SYNTHESIS, THERMAL AND SPECTRAL STUDIES OF SOME TRANSITION METAL COMPLEXES OF SCHIFF BASES

Thesis submitted to the University of Calicut
in partial fulfillment of the requirements
for the award of the degree of
Doctor of Philosophy
in Chemistry

By
ABDUL JALEEL. U.C.

DEPARTMENT OF CHEMISTRY
UNIVERSITY OF CALICUT
KERALA-673 635
JUNE
2005

Forwarded

24/6/05

HEAD OF THE DEPARTMENT
DEPARTMENT OF CHEMISTRY
UNIVERSITY OF CALICUT

Dr. Geetha Parameswaran
Professor
Department of Chemistry
University of Calicut

Calicut University P.O.
Kerala – 673 635

CERTIFICATE

This is to certify that the thesis entitled Synthesis, Thermal and Spectral Studies of some Transition Metal Complexes of Schiff Bases is an authentic record of the research work carried out by **Mr. Abdul Jaleel U. C.** under my supervision in partial fulfillment of the requirements for the degree of Doctor of Philosophy in Chemistry of the University of Calicut, and further that no part thereof has been presented before for any other degree .

Dr. Geetha Parameswaran
(Supervising Teacher)

C.U. Campus
22nd June 2005

DECLARATION

I hereby declare that this thesis entitled Synthesis Thermal and Spectral Studies of some Transition Metal Complexes of Schiff Bases submitted to the University of Calicut in partial fulfillment of the requirements for the Doctoral Degree in Chemistry is a bonafide research work done by me under the supervision and guidance of **Dr. Geetha Parameswaran,** Professor, Department of Chemistry, University of Calicut.

I further declare that this thesis has not previously formed the basis of any degree, diploma or other similar title.

C.U. Campus
22nd June 2005

Abdul Jaleel U. C

PREFACE

Coordination compounds have been a great challenge to the chemists since nineteenth century. Their versatility in the different fields of applied science is making much significance. In addition to the different applications in the applied science, structural characteristics are also gaining much momentum. In the present study, monovalent bidentate and bivalent tetradentate Schiff base ligands and their complexes are prepared and characterized on the basis of elemental analysis, magnetic and conductance measurements, UV, Visible, IR, NMR and Thermal data. These results are summarized in Part I.

The present study is focused mainly on the metal complexes of Schiff bases derived from dimedone, cyclohexanone and pyrolidone. Seven new ligands viz dimedone semicarbazone (H_2DSC), dimedone- bis -2-aminophenol (H_2DAP), dimedone bis -2-aminothiophenol (H_2DATP), cyclohexanone-2-aminophenol (HCAP), cyclohexanone-2-aminothiophenol (HCATP) pyrolidone-2-aminophenol (HPAP) and pyrolidone-2-aminothiophenol (HPATP) and their transition metal chelates have been synthesized and characterized. Mn (II), Co (II), Ni (II), Cu (II), Zn (II) and Cd (II) are the metal ions used for complexation.

Thermo analytical studies of nine selected Schiff base complexes are carried out using T. G., order of reaction, activation energy, entropy of activation, enthalpy of activation and free energy of activation are evaluated using the Coats-Redfern

equation. The results are interpreted in Part II. Thermal data further confirms the structure of the above complexes.

Part III consists of investigations on the antifungal activity of the ligands and their metal Complexes. A soil born fungus *Phytophthora capsici* that affects and destroys black pepper is used for this study. The materials and methods used for the study of antifungal activity are described in this Part III.

A detailed list of references arranged in serial order is given at the end of each part.

The research work presented in this thesis has partly been published /under publication as indicated

1) Anti fungal studies on Cu (II) Schiff base complexes .; Abdul Jaleel U.C, Dr Susheela Bhai and Dr Geetha Parameswaran in *Swedeshi Science Congress* held at M.S Swaminathan Research foundation 2003.

2) Mechanism of anti fungal activities of Schiff base complexes with special reference to the mode of inhibition on electron transfer processes in mitochondrial respiration of *Phytophthora Capsici.* Abdul Jaleel U.C. Dr Saju Kanam. Dr Susheela Bhai, Dr Anand Raj and Dr Geetha Parameswaran (to be communicated).

3) Thermo analytical and physico chemical activity studies of Cu (II),Ni (II), Zn(II) complexes of dimedone -Schiff bases . Abdul Jaleel U.C and Dr Geetha Parameswaran. (communicated).

C.U. Campus
22nd June 2005

ACKNOWLEDGEMENTS

I wish to record my profound gratitude and indebtedness to **Dr. Geetha Parameswaran,** Professor, Department of Chemistry, for her able guidance and infinite patience that enabled me to complete this work successfully. I also cherish in my mind the human touch she had given to our collective endeavor through her words of love and appreciation.

I remember with gratitude Dr Aravindakshan, Head of the Department of Chemistry, University of Calicut for providing me with all the facilities to do the research work. I also thank Mr. Prasad M Alex Research scholar in the Department of Chemistry, University of Calicut for his help and encouragement.

I am greatly indebted to Dr. Y. R. Sarma (Former Director IISR), Dr Anand Raj (Principal Scientist) and Dr Suheela bhai (Scientist), Indian Institute of Spices Research and to Dr. Saju Kanam Research Associate, Plant Pathology, I.I.S.R. for their multifarious help in carrying out the antifungal studies at their institute.

I am extremely thankful to Mr. Kripakaran,(N.I.T Trichy), and Jisha (RRL. Trivandrum) for their timely help in getting the TG , Micro analytical data and NMR spectra. Finally, I would like to express my thanks teachers, colleagues and friends at Dept of Chemistry, Calicut University. for their valuable suggestions and for all the pains they have taken to format the thesis in the present form.

Abdul Jaleel. U. C

C.U. Campus
22nd June 2005

ABBREVIATIONS

For the sake of easiness in description, the following abbreviations are used in this thesis.

H_2DSC	: Dimedone bis semicarbazone
H_2DATP	: Dimedone bis-2-aminothiophenol
H_2DAP	: Dimedone bis-2-aminophenol
HCATP	: Cyclohexanone-2-aminothiophenol
HCAP	: Cyclohexanone-2- aminophenol
HPATP	: Pyrolidone-2- aminothiophenol
HPAP	: Pyrolidone -2-aminothiophenol
M	: Central metal atom
L	: Ligand moiety in a complex

CONTENTS

PART I

SYNTHESIS AND CHARACTERIZATION

PART II

THERMO GRAVIMETRIC ANALYSIS OF SCHIFF BASE COMPLEXES

PART III

ANTIFUNGAL ACTIVITIES OF SCHIFF BASE COMPLEXES

PART I
SYNTHESIS AND CHARACTERIZATION

Abdul Jaleel.U.C "Synthesis, thermal and spectral studies of some transition metal complexes of schiff bases" Thesis. Department of Chemistry , University of Calicut, 2005

PART I

Synthesis and characterization of Schiff base complexes

Introduction and review

Introduction

One of the most productive areas of chemical research in the modern era is the development of co-ordination chemistry. The limits of coordination chemistry are difficult to define. It may range from realm of inorganic, physical and organic chemistry to the edges of theoretical physics and even bioinorganic chemistry .The progress in co-ordination chemistry and complexity and variety of coordination compounds are the main reasons for the renaissance of inorganic chemistry leading to the present period of rapid growth. The new correlations in it gave a fresh unity to whole of chemistry and the division between inorganic chemistry and organic chemistry was finally broken down.

At the very end of 18^{th}century French chemist Tassaert observed that ammonia combined with a cobalt ore to yield a mahogany colored product which is most likely the first known coordination compound. Throughout first half of nineteenth century other, often beautifully crystalline, examples of various cobalt ammoniates were prepared and in the second half ammoniates of chromium and platinum were prepared. Early milestones in the synthesis of co-ordination compounds are given in the fig 1

Figure 1

Early milestones in the development of Coordination Compounds

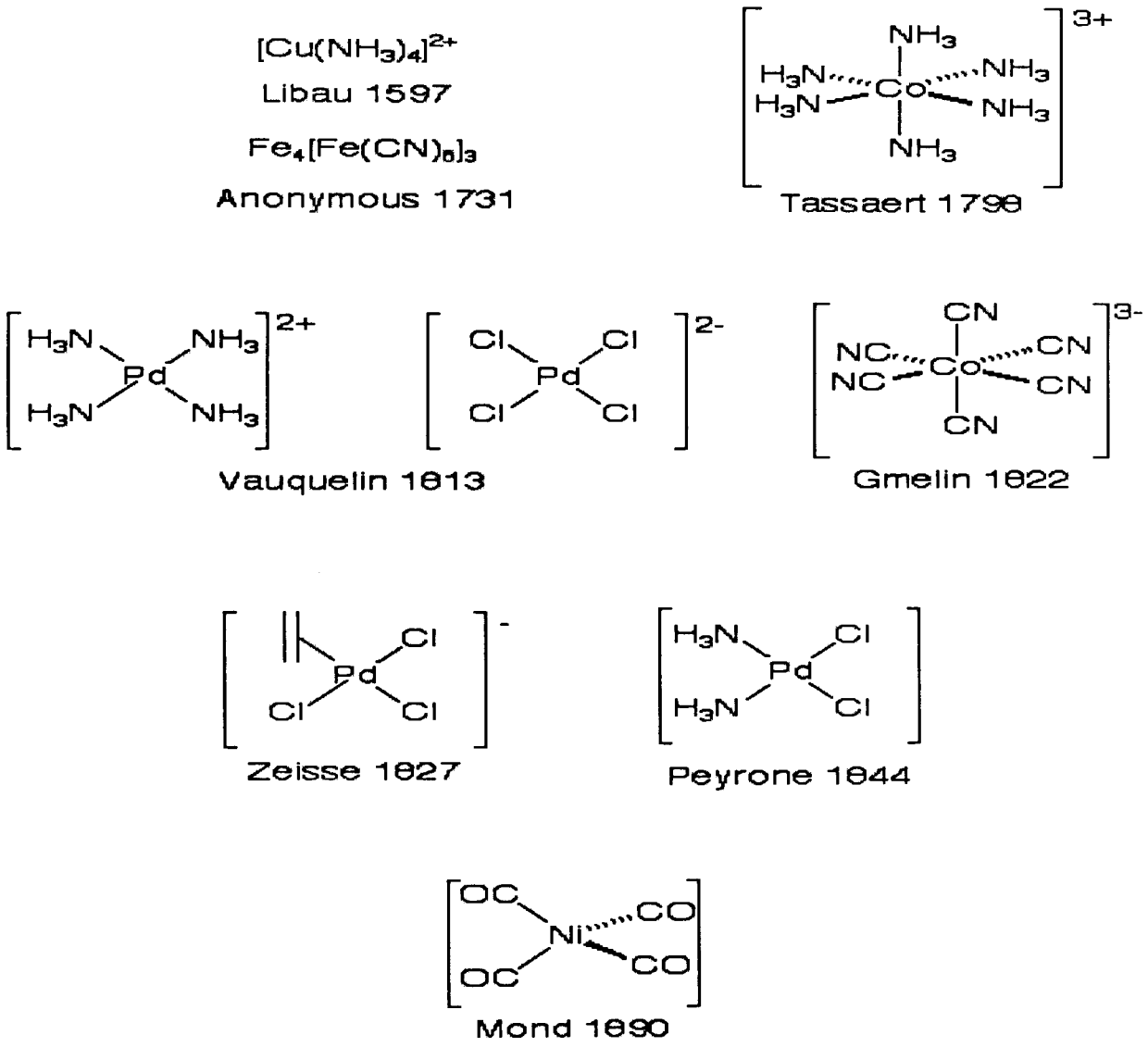

Despite various attempts, however no theoretical basis was developed to satisfactorily account for these wondrous compounds. Although Bolomstrand and Jorgensen offered some explanations for the valence state of these compounds by

chain theory , it was Werner theory which gave first scientific explanation for the valence state and stereochemistry of these compounds. Synchronized with the evolution of principles of chemical bonding, theory of coordination chemistry systematically progressed from Werner to the CFT and molecular orbital theory. Later it became possible to amalgamate CFT and MOT, the resulting ligand field theory developed by Lesle Orgel made dramatic contribution to the revival of inorganic chemistry.

Coordination compounds brought about a synthetic revolution in inorganic chemistry which led to novel products of equally novel applications in wide range of areas such as analytical chemistry, fungicides, paints, pigments, polymers pharmaceuticals, catalysis and photoconductors. Biomolecules such as hemoglobin, chlorophyll, B complex are the metal chelates, which plays an important role in life sustaining process of nature. Investigating the role and effect of chelation reveals its central role in biological systems and synthetic pathways in inorganic chemistry

The term coordination chemistry almost invariably refers to the chemistry of transition metals. Strongly perturbing, partly filled d orbitals make transition metal ion excellent in complex formation. Tendency for coordination, stereochemistry of the complexes and physical and chemical properties differ widely from metal to metal and from oxidation state to oxidation state.

Although transition elements have many useful applications and unique properties, it is being understood that complexation modifies their functional properties. Hence investigating formation and characteristics of new complexes have much significance.

Schiff bases are typically formed by the condensation of a primary amine and an aldehyde. The resultant functional group, $R'HC{=}N{-}R''$, is called an imine and is

particularly suitable for binding metal ions via the N atom lone pair, especially when used in combination with one or more donor atoms to form polydentate chelating ligands or macrocycles. Ketones will also form imines of the type $R'R''C{=}N{-}R'''$, but the reactions tend to occur less readily than with aldehydes. Examples of a few compounds of interest are given below.

I

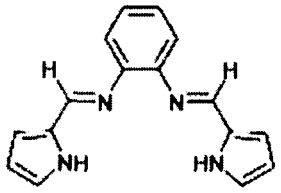

II

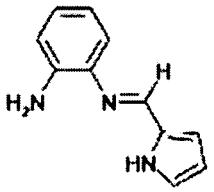

Because of the versatility offered by this ligand donor group for the design of interesting/industrially useful ligand systems, it is motivating to do further research work which aim to develop the coordination chemistry of multidentate chelating Schiff base ligands.

Review shows that transition metal complexes of Schiff bases have emerged as highly effective catalyst for various important reactions. Catalysis plays an essential role in synthesizing a diverse group of molecules for the mass production of drugs and other chemical compounds In drug development, often only one of the two mirror images of a compound generally has the desired biological effect, while the other is ineffective, or perhaps even harmful. In order to ensure the safety of a chemical compound, it must be enantiomerically pure. So asymmetric catalysis used for designing a catalyst that is able to selectively control the formation of a desired stereo isomer, where new Schiff bases are playing a central role. Such a penta denate

suphonamide ligand is reported by Karno *et al.* [1]. It was envisaged that a pentadentate ligand could coordinate to metals and leave an open coordination site that could bind and activate a substrate in a Lewis acid catalyzed reaction. These ligands are easily synthesized and should readily bind to transition metal complexes to provide chiral Lewis acids for use in asymmetric catalysis.

Another report by Genet ***et al.*** [2] also accounts for the use of palladium chiral complexes of schiff bases in the sterioselective synthesis of alpha amino acids. Benzophenone imine of glycine methyl ester palladium complex acted as prochiral nucleophile in the allylic alkylation. Good chemical yield were obtained. Catalysis can be performed at low temperature.

Study of Debabrata chatterji [3] is an example for selective catalytic activity. Tridentate Schiff base complexes of ruthenium (III) is used in the oxo transfer from tert ButOOH, to C-H bond by insertion. For that mixed-chelate complexes of ruthenium have been synthesized using tridentate Schiff-base ligands derived by condensation of aldehydes (salicyldehyde, 2-pyridinecarboxaldehyde) with 2-aminobenzoic acid, and bidentate ligands (2,2′-bipyridine or picolinic acid). $[Ru^{III}(cpsd)(bipy)(H_2O)]^+$, $[Ru^{III}(cpsd)(pic)(H_2O)]$, $[Ru^{III}(cppc)(bipy)(H_2O)]^{2+}$ and $[Ru^{III}(cppc)(pic)(H_2O)]^+$ complexes (where, $cpsd^{2-}$=(*N*-(carboxyphenyl)salicylaldiminato); $cppc^-$=*N*-2-carboxy phenyl pyridine-2-carboxaldiminato; bipy=2,2′-bipyridineand pic^-=picolinate). Catalysis of hydrocarbon oxidations for cyclohexene, cyclohexane, cyclohexanol, toluene, benzyl alcohol, and tetrahydrofuran has been studied using various O-atom transfer agents (*t*-BuOOH, H_2O_2, NaOCl, $KHSO_5$ and pyridinium-*N*-oxide). A mechanism involving intermediacy of a high valent Ru(V)-oxo species is proposed for the catalytic oxidation processes.

Lobet *et al.* reported [4] another example of specific catalytic activity of Cu (I) and Cu (II) di nuclear complexes of new hexa aza Schiff base macro cyclic ligands. It has been shown that these complexes are efficient and selective catalysts for the oxidation of 3,5-di-t-butylcatechol to 3,5-di-t-butyl-1, 2-benzoquinone. Furthermore the measured initial rate constants reveal that it reacts much faster than any of the related macro cyclic systems.

Applications of Schiff base complexes in the field of catalysis is not only limited to the field of chemical catalysis but it extend even to the field of biological catalysis. In this area report by Erskine *et al.* is very significant [5].They studied about Schiff base complexes formed by the yeast 5-aminolaevulinic acid dehydratase with inhibitor laevulinic acid which has a specific role during catalysis.

In the midst of sophisticated applications of Schiff base complexes in biological and selective catalysis, their role in traditional chemical catalysis cannot be under estimated. Following example is much relevant in this aspect. Nahar *et al.* reported [6] catalysis of dehalogenation of chloroform by Schiff base metal complexes. Effect of metal ion on the dehalogenation of chloroform promoted by the ligand substitution reaction system, consisting of bis (N-n butyl salim) M (II) (M=Zn, Cu, Ni, Pt, Pd) and N, N, N'N'tetramethyl ethylene diamine is studied. Electro negativity of metal ion and stereochemistry of complex are found to control the rate of reaction.

The next goal of this review is to demonstrate significant progress in the field of Schiff base co-ordination chemistry as it applies to medicinal field like drug designing diagnostic tool etc. This aspect has gained momentum in the development of molecule which have active role in treatment of diseases like cancer [7] and neurological [8] diseases and heart diseases (artherosclerosis) [9].

Report of Cad on [7] synthesis and biological activities of new Schiff bases of racemic gossypol and gossypolone and of (+) - and (-)-gossypol enantiomers and their Gold complexes is an interesting example. Schiff bases obtained from gossypol enantiomers are optically stable at room temperature whereas gossypolone Schiff bases racemize quickly and may be observed only at lower temperature. Their cytotoxic activities on human cancer cells were determined: it is suggested that gossypol and gossypolone dithianes and dithiolanes can be used as pro drug that target tumor cells.

Verma *et al.* has reported anticonvulsant activity of schiff bases. They synthesized [8] and screened Schiff bases of N-methyl and N-acetyl isatin derivatives with different aryl amines for anti convulsant activities against maximal electroshock (MES) and subcutaneous metrazole (ScMet). N-methyl-5-bromo-3-(p-chlorophenylimino) isatin exhibited anticonvulsant activity in MES and ScMet with LD(50) > 600 mg kg(-1), showing better activity than the standard drugs phenytoin, carbamazepine and valproic acid. Thus, compound N-methyl-5-bromo-3-(p-chlorophenylimino) isatin may be chosen as a prototype for development of new anticonvulsants.

Toshihiko Takeuchi *et al.* have reported [9] selective inhibition of Human ά -Thrombin by Cobalt (III) Schiff base complexes. Human ά-thrombin associated with the blood coagulation cascade, converts fibrinogen into fibrin, which ultimately forms blood clots. Cobalt (III) Schiff base complexes of class (acacen) bind histidine residues in active sites and on enzyme surfaces in a random fashion. Spectroscopic and chromatographic evidence indicates that the binding of these complexes is controlled by axial ligand substitution. They showed that the reaction of active site- directed peptide linked to cobalt chelate leads to selective irreversible inhibition of thrombin.

Other developments of interest in the areas of drug research include the study of anti microbial activity of Schiff base and enhancement in activity due to complexation . Following studies show remarkable advancement in the respective fields. Dashora *et al.* reported [10] the synthesis of organo silicon and organolead complexes of Schiff bases from sulpha drugs. Complexes of the type $(CH_3)_2Si(ONN)$ $(C_6H_5)_2Si(ONN)$, $(C_6H_5)_2Pb(ONN)$ have been prepared.

New (N-indolidene-DL-glycine, N-indolidene-DL-alanine and N-indolidene-DL-valine) amino acid-Schiff bases by the condensation of indole- 3-carboxaldehyde and DL-glycine, DL-alanine and DL-valine were prepared and characterized by Nursen *et al.* [11] and their antimicrobial activities tested against four different microorganisms like *B. subtilis, S. aureus, E. coli and C. albicans.* The results of the antibacterial screening of the Schiff bases ind-gly, ind-ala and ind-val at a concentration of 5000 $\mu g/cm^3$ against all bacteria have been found and the results indicate that amino acid Schiff bases shows more activity against *Staphylococcus aureus, E- coli and Bacillus polymyxa* than *Candida albicans.* Ind-gly was found to be active against both strains of *S. aureus. Escherichia coli* and *Bacillus poly myxa* were inhibited by ind-gly. Ind-val was found to be the most active of them all. *E. Coli* was the most sensitive. The activity of these substances may be due to carboxyl group. The high activity of Ind-val may be due to the presence of electron donating effect.

Acylhydrazine derived furanyl and thienyl Schiff bases and their Cu(II) complexes were prepared [12] and characterized by Zahid Chohan *et al.* The preferred enolic form of the Schiff base which function as a tetradentate ligand during coordination to the metal ion yields a square planar complex. The Schiff bases and their complexes with different anions were tested for their antibacterial activity

against bacterial species such as *Escherichia coli*, *Staphylococcusaureus*, *Pseudomonas aeruginosa and Klebsiella pneumonae.*

Raman *et al.* have synthesized [13] and characterized neutral tetradentate complexes of Cu (II), Ni(II), Co(II) and Zn(II) using the Schiff base formed by the condensation of acetyl acetone and p-anisidine.. From the data it is found that all the complexes possess square-planar geometry. All the complexes were screened for antimicrobial activity against bacteria like *S. aureus*, E. *Coli*, B. *subtilis* and the fungus, A. *Niger*, by the well diffusion technique using DMSO as solvent. The minimum inhibitory concentration (MIC) values were calculated at 37°C for a period of 24 h. It is found that all the complexes are anti microbially active and show higher activity than free ligand.

Modern researchers used to imitate the biosynthetic pathways by designing bio mimetic reactions that approximate natural reaction pathways. For example the relationship between redox properties and super oxide dismutase mimetic activity of thiohydrazone Cu (II) complexes was studied by Zdena *et al.* [14] .The redox behavior of copper (II) complexes with the open chain ligand, benzil bis thiosemicarbazone, and the macrocyclic one [3,4,10,11-tetraphenyl-1,2,5,8,9,12,13-octaazacyclotetradeca-7,14-dithione-2,4,9,11-tetraene] has been explored by cyclic voltammetry. The half-wave potential values for the copper (II)/copper (I) redox couple and the spectral data obtained on dimethylsulfoxide (DMSO) solution agree with the super oxide dismutase (SOD)-mimetic activity of the complexes. The macrocyclic complexes show more positive reduction potential and more activity than the open chain derivatives. From their results it follows that the structure and conformation of ligand has influence on the redox potential of central atom in

coordination compound. The changes in the coordination sphere are connected with the change of biological function of compounds represented by SOD-mimic activity.

Iffet Sakyyan *et al.* [15] have synthesized and characterized new complexes of Mn (III) with Schiff bases obtained by the condensation of 2-hydroxy-1-naphthaldehyde with glycine, L-Alanine, L-Phenylalanine, L-Histidine, L-Tryptophan and L-Threonine. These complexes are coordinated through the ONO donor set derived from the carboxyl, imino and phenoxy groups of the ligands. These complex molecules are proposed as model molecules where Mn plays an essential and specific role in water oxidizing complex of photosystem (II). Although manganese is essential for the oxygen evolution process in photosynthesis, its chemical role in photosystem II remains uncertain. Furthermore the chemical environment around the manganese ion is not known, which precludes the rational design of model compounds. The mechanism proposed , supported by flash photolysis data consist four discrete one-electron steps lead to oxygen evolution. Because of the multiplicity of the oxidation states of manganese and the associated coordination chemistry, it has an essential role as redox catalyst in photo system II.

In coherence with the advances in analytical chemistry Schiff bases have emerged as Cutting edge tools in sophisticated chemical analysis such as application of [16] poly vinyl chloride (PVC) membrane electrodes based on two complexes of Schiff base 2,2'[4,4'-diphenylmethane bis (nitromethylidyne)] bis phenol, with copper (II) and iron (III) ions, and used for determination of tri iodide ions with lower detection limits of 4.0×10^{-6} and 6.0×10^{-6} mol dm^{-3}, respectively. The proposed electrodes have fast response time (15 s) and their responses are independent of pH of the test solution in the range 3.5–9.0. The electrodes revealed very good selectivity for tri iodide ion over a variety of anions. They were used as an indicator electrode in the

potentiometer titration of tri iodide ions and determination of ascorbic acid in Vitamin C tablet

Optical pH sensor (optodes) based spectral response of newly synthesized Schiff bases [17] *N*, *N*'-bis (4-diaminobenzyliden)-1,2-cyclohexandiamine, *N*, *N*'-bis (4-diaminobenzyliden)-1,2-ethanediamine and 2,6-bis [(4-dimethylaminophenylimino) ethyl pyridine is designed and tested. In most of the common designs, pH optodes rely on weak acidic dyes whose dissociated and undissociated forms have different absorption or emission maxima. In their work the newly synthesized Schiff bases have been used for pH sensing in four different plasticized PVC matrices. The Schiff bases exhibited absorption and emission based optical responses to protons in the pH range of 3.0–7.8, and, therefore, can be used as an optical pH sensor for near neutral region of pH scale.

Copper in alloys can be safely estimated by using the Schiff base method without interference from many other metals in alloys. Elif Kormal and Esma KIIic used [18] N, N'-disalicylidene-1, 3-diaminopropane as a selective chelating titrant for copper (II). The standard solutions of copper (II) (10^{-3}–10^{-5} M) were potentiometrically titrated using *N*,*N*'-disalicylidene-1,3-diaminopropane (Schiff base) as titrant and copper(II)-selective electrode for end-point indication in both ammonium acetate and ammonia/ammonium chloride buffer media. The stoichiometry of titration reaction and interference effects of some metal ions on titration of copper was studied. There was a good agreement between the results obtained by the proposed titration method and ethylenediaminetetraacetic acid (EDTA) titration method. The accuracy and precision of Schiff base method were tested .

In another report Papi *et al.* studied [19]the synthesis characterization and application of metal complex of nickel with Schiff bases, 2-(2-pyridylmethyleneamino) phenol (PMAP) and 2-(2-quinolylmethyleneamino) phenol (QMAP). It was found that, for the Ni-PMAP complex, two ligands were bonded to one metal ion, giving a neutral complex with one molecule of water probably bonded in the inner sphere of the complex. In the case of QMAP, nickel forms cationic complexes with a metal-to-ligand ratio of 2:2 and two molecules of acetate as anions. The solution properties of Ni-QMAP were investigated at different pH. The chromophoric properties of the complex were enhanced with increase in pH, while stability decreased with time. The application of QMAP as a spectrophotometric reagent for the determination of small amounts of nickel was investigated. Adherence to Beer's law was observed from 0.00 to 5.00 μg/ml at pH 8, the most appropriate pH in respect to sensitivity and acceptable time stability of the complexes. Dyeing properties of both complexes were investigated on polyamide 66 and the influence of the addition of another phenyl ring to the ligand molecule on the dyeing properties of the complex is also investigated.

Guidelines for the molecular design of non-doping red emissive materials for OLED applications are presented in the investigation of Jia-An Gan *et al.*. They have reported [20] the synthesis of Schiff base derivatives of 1,8-Naphthalimides for non-doping OLEDs (organic light emitting diode) showing tunable emission color from blue, green to red Substitution at the 4-position of 1,8-naphthalimide with electron-donating groups can increase fluorescent quantum yields and change emissive wavelengths from blue to red . Based on this molecular design concept, novel naphthalimide derivatives containing Schiff base moiety were prepared by condensing 4-hydrazino-1,8-naphthalimides with the aldehydes. Amino conjugation between the

4-amino-1, 8-naphthalimide and the substituted moiety resulted in red shift of the absorption and fluorescence maximum wavelengths in the aceto nitrile solution and in the net solid film. Some of these dyes emit brilliant red fluorescence in solid films and were used as non-doping emissive materials to fabricate electro luminescence devices.

Review of Schiff base complexes of semicarbazones

Like other Schiff bases semicarbazone are also excellent chelating agents. Diversity in structural aspects and predominance in applications like anticonvulsant, anti cancer and anti HIV activity might be the other reason for the vide study of semicarbazide complexes. A review with much priority for structure and synthesis follows.

Dixit, Purnima *et al.* have synthesized [21] and characterized organotin (IV) complexes of acetoin and benzoin semicarbazones and thiosemicarbazones. By the condensation of benzoin and acetoin with semicarbazide hydrochloride and thiosemicarbazones corresponding Schiff bases are obtained. These when reacted with dimethyl tin dichloride and dibutyl tin oxide, lead to the formation of substitution products of the type, R_2SnL (where R = Me or Bu and LH_2 = ligand molecule). The resulting complexes have been characterized on the basis of elemental analysis, molecular weight determination and conductivity measurements. The mode of bonding of the ligands with the metal atom has been deduced on the basis of IR, ^1H NMR and electronic spectral studies. All the ligands have been found to behave as bifunctional tridentate donors .

Francisco Hueso-Urena have reported [22] the synthesis, spectral and XRD studies on three O-nitrito-complexes with new N, N, O-tridentate Schiff bases derived from 6-amino-5-formyl-1, 3-dimethyluracil and semicarbazide, acetylhydrazine and benzoylhydrazine From the reaction between Cu (II) and Zn (II) nitrates and three

Schiff bases derived from 6-amino-5-formyl-1, 3-dimethyluracil and semicarbazide (H_2SDO), acetylhydrazine (H_2ACEDO) and benzoylhydrazine (H_2BEZDO) in DMF, three nitrito-complexes with simplified formulas $[Cu(HSDO)(NO_2)]$, $[Cu(HACEDO)(NO_2)(H_2O)]$ and $[Zn(HBEZDO)(NO_2)(H_2O)]$ have been obtained. In the three compounds the Schiff base acts as tridentate mono deprotonated ligand, making two five- and six-membered chelate rings.

Agarwala *et al.* conducted [23] synthetic and physicochemical studies of uranium complexes with semicarbazone and hydrazones. Uranyl complexes of two Schiff bases, semicarbazone and hydrazones containing OON donor atoms have been synthesized .The coordination number of the *o*-vanillin semicarbazone (oVSC) complex is 6 whereas, that of the *o*-vanillin isonicotinic acid hydrazone (oVINAH) complex is 8, in addition to the two oxygen atoms already bonded to U (VI) in each species, The thermograms showed the presence of 3 and 2 water molecules in these complexes, respectively and the IR spectral data also supported the above conclusion. Vasile Lozan *et al.* [24] reported the synthesis of dinuclear nickel (II) and palladium (II) complexes with Schiff-base ligands (derived form salicylaldehyde condensed with 2-amino-1-alcohols or from 2-hydroxy-5-methyl isophthaldialdehyde and pyridine-2-carboxaldehyde condensed with semicarbazide, thiosemicarbazide, carbonodihydrazide, or thiocarbonodihydrazide) which can be activated with the co-catalysts methylalumoxane (MAO) or tris (pentafluorophenyl) borane for the vinyl/addition polymerisationof Norbornane.

Singh *et al.* have reported [25] the synthesis of Schiff bases 1-acetyl ferrocene thio semicarbazone and l-acetyl ferrocene semicarbazone by the condensation of l-acetyl ferrocene with the corresponding thiosemicarbazide and semicarbazide hydrochloride, respectively. These Schiff bases on interaction with diorganosilicon

(IV) chlorides yield complexes having Si-S or Si-O and Si- N bonds. The structure of the ligands and their compounds have been elucidated .Spectroscopic data indicated that the Schiff bases act as bidentate ligands and coordinate to silicon via nitrogen and either the S or O atoms giving trigonal bi pyramidal and octahedral geometries for the resulting complexes.

In another study Ferenc makkay *et al.* have discribed [26] the formation conditions, composition, stability and analytical application of some ternary complexes Co (II):L^1:X (L^1=aliphatic and alycyclic α-dioximes; X=N^{-3}, I^-), binary derivatives: Co(II):L^2 (L^2=α-ketoximes diacetylmonoxime, methyl-isopropyl dione monoxime, 1,2,3-cyclohexane trione dioxime (1,3)), Co(II): L^3 (L^3 = Condensation products of ketoximes with semicarbazide, thiosemicarbazide) and Co(II):L^4 L^4=Schiff bases with ethylenediamine and hydrazine) were studied spectrophotometrically. The electronic spectra of these complexes were recorded and discussed.

Leovac *et al.* have synthesized [27] octahedral Co (III) complexes with tridentate salicylaldehyde semi-thio semi -and iso thiosemicarbazone and pyridine of general formula [Co III (L^{1-3})$(py)_3$] X , H_2L^1 = salicylaldehyde semicarbazone, X = [Co(II) $Cl_3(py)]^-$,ClO_4^-.H_2O, I^-. H_2L^2 = salicylaldehyde thiosemicarbazone, X = [Co(II) $Cl_3(py)]^-$, [Co(II) $Br_3(py)]^-$,ClO_4^-, H_2O, I_3^- ; H_2L^3 = salicylaldehyde S-ethyl iso thio semi carbazone, X = [Co(II) $Br_3(py)]^-$,ClO_4^-. H_2O, BF_4^-). The tridentate coordination of all the three di anionic forms of the ligands involves the phenol oxygen, hydrazine nitrogen and the chalcogen (O or S) in the case of salicylaldehyde semi-, thiosemicarbazone and the terminal nitrogen atom in the case of iso thio semi -carbazone. For all the complexes, octahedral arrangement is proposed, which is a consequence of the planarity of the chelate ligand. By using

elemental analysis, molar conductivity, magnetic susceptibility, IR and electronic absorption spectra the compounds have been characterized. The thermal decomposition of the complexes was investigated by thermo-gravimetry, coupled TGMS and DSC.

In another report [28] synthesis, physico chemical and voltammetric characterization of iron (III) complexes with pyridoxal semi-, thiosemi-and S-methyl isothiosemicarbazones are described .The reaction of warm EtOH solutions of $FeX_3.nH_2O$ (X =Cl, NO3) with tridentate O N X (X = O, S, N) pyridoxal semi-,thio semi and S-methyl iso thio semicarbazones (H_2L^1 ,H_2L^2 ,H_2L^3 , respectively) yielded high-spin octahedral mono and bis(ligand)complexes of the formula $[Fe(H_2L^{1-3})Cl_2(H_2O)]Cl$,$[Fe(HL^{1-2})_2]$ Cl. nH_2O and$[Fe(H_2L^3)(HL^3)](NO_3)_2.H_2O$. Elemental analysis, conductometric and magneto chemical measurements, and IR and UV-VIS spectra proved the stability and structure.

Apart from the structural and theoretical point of application, complexes of semicarbazone posses high level significance in the applied chemistry. The following examples will provide the importance of semicarbazone complexes in advanced applications that are useful to mankind.

Pandeya *et al.* have studied [29] anticonvulsant and neurotoxicity evaluation of 5-(un)-substituted isatin imino semicarbazide derivatives. Schiff bases were prepared by reacting 5-(un)-substituted isatin with some heterocyclic compound, viz., N- [4-(4'-chlorophenyl)-thiazol-2-yl] semicarbazide, The compounds were evaluated for anticonvulsant and neurotoxin properties and found active. The above compound showed lower neurotoxicity than phenytoin and carbamazepine .

Elzbieta Pomarnacka *et al.* have reported [30] synthesis of 1-(6-chloro-1,1-dioxo-1,4,2-benzodithiazin-3-yl)semi-carbazides and their transformation into 4-

chloro-2-mercapto-*N*-(4,5-dihydro-5-oxo-4-phenyl-1*H*-1,2,4-triazol-3-yl)benzene sulfona- mides as potential anticancer and anti-HIV agents compounds and these were tested at the US National Cancer Institute for their in vitro anticancer and anti-HIV activities. Results of anticancer screening showed moderate activity of and while was found to have encouraging anti-HIV activity.

Schiff base complexes of 2-aminophenol and 2 -aminothiophenol

Review shows that higher tendency for chelation stability and diversity of the structure and speciality in applications are the reasons for wide interest in the Schiff base complexes of 2-aminophenol and 2-aminothiophenol. Salam ***et al.*** [31] has synthesized Cu (II) and Ni (II) complexes of some dibasic tridentate Schiff bases prepared by condensation of 2 aminophenol with 2-hydroxy-1-naphthaldehyde. Syamal ***et al.*** [32] have characterized Fe (III) complexes of tridentate Schiff bases derived from simple or substituted salicylaldehyde and 2-aminophenol.

Tez Can has [33]prepared and characterized the complexes of transition metals, rare earths metals and main group metals with Schiff base salicylidene 2- aminophenol and salicylidene -2-hydroxy -1- naphthyl amine.

The synthesis of several new coordination compounds of Cu (II), Ni (II), Co (II), Sn (II), Hg (II) etc with Schiff bases derived from 7 formyl-8- hydroxy quinoline (Oxine) and 2 aminophenol have been reported by Sonabati and bindary[34], the ligands and complexes were characterized by elemental analysis, IR, U.V, EPR, and NMR studies showed that the Schiff bases behave as mono basic and tridentate ligands coordinating through the oxygen atom of the deprotonated phenolic group, the nitrogen atom of the azomethine group and pyridine.

Schiff bases derived from salicylaldehyde and 2- aminophenol were synthesized and characterized by Naik[35] and co workers. Magnetic and electronic

spectral studies provide the evidence for the existence of octahedral geometry for the complexes.

Mehtha *et al.* [36] have synthesized Schiff bases derived from the condensation of 2 hydroxy-1- naphthaldyhyde and 2-aminophenol. The copper complex was characterized by elemental analysis U.V, IR, NMR and magnetic data .

New complexes [37] of the vanadium (IV) and oxovanadium (IV) with Schiff base ligands derived from the beta diketone and 2- aminophenol were prepared and characterized. A distorted octahedral environment was proposed for the vanadium (IV) and oxovanadium (IV) complexes. The spectroscopic results were used to compute the important ligand field parameters. Vanadium (IV) complexes exhibit promising catalytic activity towards the aerobic oxidation of phenylene diamine to the corresponding semi oxide form.

Copper (II) complexes[38] of Schiff bases derived from equimolecular amounts of 5-nitro salicylaldehyde and the amines, 2 -aminophenol and 4-aminophenol were prepared by Murthy *et al.* . Copper complexes of the two ligands had a stochiometry 1:2. The complexes were tested for the anti bacterial activity against common pathogenic organism, and they showed mild to moderate activity .

Jejukumar *et al.* [39]have synthesized Schiff base complexes of Cu (II) and Ni (II) derived from phenyl butazone and 2- aminophenol. They were characterized by the elemental analysis, magnetic measurements, and X ray diffraction and IR. The Schiff base ligands and their metal complexes were tested for their anti bacterial behavior using *E.coli* as a test organism.

Chae *et al.* [40] have prepared the Schiff base ligands by the reaction of the salicylaldehyde and 2 hydroxy-1- naphthaldeyhde with 2-aminophenol and 2 amino-p- cresol respectively. The structures and the properties of the ligands and their Co

(II) complexes were studied by using the elemental analysis, NMR, U.V IR, and TGA .

The synthesis and characterization of the Schiff base from the 2-aminophenol and crocetinadialdehyde 2, 7- dimethyl octatrienedial or terephthaldehyde were carried out by Armin *et al.* [41].

Maya Devi *et al.* [42] have synthesized and characterized some transition metal complexes of Schiff base quinoxaline-2-carboxaline-2-aminophenol. A tetrahedral structure was assigned for the Mn (II), Co (II), Ni (II) and Cu (II) complexes. For the Fe (III) complexes an octahedral dimeric structure was suggested . Platinum complexes[43] derived from the 2- aminophenol and salicylaldehyde and 2 hydroxy-1-naphthaldyhyde were prepared and characterized by the elemental analysis conductance, magnetic measurements. IR and electronic spectral data. The tridentate dibasic nature of the ligand was established on the basis of IR studies,. The complexes are non-electrolytes, diamagnetic and square planar.

Sanchez *et al.* have synthesized [44] new palladium (II) complexes with a tridentate PNO Schiff base ligand of aminophenol. Deprotonation of the Schiff base formed by condensation of 2-(diphenylphosphino) benzaldehyde with 2-aminophenol in the presence of the appropriate palladium precursor ([Pd $(AcO)_2$] or [$PdCl_2$ $(PhCN)_2$]) form the corresponding neutral complexes [Pd(2-(2-$Ph_2PC_6H_4$-CH=N)C_6H_4O)(AcO)] or [Pd(2-(2-$Ph_2PC_6H_4$-CH=N)C_6H_4O)(Cl)] in good yield. The first reacts smoothly with thiols and activated phenols to give complexes of general formula [Pd {2-(2-$Ph_2PC_6H_4$-CH=N)C_6H_4O}(X)] (X = OC_6F_5 , SEt , S^tBu , SC_6H_5 , SC_6H_4-4Me , SC_6H_4-4NO_2). When the chloro complex is treated with silver per chlorate and tertiary phosphines (L) the cationic derivatives [Pd {2-(2-$Ph_2PC_6H_4$-CH=N)C_6H_4O}(L)][ClO_4] (L = PPh_3 , $PMePh_2$, PMe_2Ph , PEt_3) were obtained. The

new complexes were characterized by partial elemental analyses and spectroscopic methods (IR, ^{1}H,^{19}F and^{31}P NMR).

Minu *et al.* have synthesized. [45] several ruthenium(II) Schiff base complexes derived from bis (pyrrole-2-carboxaldehyde)-3,4-toluenediimine, bis(pyrrole-2-carboxaldehyde)-1, 2-cyclohexanediimine, bis(pyrrole-2-carboxaldehyde)-1,8-naphthalindi-imine, bis(pyrrole-2-carboxaldehyde)-1,3-propylenediimine,bis(pyrrole-2-carboxaldehyde)-1,2-phenylenediimine and bis(pyrrole-2-carboxaldehyde)-ethylenediimine, Lanthanide(III) Schiff base complexes derived from N-(2-pyrrolylmethylene)-2-aminophenol were synthesized. All the complexes were characterized by analytical and spectroscopic methods. The ruthenium Schiff base complexes were found to be effective catalysts for the oxidation of primary alcohols in the presence of N-methyl morpholine-N-oxide as oxidant.

Jung-Sook Kim *et al.* have synthesized [46] six-coordinate molybdenum (V)-oxo complexes with N-salicylidene-2-aminophenol and its derivatives as ONO-donor ligands. The spectral and electrochemical properties of the complexes have been studied by elemental analysis, molar conductivity, UV- IR and NMR .

Salavati *et al.* reported [47] application of Alumina-supported Mn (II), Co (II), Ni (II) and Cu (II) bis (2-hydroxyanil) acetylacetone complexes as catalysts for the oxidation of cyclohexene with *tert*-butylhydroperoxide complexes of a tetradentate Schiff base ligand[bis(2-hydroxyanil)acetylacetone], 2-[{1-methyl-3-[(2-hydroxy phenyl) imino]butylidene} amino]phenol (H2haacac) . It has been prepared and characterized by elemental analyses, IR and conductometry. The results suggest that the Schiff base is a bivalent anion with tetradentate ONNO donors derived from the phenolic oxygen and azomethine nitrogen. The formula was found to be [M (haacac)]

for the 1:1 non-electrolytic complexes. Alumina-supported [M(haacac)] complexes catalyze the oxidation of cyclohexene with *tert*-butylhydroperoxide (TBHP).

Schiff-base 2,5-pyrrolediyl bis [*N*-(*o*- hydroxyphenylaldimine)] (SBH_2) has been synthesized by the condensation of 2,5-pyrroledicarboxaldehyde and *o*-aminophenol. The reactions of the Schiff-base with several transition- and post-transition-metal ions have been investigated. The Schiff-base reacts as a tetradentate dianion without deprotonation of the pyrrole. The complexes M (SB) nH_2O have been isolated and characterized with n = 1, 2 or 3; SB is the dianion of the Schiff-base ; and M = divalent Mn, Co, Ni, Cu, Zn, Pd, Cd, Pb or UO_2. The binuclear complexes M (SB) MX_2 for M = Cu, X =NO_3, and M = Ni or Pd, X = Cl, have also been isolated by Tayim *et al.* [48].

Besides the traditional applications, Schiff bases have emerged as analytical tool for precise determination of traces in even in physiological systems as the application of aluminium (III) [49] complex with salicylidene-*o*-aminophenol to the fluorometric determination of nucleic acids, is a very good devolopment in this field .In buffer medium of hexamethylene tetraamine–HCl at pH 5.9 the aluminium(III) complex with salicylidene-*o*-aminophenol (SAP) has a fluorescence peak at 508 nm with excitation at 410 nm. When nucleic acid coexists, it reacts with the complex within 8 min at room temperature to produce a non-fluorescent product, resulting in the decrease of fluorescence intensity of the aluminium complex. On basis of this, a new fluorometric method for nucleic acids determination is proposed. Compared with some established fluorometric methods, this procedure is sensitive, selective, reliable, and reproducible.

Xiaoyuan Chen *et al.* has studied the synthesis [50] and structural characterizations of a series of novel `3+2' and `2+2+1' mixed-ligand complexes carrying 8-hydroxy-5-nitroquinoline (HL) as the bidentate N, O donor atom system. Thus, reactions of $[ReOCl_3(PPh_3)_2]$ with dianionic tridentate ligands H_2L'' (where H_2L^1=HOC_6H_4-2-CH=NC_6H_4-2-OH; H_2L^2=HOC_6H_4-2-CH=N---C_6H_4-2-SH; H_2L^3=HOC_6H_4-2-CH=NN=$C(NHC_6H_5)$---SH; H_2L^4=2-CH_2OH---C_5H_3N-6-CH_2SH; and H_2L^5=2-CO_2H---C_5H_3N-6-CO_2H) and HL afforded a series of `3+2' oxorhenium complexes of the type $[ReO(H_2L'')(L)]$ which exhibit distorted octahedral geometries.

Investigations[51] on new transition metal chelates of the 3-methoxy-salicylidene-2-aminothiophenol Schiff base have been carried out by Soliman *et al.* Co (II), Cu (II) and Zn (II) complexes of a Schiff base have been prepared and characterized by elemental analyses, IR, and ^{1}H-NMR spectroscopy, thermogravimetric analysis, conductometric and magnetic measurements. The results suggested that the Schiff base is a bivalent anion with tridentate ONS donors derived from the phenolic oxygen, azomethine nitrogen and thiophenolic sulfur. The formulae were found to be $[ML{\cdot}H_2O]$ and $[ML_2]$ for the 1 : 1 and 1 : 2 non-electrolytic complexes, respectively. The thermal decomposition of the complexes follows first order. Complexes show ligand field transitions at 815 and 760 nm at room temperature which are independent of the solvents used and are consistent with a pseudo tetrahedral kinetics and the thermodynamic parameters of the decomposition were calculated.

Subrata Mandal *et al.* have reported [52] synthesis and characterization of CuN_2S_2 complexes for modelling the blue protein active sites. Two new tetradentate ligands have been synthesized by Schiff base condensation of di isobutyraldehyde

disulphide with 2 -mercaptoethylamine (L^1) and 2-aminothiophenol (L^2) respectively and then reducing the imine linkages with $NaBH_4$ in refluxing methanol. In the free ligands the thiolate sulphur is protected with tertiary butyl groups, which are cleaved in the presence of Cu^{II}-salts to give neutral CuN_2S_2 complexes.

Chinnasamy Jayabalakrishnan *et al.* studied [53] the products obtained by reacting ruthenium (II) complexes [RuHCl(CO)(PPh3)2(B)] [B = PPh3, pyridine (py) or piperidine (pip)] with tridentate Schiff base ligands derived by condensing salicylaldehyde or *o*-vanillin with *o*-aminophenol and *o*-aminothiophenol. Thesecomplexes have been characterized by analytical, IR, Electronic, ^{1}H-n.m.r. and ^{31}P-n.m.r. Spectral studies and formulated as [Ru (L)(CO)(PPh3)(B)] (L = bifunctional tridentate Schiff base anion, B = PPh3, py or pip). An octahedral structure has been proposed for the new complexes. Some have been tested for the *in vitro* growth inhibitory activity against bacteria *Escherichia coli*, Bacillus sp. and *Pseudomonas* sp.

Thangaian Daniel Thangadurai *et al.* [54] studied ruthenium (II) carbonyl complexes containing tetradentate Schiff bases such as *bis* anthranilic acid) acetylacetimine (H_2-anthacac), *bis* (anthranilic acid) dibenzoylmethimine (H_2-anthdibm), *bis*(2-aminothiophenol) acetylacetimine (H_2-2-amptacac) or *bis*(2-aminothiophenol) dibenzoylmethimine (H_2-2-amtpdibm), with a general formula [Ru (CO)(LL')(B)] (where, LL' = anthacac, anthdibm, 2-amtpacac or 2-amtpdibm; B = PPh_3 or py or pip or morph) .The complexes have been characterised by elemental analyses and spectral (I.R. Electronic spectra, ^{1}H- and ^{31}P-n.m.r.) data. An octahedral structure has been proposed for the complexes, which were also tested for their antibacterial properties.

Schiff base complexes of keto compounds.

For the last few years the properties and syntheic viability of cyclic ketones attract a keen attention to several scientists. Some of these complexes have very remarkable practical applications like anti cancerous, antibacterial activities etc A review of Schiff base complexes of keto compounds including those of dimedone, cyclohexanone and pyrolidone are presented here. Kamal *et al.* reported [55] the preparation and characterization of novel asymmetrical Schiff-Base ligands derived from dimedone with both ethylenediamine or p-phenylenediamine and 2-methyl-7-formyl-8-hydroxy quinoline and their metal complexes. These were prepared by reacting two half-unit Schiff-base compounds with 2-methyl-7-formyl-8-hydroxyquinoline. The two half-unit Schiff-base compounds were initially prepared by condensing dimedone with either ethylenediamine or p-phenylenediamine, respectively. Both ligands are dibasic and contain two sets of NO coordinating sites. Twelve metal complexes were obtained by reacting both ligands with Cu (II), Ni (II), Co (II), Mn (II), Fe (III), VO (IV) cations. The ligands and their metal complexes were characterized by elemental analysis; IR, UV-Vis, ESR ,mass spectra and magnetic moments of the complexes were determined. Visible spectra of the complexes indicated distorted octahedral geometries around the metal cations. ESR spectra indicated mononuclear and dinuclear structures of the complexes of ligands. Magnetic moments of the complexes were rather low compared with those expected for octahedral geometries and indicated polymeric linkage of the metal complex molecules within their crystal lattices. The insolubility of the metal complexes in most organic solvents supports the polymeric structures.

Sergej *et al.* reported [56] the biological activity of cobalt(III) complexes with tetradentate Schiff bases and different biogenic nitrous bases or an analogous synthetic ligands. Co $(acac_2en)(NH_3)_2]Cl$, and their analogs with different ligands were tested in vivo. Tumor-s response to treatment was estimated by standard methods. It was found all cobalt complexes have been shown to display substantial anticancer, in particular antimetastatic activity.

Ahmed *et al.* [57] have synthesized Co(II), Ni(II), Cu(II), Zn (II), Cd(II), and UO_2 complexes of 5, 5-dimethyl-1, 3-cyclohexanone bis(4-phenylthiosemicarbazone), H_2CPT. These complexes have been characterized by elemental analysis, IR. and reflectance spectral studies, and magnetic moment measurements. IR. spectra show that H_2CPT gives rise to dibasic quadridentate SNNS donor.

Wang Dongmei *et al.* studied [58] about the reaction of metallic copper powder with 2-thenoyltrifluoroacetone and bis (diphenylphosphino) ethane which gave the binuclear copper (I) complex $[Cu (dppe)(tfac)]_2$. The complex has been characterized by physico-chemical and spectroscopic methods. X-Ray structure of the title complex shows that 2-thenoyltrifluoroacetone behaves as chelating ligand and dppe coordinates as bridging ligand to Cu^I atoms in the newly prepared copper complex.

Kozlov *et al.* have reported [59] synthesis of benzo phenanthridine derivatives by condensation of N-Arylmethylene-2-naphthylamines with 5-Phenyl- and 5-(p-Methoxyphenyl)-1,3-cyclohexanediones. Condensation of *N*-arylmethylene-2-naphthylamines with 5-phenyl- and 5-(*p*-methoxyphenyl)-1,3-cyclohexanediones in various solvents gave new hexahydrobenzophenanthridin-4-one derivatives.

Casas *et al.* have studied [60]the crystal and molecular structures of cyclohexanone thiosemicarbazones . It crystallizes in the triclinic crystal system and the following

unit cell parameters: a = 6.2989, b = 7.97, and c = 9.41 A^0 ; α = 79.60 ^{0}, β = 85.519 ^{0} and $\gamma = 73.50^0$.

Agarwal and Sharma synthesized [61] some novel Cu (II) complexes of biologically important hydrazones of isonicotinic acid hydrazide various hydrazones of isonicotinic acid hydrazide (INH) were isolated by condensing isonicotinic acid hydrazide with various aromatic ketones, viz, benzophenone (BPN), cyclohexanone (CHN) or benzylacetone (BzAN). The interaction of these hydrazones with Cu(II) salts in non-aqueous solvent resulted in the coordination complexes with the general composition CuX2 2L (X = Cl, Br, NO3 or CH3COO and L = INH-BPN, INH-CHN or INH-BzAN).These complexes were characterized through elemental analyses, electrical conductance, infrared and electronic spectra.Biological activity of these complexes were also investigated.

Scope of present investigation

Literature survey shows that the study of coordination compounds especially those of Schiff base are highly relevant. Wide range of applications of Schiff base complexes in general and those of semicarbazone, 2-amino phenol, 2-amino thiophenol,cyclohexanone, dimedone etc in particular give us great hope for the future research which may be useful to mankind. The dull period in the history of Schiff base complex in the 1990s has give way to the uprising in the new millennium especially regarding the advanced application in drug designing, as analytical tools and for asymmetric catalysis. Hence the decision to go for synthesis and investigations on Schiff bases and their complexes with new combination of semicarbazone, aminophenol and aminothiophenol, has much relevance. The survey has also revealed that Schiff bases of keto compounds are very rare. So new combination of Schiff bases involving keto compound such as dimedone,

cyclohexanone and pyrolidone with semicarbazide, aminophenol and aminothiophenol were studied. And their complexes of transition d block elements were prepared. For the characterization of ligands and complexes data from elemental analysis by IR, UV, NMR ,magnetic and conductance studies were used. Kinetics of thermal decomposition is studied using the TG.

In application level anti fungal activity of the ligands and representative complexes are tested. The anti fungal activity of the co-ordination compounds on certain fungi like *Phytophthora capsici* which may contribute to development of specific fungicide for the crop protection.

CHAPTER 2

MATERIALS AND METHODS

In this chapter a concise report of the reagents, apparatus used and the methods adopted for the synthesis, characterization of the ligands and complexes are presented. Detailed descriptions are provided in suitable contexts. Materials and methods for antifungal studies are given as a separate chapter in part III.

1) Chemicals:

Analar grade chemicals (BDH, E.Merck, Glaxo) are used for the synthesis. For the preparation of the ligands reagents Dimedone, 2-Aminothiophenol, 2-Aminophenol, Cyclohexanone and Pyrolidone were used. The metal salts used for the synthesis of the complexes are acetates of Mn (II) Co (II), Ni (II), Cu (II), Zn (II) and Cd (II). The solvents used for the synthesis, purification and analysis of ligands and complexes are ethanol, methanol, acetone, diethyl ether, petroleum ether, and dimethyl formamide and dimethyl sulphoxide. Solvents ethanol and methanol are purified by standard methods [62].

2) Synthesis of ligands and complexes

The procedures for the preparation of the ligands and complexes are given in the following chapters.

3) CHN analysis

Carbon, Hydrogen, and Nitrogen content of the ligands and their metal complexes were determined by microanalysis on PERKIN ELMER CHNS/O analyzer

4) Estimation of metals

Standard methods [63,64] like volumetric, gravimetric or pyrolytic techniques were adopted for the estimation of metal content. The atomic absorption spectroscopy is also used for the conformation of the metal percentage in selected samples.

For the volumetric and gravimetric estimations, a common method was used for decomposing the metal complexes. About 0.2 g of the complex was digested with concentrated nitric acid –perchloric acid mixture followed by con. HCl. The resultant solution was then quantitatively made up to 100 ml. By using a definite volume of the solution the metal content of the complex was estimated.

Amount of the copper was determined iodometrically by the addition of KI and subsequent titration of liberated iodine by standard sodiumthiosulphate. Cobalt and cadmium were estimated volumetrically by complexometric titration using standard EDTA solution and xylenol orange indicator. Gravimetrically nickel was estimated by precipitating as dimethyl glyoximate. Zinc and Manganese were estimated by complexometric titration using standard EDTA and eriochrome black T indicator.

Almost all of the metals were estimated by pyrolysis method. About 0.2 g of each complex was weighed out in a silica crucible and heated strongly. During the heating all the organic particles in the chelate was burnt off and the metallic oxide left behind was weighed. From the weight of the oxide metal percentage was calculated.

5) Electrical conductance

Molar conductance measurements of the complexes were carried out in nitrobenzene or DMSO solvent at $25^0C \pm 2^0C$ on a Toshniwal conductivity bridge Approximately $10^{-3}M$ solutions were used for these studies.

6) Magnetic measurements

Magnetic susceptibilities of the complex were determined at room temperature by Gouy method. [65,66] Diamagnetic corrections were applied using Pascal's constants taking into consideration of the magnetic contribution of the various atoms and structural units. Effective magnetic moment was calculated from the corrected molar susceptibility equation.

$$\mu_{eff} = 2.84 \sqrt{(\Psi'_m T)}$$

Ψ'_m=molar susceptibility corrected for diamagnetism and T = absolute temperature. The theoretical magnetic moments were calculated using the formula $\mu_{eff} = g\sqrt{(S(S+1))}$.

7) Infra red spectra

The infra red spectra of the ligands and metal complexes were recorded in the range 4000-400cm^{-1}nm on a Shimadzu –IR 470 infra red spectrophotometer by KBr disc technique .The importance of IR spectroscopy lies in the fact that the characteristic infrared absorption bands of a group occur at about the frequency irrespective of the molecule in which the group is present.

8) Electronic spectra

The UV – Visible spectra of the ligands and complexes were carried on a Shimadzu recording spectrophotometer using DMSO as solvent. For each complex, the peak was assigned to a particular d-d transition. Electronic spectral studies were used to supplement the information obtained from magnetic measurements.

9) Thermo gravimetric analysis

Thermo gravimetric analysis was carried out on a PERKIN ELMER 7 series thermal analyzer in static air atmosphere maintaining the rate of heating at $10^0 Cmin^{-1}$.

10) NMR spectra

NMR spectra of ligands and complexes of selected complexes (Zn (II) and Cd (II) complexes of H_2PAP, H_2PATP , H_2 CAP and H_2CATP) were carried on Brucker DPX 300 MHz machine using DMSO as solvent. In each case the spectra were analyzed by considering the standard chemical shift values

11) 3D sketches and Naming of ligands

For the naming of the ligand molecules and the drawing of 3d structures the 'Chem. Sketch' soft ware by Advanced Chemistry Devolopment Inc is used. For the naming of the

ligands same software with the norms of *Journal of American Chemical* society is used. In the 3D drawing of the complexes, the stereo chemical factors are not considered since the parameters tested was in sufficient to explain the exact stereochemistry of the molecule.

CHAPTER 3

Studies on Mn (II), Co (II), Ni(II),Cu(II),Zn(II) and Cd(II) Complexes of Dimedone bis Semicarbazone (H_2DSC)

During the past few decades, major developments have been achieved in the research of coordination compounds with special emphasis on metal complexes of Schiff bases containing nitrogen and oxygen donors [67-71] . This may be due to their stability, biological activity[71,72]and potential applications in many fields[75, 76]. Biological activity of complexes derived from semicarbazide has been widely studied [71] and contrasted for processes such as, antitumor, antiviral, anti malarial and anti tuberculosis activities. [71,72, 73,74] We have attempted to synthesise a novel ligand dimedone bis semicarbazone and to explore its possibilities as active and potential biological agent. With the aim of further research complexes of semicarbazone of dimedone were synthesized.

Semicarbazone of dimedone can act as a tetradentate dianionic ligand containing the ONNO donor group. Besides two azomethine groups the ligand contains two-carbonyl oxygen, which are enolisable and hence act as potential donor sites. A perusal of literature shows that studies about Schiff base complexes of dimedone are very rare and those of semicarbazide are a few in number [23,30,59,77,78] . But complexes of H_2DSC are not reported so far and hence seeks a special attention.

So it seems to be very essential to synthesize and characterize the complexes of dimedone bis semi carbazone and to conduct detailed investigation about the structure, magnetic properties, thermal stabilities, decomposition patterns and biological activities of these complexes.

A. Experimental

1. Materials and methods

Specifications regarding the reagents used the procedural details adopted for the characterization of the ligand and complexes are given in chapter II.

2. Preparation of ligand - Dimedone bis semicarbazone

A hot ethanolic solution of dimedone (0.01mol) was added drop wise to a stirred solution (0.02 mol) of semicarbazide dissolved in 20ml of water and 20 ml of ethanol. The mixture was refluxed for about 15 minutes and then cooled .The pale yellow precipitate formed was filtered, washed with alcohol and then dried. To obtain dimedone bis semi carbazone a hot saturated solution of it was neutralized with very dilute solution of sodium hydroxide. As the solution was cooled pale yellow crystals of dimedone bis semicarbazone got separated.

3.Synthesis of complexes of Dimedone bis Semicarbazone

The complexes were prepared by adding slowly a hot aqueous solution of the metal acetate to a refluxing ethanolic solution of the ligand containing sodium acetate (0.5gm) until the metal ligand ratio reached 1:1. The reaction mixture was refluxed for one hour and the complexes were precipitated. The complexes were washed with water followed by ethanol and dried over anhydrous Ca Cl_2.

The complexes of Mn (II), Co (II), Ni (II), Cu (II), Zn (II) and Cd (II) were prepared by the above method.

B. Results and discussion

Analytical and physicochemical data obtained, have been correlated in a logical way to explain the properties, structure and bonding in the compounds.

1. Characterization of Ligand

TLC established the purity and homogeneity of the ligand. CHN and IR data given in the Table I.3.1-I.3.2. showed close agreement with empirical formula for dimedone bis semicarbazone. The structure of H_2 DSC is given in figure I.3.1.

2. Formulae and general properties of complexes

All the complexes are colored, stable and non-hygroscopic. The solubility of these complexes in common organic solvents are very low but they are soluble in DMF and DMSO. The values of electrical conductivity of these complexes in DMSO showed that they are non-electrolytic compounds.

The complexes were analyzed for metal, estimated by using atomic absorption spectroscopy and carbon, hydrogen and nitrogen estimated by standard micro analytical methods. The analytical data of the complexes corresponds to the formulae ML $(H_2O)_2$ where M = Mn (II), Co (II), Ni (II), Cu (II), and ML where M = Zn (II) and Cd (II). Results are given in the Tables I.3.1- I.3.3.

3. Magnetic behavior

Magnetic measurements are extremely useful in the structural determination of inorganic coordination compounds [79,80]. Here the magnetic susceptibility of complexes were determined by the Gouy balance. The measurements were made at room temperature. The Gouy balance was standardized using Hg $[Co(NCS)_4]$ as calibrant [81]. Table 1.3.1 shows effective magnetic moment values calculated from the corrected magnetic susceptibility.

When a sample is weighed in the presence and absence of magnetic field a weight change is observed. Diamagnetic materials have no unpaired electrons and show a slight decrease in weight. Paramagnetic materials have unpaired electrons and they show an increase in weight in presence of magnetic field. From this

change in weight the paramagnetic susceptibility and effective magnetic moment can be calculated [79] . The magnetic moment values provide information regarding the number of unpaired electrons present in a molecule and orbitals in which they are situated. Some indications of the structures and geometries of the complexes are also obtained from magnetic moment values. [79]

In the case of Mn (II) complex the electronic d-d- transition from a high spin d^5 configuration must necessarily involve the pairing of some electron spins, such transitions are both spin forbidden and orbitally forbidden, therefore the bands are weak. Octahedral geometry is common among high spin d^5 configuration and spin only magnetic moment in the range 5.9 BM is expected [80]. The H_2DSC complex shows a moment of 5.85 BM indicating d^5 octahedral geometry.

Octahedral and tetrahedral Co (II) complexes differ in their magnetic properties. In high spin octahedral complexes of Co (II), ground term is ^4T_1g which results in considerable orbital contribution. Hence the observed magnetic moment values are in the range ~5.20 BM which is higher than the spin only value for three unpaired electrons. [79,80] The low spin octahedral Co (II) complex has ground state ^2E_g hence no orbital contribution is expected. So the observed values are very close to the spin only values for 1 un paired electron (1.73 BM). In tetrahedral high spin complex of Co (II) the ground term is $^4A_2$ and there is no orbital contribution. The expected magnetic moment is the spin only value for the three unpaired electrons i.e. 3.87 BM.

However observed values are in the range 4.40~4.80 BM. The high value is due to spin orbit coupling perturbations. In the case of four coordinated low spin complexes, which are square planar, it is difficult to predict accurately the magnetic properties. A magnetic moment rather above the spin only value for

unpaired electron 1.73 BM is expected [79,80] The Co (II) complex of H_2DSC shows magnetic moment of 4.89 indicating octahedral geometry, which is further supported by electronic spectral data .

When we are considering the magnetic properties of the complexes of Ni (II), it can be classified in to three categories [79,80]. Six coordinated octahedral complexes with paramagnetic character and ^3A_2g ground term, four coordinated square planar diamagnetic complexes with a spin singlet ground term and the four coordinated approximately tetrahedral paramagnetic complexes with a triplet ground term. Between the two paramagnetic types the octahedral complexes show magnetic moments in the range 2.90-3.30 BM, because no orbital contribution is expected, as the ground term is ^3A_2g. A slightly higher value than the spin only moment is expected for the complexes because of the spin orbit coupling or higher state mixing with ground state .[80]

For tetrahedral complexes the magnetic moment values are in the range of 3.20-4.00BM. The higher value is due to the appreciable orbital contribution of the T ground state. Large distortions and inequalities in the field of coordinated ligands may result in magnetic moments with small orbital contributions and the observed values are as low as 3.20 BM. Square planar complexes have a spin singlet ground state and hence are diamagnetic.

The Ni (II) complex of H_2DSC shows a magnetic moment of 3.1BM, which indicates an octahedral geometry, which is further supported by electronic spectral data.

The Cu (II) complexes usually have a distorted octahedral stereochemistry. A few are known with square planar or approximately tetrahedral geometry. But

stereochemistry has little effect on the magnetic moment of Cu (II) complexes and magnetic moment is about 1.90 BM.

In regular octahedral Cu (II) complexes ground term is ^2Eg and hence no orbital contribution is expected. The spin only magnetic moment value corresponding to one unpaired electron is 1.73 BM, but the observed values fall in the range 1.80-2.10 BM. The slightly higher value is due to the spin orbit coupling. In regular tetrahedral Cu (II) complex the ground term being a triplet state, orbital contribution is expected and theoretically predicted value of magnetic moment is 2.20 BM [82] . But the reported values are in the range 1.95-2 BM [83] .The observed magnetic moment values of Cu (II) complexes of H_2DSC is 1.77BM which indicates octahedral geometry of the Cu (II) complex.

4.IR spectra

Among the different analytical techniques, Infrared spectroscopy is one of the powerful methods for structural analysis. It can be used for the identification and characterization of a compound and assigning structures. The significant vibrational bands and their assignments of the ligand and the complexes are given in the tables. Assignments are made on the basis of comparison with similar known systems [84].

IR spectra of H_2DSC shows band at 1613cm^{-1} and 1671 cm^{-1} which are due to C=N stretching and C=O stretching respectively [84]. The band at 3350 cm^{-1} is probably due NH stretching and that at 3450cm^{-1} is probably due to stretching of NH_2 groups [84] .The IR spectra of the complexes are compared with that of the free ligand to determine the changes that might have taken place during the complexation. The band at 1613 cm^{-1} is the characteristic of the azomethine group present in the free ligand. The lowering in this frequency region (1543 - 1599cm

$^{-1}$), observed in all the complexes, indicates the involvement of the azomethine nitrogen atom in coordination [85,86]. The band at 1671 $cm^{-1}$is characteristic of the C=O in the free ligand. In all the complexes this band disappears and new band appears around 1000cm^{-1} due to γ C-O. This may be due to enolisation and subsequent coordination of this carbonyl group[87].The band at 3350 is assigned to the >NH stretching, this band disappears in all the complexes, supporting enolisation. Ligand shows absorption at the frequency 3450cm^{-1} which may be assigned to the NH_2 stretching [84]. The bands at 521-517 cm^{-1} and 424–418 cm^{-1} are due to the formation of M–N and M–O bonds respectively. [84,88] Presence of a broad band around 3447 cm^{-1} (except in Zn (II), Cd (II) complexes) may be due to the OH stretching of coordinated water. But in some of the complexes this band are not obvious due to the overlapping of some other bands [84,88]. In addition to that a medium band approximately at 944-966 suggests that the water molecules are coordinated . The characteristic frequency of free acetate ion [84,89] at 1560, 1415 are absent in all the complexes. But the non-conducting nature and stoichiometry of this complex indicate that acetate ion is not present in them.

5.Electronic spectra

The electronic spectra of all the complexes of H_2DSC are recorded in DMSO. The important spectral bands of the complexes and their probable assignment are given in the Table.I.3.3. The electronic spectrum depends on energy of metal d orbitals, their degeneracy and the number of electrons distributed. These features in turn are controlled by the oxidation state of the metal, number and kind of the ligand and the geometry of the complex [90].

The majority of Mn (II) complexes have high spin octahedral d^5 configuration. A high spin octahedral field gives spin forbidden as well as parity

forbidden transitions. Hence octahedral Mn(II) complexes are usually pale in color and the absorption are very weak. The tale of CT bands overlap with weak transition thus obscuring them.

In tetrahedral environments the transitions are still spin forbidden but no longer parity forbidden. These transitions are there for about 100 times stronger and complexes have noticeable light yellow green color [91].

In the present investigation Mn (II) complex of H_2DSC shows a number of weak bands which may be assigned to charge transfer or d-d transition in octahedral field.

Octahedral geometries are commonly found in Co (II) complexes and such complexes are pink in color. The expected d-d transitions are [92,93,94]

$$^4T_{1g}(F) \rightarrow {}^4T_{2g}(F) \quad ======= \quad 1250\text{-}1000 \text{ nm}$$

$$^4T_{1g}(F) \rightarrow {}^2E_g(F) \quad ======= \quad 880 \text{ nm}$$

$$^4T_{1g}(F) \rightarrow {}^4A_{2g}(F) \quad ======= \quad 700\text{-}500 \text{ nm}$$

$$^4T_{1g}(F) \rightarrow {}^4T_{1g}(P) \quad ======= \quad 500\text{-}400 \text{ nm}$$

However the visible spectrum will be dominated by the highest energy transition and spectrum is usually complicated by poor resolution of several of these bands. This makes the assignment of this spectrum somewhat difficult. Tetrahedral Co (II) complexes are generally deep blue in color and expected transitions are

$$^4A_2(F) \rightarrow {}^4T_1(F) \quad ======= \quad 1600 \text{ nm}$$

$$^4A_2(F) \rightarrow {}^4T_2(F) \quad ======= \quad 650 \text{ nm}$$

$$^4A_2(F) \rightarrow {}^4T_1(P) \quad ======= \quad 500 \text{ nm}$$ [95]

Both environments give rise to bands in the same region around 500 nm, although tetrahedral complexes more frequently exhibit maxima near 700nm. So the best

spectral indicator of stereochemistry is the intensity especially when the spectrum is complicated by the overlap with a strong charge transfer tail.

For square planar complexes which are generally dark brown in color weak and broad bands are present in the region 1200 – 1000 nm.

In the present investigation Co (II) complex shows absorptions which can be assigned to the d-d transitions of octahedral geometry as given in the Table.I.3.3. Low intensity of bands and purple color support octahedral geometry.

Studies by Jorgensen revealed that in the case of Ni (II) [96] four bands corresponding to the transitions are observed in the given ranges

$^3A_2g\ (F) \rightarrow {}^3T_2g\ (F)$ - 1100 -900 nm

$^3A_2g\ (F) \rightarrow {}^1Eg\ (F)$ -800-750 nm

$^3A_2g\ (F) \rightarrow {}^3T_1g\ (F)$ -650-520 nm

$^3A_2g\ (F) \rightarrow {}^3T_1g\ (P)$ -400-350 nm

The ratio of the wave numbers of the first and third band lies in the range 1.6 –1.8 that is one of the distinguishing characteristics of octahedral Ni (II) complexes. Most of the tetrahedral complexes of Ni (II) have intense blue color due to the presence of an absorption band in the red part of the visible region. The occasional appearance of green or red color in tetrahedral complexes is due to the charge transfer absorption tailing in to the visible region from the ultra violet region. The two readily accessible bands in the spectrum of tetrahedral Ni (II) complexes are

$^3T_1\ (F) \rightarrow {}^3A_2\ (F)$ 1250-1500 nm

$^3T_1\ (F) \rightarrow {}^3T_1\ (P)$ 700-600 nm

$^3T_2\ (F) \rightarrow {}^3T_1(F)$ 3300-2000 nm

The third band is usually over lapped by absorption of organic part in the molecule or the solvent

The square planar complexes of Ni (II) [96] are generally red yellow or brown and this may be due to the presence of absorption bands of medium intensities. However other colors do occur when additional bands are present. [97] The different bands and the assignments are the following [97,98,99]

$^1A_1g \rightarrow {}^1B_1g$ - 600-570 nm

$^1A_1g \rightarrow {}^1A_2g$ ~ 480 nm

$^1A_1g \rightarrow {}^1Eg$ ~ 400 nm

CT bands usually overlap the second and third bands

In the present investigation Ni (II) complex of H_2DSC shows three absorption bands which are assigned as given in the Table I.3.3 and obtained data support the octahedral geometry. The ratio of wave numbers of transitions

$^3A_2g(F) \rightarrow {}^3T_2g(F)$ - 929

$^3A_2g(F) \rightarrow {}^3T_1g(F)$ -512 is in the range 1.6 to 1.8 which confirms the octahedral geometry.

For octahedral Cu (II) complexes only a single band due to the transition ^2Eg- $^2T_{2g}$ would result but the observed band is very broad and clearly contain several components which is a result of tetragonal distortions due to Jhan -Teller effect [90] . In tetrahedral Cu (II) complexes d-d transition occur in the range 1400-1000 .In square planar and octahedral complexes band appears in the region 1000-500 . If this region is blank then it can be inferred that the complexes are tetrahedral in nature. It can also be inferred that the complexes have tetrahedral geometry if the energies of the bands are low compared to those of square planar or tetragonal complexes. A greenish blue color is associated with penta or hexa coordinated Cu (II) and brown and violet color indicate 4 coordinate Cu (II) [100,101].

In the case of the Cu (II) H_2DSC complex an absorption band present 674 nm is assigned to the d-d transition in octahedral complexes.

6.Conclusion

The complex compounds of Mn (II), Co (II), Ni (II), Cu (II) , Zn(II) and Cd(II) with dimedone bis semicarbazone are synthesized . The physico chemical properties of all the complexes were studied . The complexes have the general formula [M (L)$(H_2O)_2$] where M= Mn (II) Co (II) Ni (II) Cu(II), and L is tetra dentate di anion obtained from $H_2DSC(H_2L)$. The other complexes are assigned the formula [ML] where L is the tetra dentate di anionic ligand obtained from H_2DSC [H_2L] and M=Zn (II) or Cd (II) .

In all metal complexes the carbonyl group is enolised and ionizes and then coordinated to the metal ion. The IR data, conductance values and stochiometry of the compound strongly prove this assumption. The data obtained are insufficient to prescribe the exact geometry of Zn (II) and Cd (II). However in comparison with structure of other complexes and considering common coordination numbers exhibited by these metal ions, a four coordinated tetrahedral geometry may be assigned to them .

7.Structure of Ligand and complexes

By considering the analytical data the structure of the ligand Dimedone bis semicarbazone and its Mn (II),Co (II), Ni (II),Cu(II),Zn (II) and Cd (II) are drawn . The proposed structure is given in Fig I.3.2 and I.3.3.

Ligand

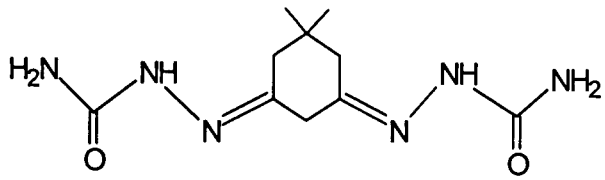

H_2DSC

Figure I. 3. 1

Octahedral Complexes

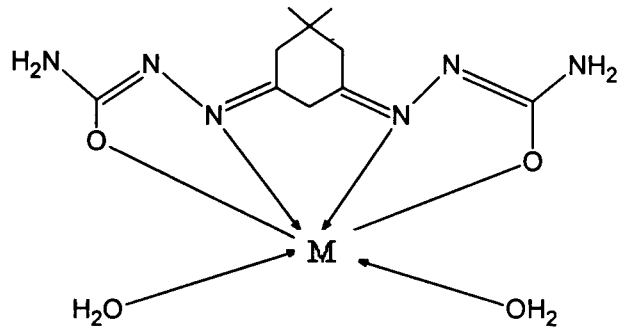

Complexes of H_2DSC where M = Mn(II)Co(II),Ni(II),Cu(II)

Figure I.3.2

Tetrahedral Complexes

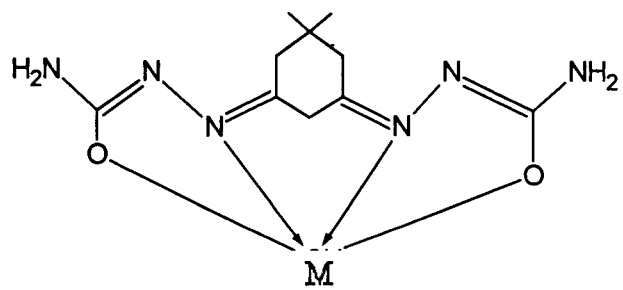

Complexes of H_2 DSC where M = Zn(II)Cd(II).

Figure I.3.3

Table I.3.1

Micro analytical, magnetic and Conductance data of transition metal chelates of Dimedone bis semicarbazone (H_2DSC)

Complexes

Compound	Molecular formula	Conductance $Ohm^{-1}cm^2mol$	$\mu_{effective}$ (BM)	Found (calculated)%			
				Metal	C	H	N
H_2DSC(LIGAND)	$C_{10}H_{18}O_2N_6$				46.7 (47.2)	7.8 (7.1)	32.3 (33.1)
$[MnL(H_2O)_2]$	$[MnC_{10}H_{16}O_2N_6(H_2O)_2]$	43	5.85	16.01 (16.02)	34.1 (34.99)	5.77 (5.83)	24.00 (24.49)
$[CoL(H_2O)_2]$	$[Co_{10}H_{16}O_2N_6(H_2O)_2]$	23	4.89	17.02 (16.97)	34.01 (34.59)	5.18 (5.76)	23.2 (24.21)
$[NiL(H_2O)_2]$	$[NiC_{10}H_{16}O_2N_6(H_2O)_2]$	34	3.1	16.5 (16.93)	34.6 (34.61)	5.3 (5.76)	23.9 (24.22)
$[CuL(H_2O)_2]$	$[CuC_{10}H_{16}O_2N_6(H_2O)_2]$	16	1.77	18.04 (18.07)	33.2 (34.13)	5.12 (5.68)	23.1 (23.89)
[ZnL]	$[ZnC_{10}H_{16}O_2N_6]$	23	D	21.00 (20.58)	36.3 (37.8)	5.01 (5.04)	25.9 (26.47)
[CdL]	$[CdC_{10}H_{16}O_2N_6]$	14	D	29.06 (30.84)	32.88 (32.93)	4.27 (4.39)	24.56 (23.05)

D= diamagnetic

Table I.3.2.
Characteristic Infrared absorption frequencies (cm^{-1})of transition metal chelates of H_2DSC

Compounds	υ (H_2O)	υ-(C=O)	υ(>C=N-)	γ(OH) (H_2O)	υM-N	υM-O
Ligand (H_2DSC)	---	1671m	1613.s	----	----	----
$[MnL(H_2O)_2]$	3436 m	989m	1597s	944w	520w	413m
$[CoL(H_2O)_2]$	3451br	979m	1599s	952w	517w	418w
$[CuL(H_2O)_2]$	3412br	988m	1543s	966w	517.8w	418m
$[NiL(H_2O)_2]$	3410br	964m	1578s	945w	521w	424m
[ZnL]	----	976m	1585s	----	517m	418m
[CdL]	----	934m	1543s	----	517m	418m

Strong = s, Medium= m, Weak=w broad =br

Table I.3.3

Characteristic ultraviolet frequencies

and

probable assignment of transition

with geometry of H_2DSC complexes

Complex	Band(nm)	Assignment	Geometry
[Mn L $(H_2O)_2$]	412	CT	Octahedral
[Co L$(H_2O)_2$]	1075 666	$^4T_{1g}(F) \rightarrow {}^4T_{2g}(F)$ $^4T_{1g}(F) \rightarrow {}^4A_{2g}(F)$	Octahedral
[Ni L$(H_2O)_2$]	929 512	$^3A_2g(F) \rightarrow {}^3T_2g(F)$ $^3A_2g(F) \rightarrow {}^3T_1g(F)$	Octahedral
[CuL$(H_2O)_2$]	674	$^2Eg \rightarrow {}^2T_2g$	Distorted octahedral
[ZnL]	395	CT	Tetrahedral
[CdL]	323	CT	Tetrahedral

3D Sketches

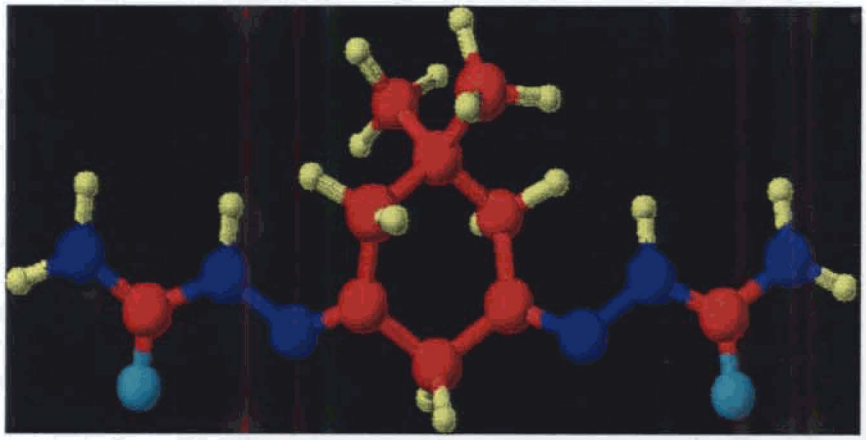

5,5-Dimethylcyclohexane-1,3-Dione Disemicarbazone (H_2DSC)

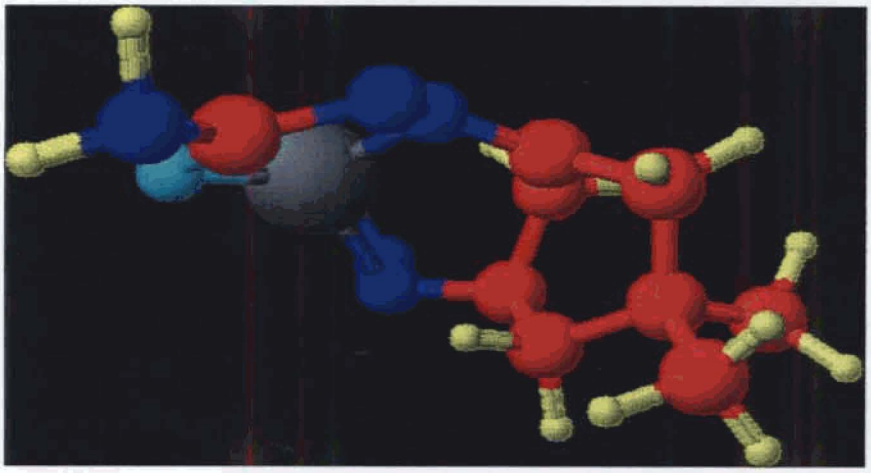

TETRAHEDRAL COMPLEXES OF H_2DSC

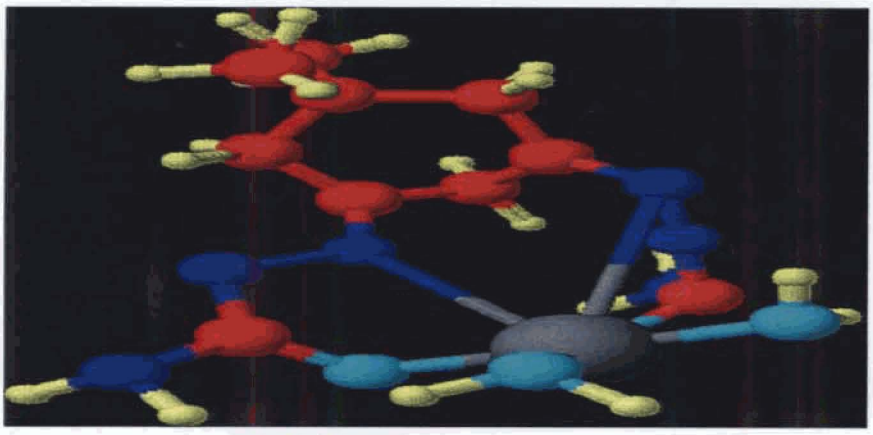

OCTAHEDRAL COMPLEXES OF H_2DSC

Yellow = Hydrogen; Red = Carbon; blue= Nitrogen; Cyan= oxygen/ sulphur
Gray = metal

The 3D structures and naming ligand are based the on the drawings of ACD soft ware which follows on *Journal of American Chemical Society* and the stereochemistry of the molecules is only an approximation

CHAPTER 4

Studies on Mn (II), Co (II), Ni (II),Cu(II),Zn(II) and Cd(II) Complexes of Dimedone bis-2-Aminothiophenol (H_2DATP) and Dimedone bis -2 Aminophenol (H_2DAP)

Two Ligands dimedone bis-2-aminothiophenol (H_2DATP) and dimedone bis -2-aminophenol (H_2DAP) have been synthesized for the first time. These two novel ligands form various complexes with different transition metal ions. Both ligands are found to be tetradentate. Schiff base complexes of aminophenol [50-,54] and aminothiophenol [47-49 ,102] are widely studied. Literature survey reveals that not much work has been done on the Schiff bases derived from 5,5 dimethyl 1,3 cyclohexanedione (dimedone), and dimedone bis-2-aminothiophenol (H_2DATP), and dimedone bis -2-aminophenol (H_2DAP) are the ligands reported for the first time.

In this chapter detailed investigation of the ligands H_2DAP and H_2DATP were made with a special attention on structure, magnetic property, thermal stabilities, decomposition patterns and biological activities of these complexes derived from them.. Here H_2DAP can act as a tetra dentate dianionic ligand containing the ONNO donor group while H_2DATP can act as a tetra dentate dianionic ligand containing the SNNS donor group.

A. Experimental

1. Materials and methods

Specifications regarding the reagents used and the procedural details adopted for the characterization of the ligand and complexes are given in chapter 2

2.Preparations of ligands H_2DAP and H_2DATP

A hot ethanolic solution of dimedone (0.01mol) was added drop wise to a stirred solution contaning.02 mol of 2 aminophenol dissolved in ethanol. The mixture was refluxed for about 20 minutes and then cooled. The pale yellow precipitate formed was filtered, washed with alcohol then dried. Melting point 141^0C.To obtain H_2DATP the same procedure adopted for H_2DAP is used. Melting point 130^0C .

3. Synthesis of complexes of H_2DAP and H_2DATP

The complexes were prepared by adding slowly a hot aqueous solution of the metal acetate to a refluxing ethanolic solution of the ligand until the metal ligand ratio reached 1:1.The reaction mixture was refluxed for 45 minutes and the complexes precipitated were separated. It was washed with water followed by ethanol and dried over anhydrous Ca Cl_2. Complexes of Mn (II), Co (II), Ni(II), Cu(II), Zn(II)and Cd(II) were prepared by the above method .

B.Results and discussion

The complexes were characterized on the basis of elemental analysis, UV and IR spectral data, magnetic studies, conductance measurements and the thermal data

1. Characterization of Ligand

TLC established the purity and homogeneity of ligand. CHN, and IR data given in the Table I.4.1-I.4.5 showed close agreement with empirical formula for H_2DAP and H_2DATP .

2. Formula and general properties of complexes

All the complexes are colored, photo stable and non-hygroscopic. The solubility of these complexes in common organic solvents are very low but they

are soluble in DMF and DMSO. The values of electrical conductivity of these complexes in DMSO show that they are non-electrolytic compounds.

The complexes were analyzed for metal estimation by using atomic absorption spectroscopy and carbon hydrogen and nitrogen estimated by standard micro analytic methods. The analytical data of the complexes corresponds to the formulae ML (H_2O) where M= Mn (II), Co (II), Ni (II), Cu (II) and ML where M= Zn (II) and Cd (II) Results are given in the Table I.4.1, -I.4.6.

3. Magnetic behavior

The details of the methods for theoretical prediction by magnetic behavior of complexes are already explained in the chapter III. The observed magnetic moment values are summarized in Table I.4.1 and I.4.4. The Mn (II) complexes are showing magnetic moment values 5.91 and 5.97BM (H_2DAP,H_2DATP) indicating octahedral geometry [80] with high spin d^5 configuration.

The observed magnetic moments for the spin free octahedral Co (II) ($^4T_{1g}$) is higher than spin only values and it may be due to orbital contribution of both the ground state ($t_{2g}^5e_g^2$) and the first excited state ($t_{2g}^4e_g^3$). It is reported that the octahedral high spin geometry can be assigned to Co(II) complexes, if the observed magnetic moment values are in the range of 4.7 -5.2 BM [80]. The cobalt (II) complexes of H_2DAP and H_2DATP possess magnetic moment values of 4.9 and 4.8 BM that proves the octahedral geometry. The H_2DAP and H_2DATP complexes of Ni (II) have magnetic moment value of 3. 1 BM and 3.01 BM which is very close to the spin only value of octahedral geometry[80]. The magnetic moment of Cu (II) complexes of H_2DAP and H_2DATP possess normal values 1.97BM and 2.1 B.M as expected for octahedral geometry[80, 103]. The Zn(II) and Cd (II) complexes are found to be diamagnetic.

4. IR spectra

H_2DATP shows bands at 1610 cm^{-1} and 2650 cm^{-1} which are due to C=N stretching and S-H stretching[104] respectively. The band at 701 cm^{-1} is probably due C- S stretching [104].The IR spectra of the complexes are compared with that of the free ligand to determine the changes that might have taken place during the complexation. The band at 1610 $cm^{-1}$is characteristic of the azomethine group present in the free ligand. The lowering of this frequency to the region (1582 - 1589cm^{-1}), observed in all the complexes, indicates the involvement of the azomethine nitrogen atom in coordination [85,86] The stretching vibrations of (SH) have no apparent help since they display very weak bands in both the free and in the complexes however, the participation of SH group in chelation is ascertained from the shift of γ C-S from frequency from 701 cm^{-1}. [51,104] The bands ranging from 418 to 450 cm^{-1} are due to the presence of M–N bonds [84,88]. Presence of a broad band around 3447 cm^{-1} in the case of Ni (II), Co (II),Mn(II) and Cu(II) may be due to the OH stretching of coordinated water The presence of OH bending frequency at 931 to 937 cm^{-1} [104,51] further confirms the presence of coordinated water. The characteristic frequency of free acetate ion at 1560 and 1415 cm^{-1} are absent in all the complexes. [84,89] The non conducting nature and stoichiometry of this complex indicate that acetate ion is not present

In IR spectra of H_2DAP bands at 1605 cm^{-1} and 3450 cm^{-1} are due to C=N stretching and O-H stretching respectively [84]. The band at 1240 cm^{-1} is probably due to C- O [84]. The IR spectra of the complexes are compared with that of the free ligand to resolve the changes that might have taken place during the complexation. The band at 1605 $cm^{-1}$is characteristic of the azomethine group present in the free ligand. The lowering in this frequency region (1588- 1560cm –1), observed in all the

complexes, indicates the involvement of the azomethine nitrogen atom in coordination [85,86]. The band at 1240cm^{-1} is characteristic of the C-O in the free ligand [51]. The shifting of this band to lower frequency region, observed in all the complexes, indicates O-H group ionized and coordinated. The bands at 627-608 cm $^{-1}$ and 418-447cm $^{-1}$ are due to the formation of M–N and M–O bonds respectively [84,88]. The presence of water in the above mentioned complexes is confirmed by the presence of weak band in the 931- 937 range which may be attributed [51] to bending vibration of water molecules in Mn (II), Co (II),Ni (II) and Cu (II) complexes. The other bending vibrations usually found at 1600cm^{-1} which usually interferes with the skeleton vibration of benzene ring. The non-conducting nature and stochiometry of these complexes indicate that acetate is not present.

5. Electronic spectra

The electronic spectra of all the complexes of H_2DAP and H_2DATP are recorded in DMSO. The important spectral bands of the complexes and their probable assignments are given in the Tables I.4.3 and I.4.6.

In the present investigation Mn (II) complexes of H_2DAP and H_2DATP show bands which corresponds to octahedral geometry [91]. The magnetic and other data also support octahedral geometry. In the present investigation Co(II) complex of H_2DAP shows absorptions at 560nm which can be assigned ($^4T_{1g}$ (F) $\rightarrow$ $^4A_{2g}$ (F)) in H_2DAP and 473nm and 545nm in H_2DATP ($^4T_1g(F) \rightarrow {}^4T_2g(P)$), ($^4T_1g$ (F)$\rightarrow$ $^4A_2g(F)$) the transitions of octahedral geometry. Low intensity of bands and purple color supports octahedral geometry color and other data also supports this observation [91].

In the Ni (II) complex of H_2DATP, absorption bands at 561and 972 nm and H_2DAP complex bands at 564nm and 978 nm are assigned as given in the Table I.

4.3 and I.4.6 . These data supports the octahedral geometry [96]. In the case of copper (II) complexes of H_2DATP and H_2DAP absorption bands present at 678nm and 690nm respectively are assigned [100,101] to the d-d transition in octahedral geometry.

6. Conclusion

The complexes of Mn(II) Co(II)), Ni(II) Cu(II) Zn(II) and Cd(II) with H_2DAP and H_2DATP are synthesized (H_2L) .The physico chemical properties of all the complexes were studied . The octahedral complexes have the general formula [M (L) $(H_2O)_2$] where M= Mn (II) Co (II)), Ni (II) Cu (II) and L is tetra dentate dianion obtained from H_2DAP and H_2DATP) . The other tetrahedral complexes are assigned the formula [ML] where L is the tetra dentate dianionic ligand obtained from H_2DAP and H_2DATP where M= Cd (II). Zn (II) The IR data, conductance values and stoichiometry of the compound strongly proves this assumption .

7.Structure of ligands and complexes

By considering the analytical data the structure of the ligand H_2DAP and H_2DATP and its Mn (II),Co(II), Ni(II),Cu(II),Zn(II) and Cd(II) complexes are drawn . The proposed structure is given in Figures I.4.1-I.4.6.

Ligand- H_2DAP

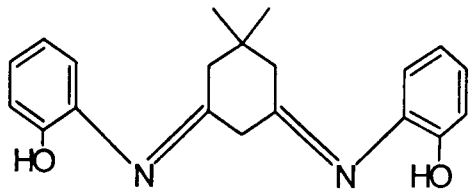

Figure I.4.1.

Octahedral Complexes

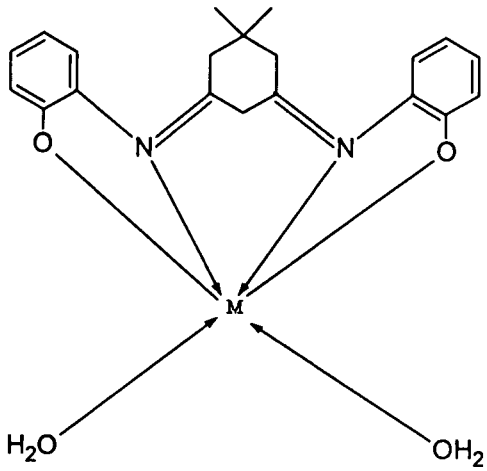

Figure I.4.2.
Complexes of H_2DAP where M = Mn (II),Co,(II),Ni(II) and Cu(II).

Tetrahedral complexes

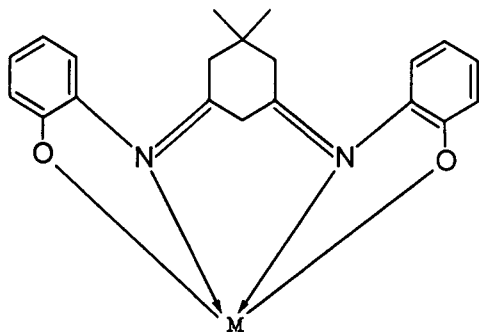

Figure I.4.3.
Complexes of H_2 DAP where M = Zn(II),Cd(II)

Ligand –H_2DATP

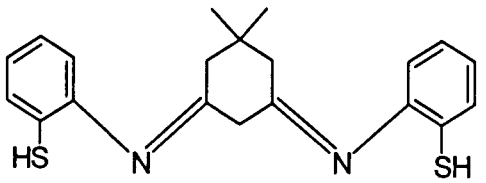

Figure I.4.4.

Octahedral complexes.

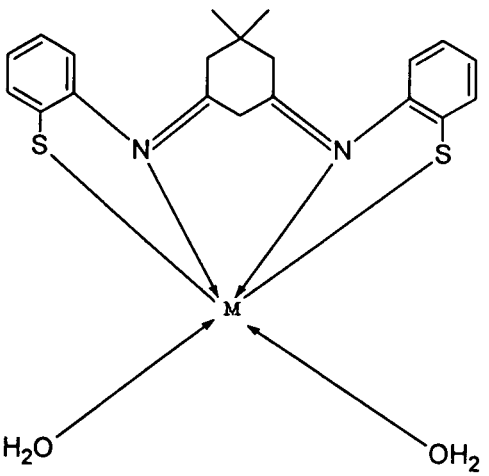

Figure I.4.5.
Complexes of H_2DATP where M = Mn (II),Co,(II),Ni(II) and Cu(II).

Tetrahedral complexes.

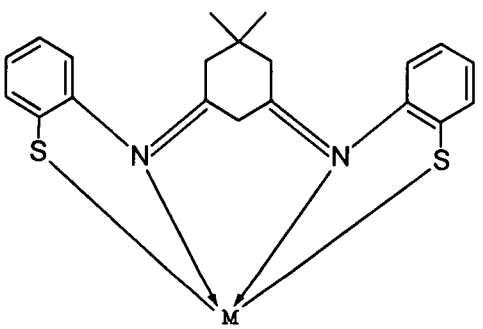

Figure I.4.6.
Complexes of H_2DATP where M = Zn (II), Cd(II)

Table I.4.1.

Micro analytical, magnetic and Conductance data of transition metal chelates of Dimedone bis –2-amino phenol (H_2DAP)
Complexes

Compounds	Molecular formula	Conductance $Ohm^{-1}cm^2mol$	μ_{eff} BM	found (calculated) %			
				Metal	C	H	N
H_2DAP(Ligand)	$C_{20}H_{22}O_2N_2$				73.6 (74.5)	6.6 (6.83)	8.1 (8.69)
$[MnL(H_2O)_2]$	$MnC_{20}H_{24}O_4N_2$	22	5.91	13.32 (13.36)	58.2 (58.40)	5.76 (5.84)	6.88 (6.81)
$[CoL(H_2O)_2]$	$CoC_{20}H_{24}O_4N_2$	23	4.9	14.2 (14.19)	57.6 (57.84)	5.5 (5.78)	5.98 (6.74)
$[NiL(H_2O)_2]$	$NiC_{20}H_{24}O_4N_2$	22	3.1	14.5 (14.15)	56.98 (57.87)	5.77 (5.78)	6.66 (6.75)
$(CuL(H_2O)_2]$	$CuC_{20}H_{24}O_4N_2$	32	1.97	16.2 (15.14)	57.1 (57.20)	5.01 (5.72)	6.01 (6.67)
[ZnL]	Zn $C_{20}H_{20}O_2N_2$	12	D	15.98 (16.96)	62.1 (62.27)	4.97 (5.1)	7.25 (7.26)
[CdL]	Cd $C_{20}H_{20}O_2N_2$	16	D	24.8 (25.99)	55.4 (55.50)	3.92 (4.62)	6.40 (6.47)

Table.I. 4.2.

Characteristic Infrared absorption frequencies (cm^{-1})of transition metal chelates of H_2DAP

Compounds	υ (>C=N-)	υ (-C-O)	γ(-OH)	υ (M-N)	υ (M-O)
Ligand H_2DAP	1605s	1240m	---	-----	-----
$[MnL(H_2O)_2]$	1573m	1204m	937w	615w	447w
$[CoL(H_2O)_2]$	1588m	1194m	932m	609w	415w
$[NiL(H_2O)_2]$	1580s	1232m	931w	627w	418w
$[CuL(H_2O)_2]$	1582s	1232m	933w	627m	418w
[ZnL]	1560s	1234m	----	621m	418m
[CdL]	1560s	1196w	----	608m	415m

Strong = s, Medium= m, Weak=w broad =br

Table. I. 4.3.
Characteristic ultraviolet frequencies
and
probable assignment of transition
with geometry of H_2DAP complexes

Complexes	Band	Assignment	Geometry
$[MnL(H_2O)_2]$	406	CT	Octahedral
$[CoL(H_2O)_2]$	560	$^4T_1g\ (F) \rightarrow {}^4A_2g(F)$	Octahedral
$[NiL(H_2O)_2]$	564 978	$^3A_2g\ (F) \rightarrow {}^3T_1g(F)$ $^3A_2g\ (F) \rightarrow {}^3T_2g(F)$	Octahedral
$[CuL(H_2O)_2]$	690	$^2Eg \rightarrow {}^2T_2g$	Octahedral
[ZnL)	420	CT	Tetrahedral
[CdL]	439	CT	Tetrahedral

Table. I. 4.4.

Micro analytical, of transition metal chelates of Dimedone bis aminothiophenol (H_2DATP) Complexes

Compounds	Molecular formula	Conductance $Ohm^{-1}cm^2mol$	μ eff BM	Found (calculated)%			
				Metal	C	H	N
H_2DATP (Ligand)	$C_{20}H_{22}S_2N_2$	----	---	----	67.6 (67.8)	6.00 (6.21)	7.1 (7.91)
$[MnL(H_2O)_2]$	$MnC_{20}H_{24}S_2N_2O_2$	22	5.97	12.0 (12.40)	54.0 (54.18)	5.9 (5.42)	6.3 (6.32)
$[CoL(H_2O)_2]$	$CoC_{20}H_{24}S_2N_2O_2$	13	4.8	13.2 (13.17)	54.9 (53.70)	5.40 (5.37)	6.22 (6.26)
$[NiL(H_2O)_2]$	$NiC_{20}H_{24}S_2N_2O_2$	12	3.01	12.2 (13.14)	53.5 (53.72)	5.32 (5.37)	6.22 (6.26)
$[CuL(H_2O)_2]$	$CuC_{20}H_{24}S_2N_2O_2$	11	2.1	13.22 (14.07)	52.1 (53.15)	4.99 (5.31)	6.22 (6.20)
[ZnL]	Zn $C_{20}H_{20}S_2N_2$	8	D	14.9 (15.66)	56.9 (57.50)	4.48 (4.79)	6.1 (6.70)
[CdL]	Cd $C_{20}H_{20}S_2N_2$	6	D	23.6 (24.20)	51.2 (51.67)	4.1 (4.31)	5.9 (6.02)

D= diamagnetic

Table.I. 4.5.
Characteristic Infrared absorption frequencies (cm^{-1}) of transition metal chelates of H_2DATP

Compounds	υ (>C=N-)	υ (-C-S)	γ .(-OH)	υ (M-N)
Ligand H_2DATP	1610s	701m	----	----
$[MnL(H_2O)_2]$	1583s	690m	933m	418w
$[CoL(H_2O)_2]$	1584s	689m	935m	420m
$[NiL(H_2O)_2]$	1589s	686m	931m	418m
$[CuL(H_2O)_2]$	1583s	694w	930m	418s
[ZnL]	1582m	675w	937s	450w
[CdL]	1589s	675w	932m	436w

Strong = s, Medium= m, Weak=w broad =br

Table. I. 4. 6.
Characteristic ultraviolet frequencies
And probable assignment of transition
with geometry of H_2DATP complexes

Complexes	Band nm	Assignment	Geometry
[Mn L $(H_2O)_2$]	389	CT	Octahedral
[Co L $(H_2O)_2$]	473 545	$^4T_{1g}$ (F) → $^4T_{1g}$ (P) ^4T_1g(F) → $^4A_{2g}$ (F)	Octahedral
[Ni L $(H_2O)_2$]	561 972	^3A_2g(F)→^3T_1g(F) ^3A_2g(F)→^3T_2g(F)	Octahedral
[Cu L$(H_2O)_2$]	678	^{2}Eg→^2T_2g	Octahedral
[ZnL]	420	CT	Tetrahedral
[CdL]	529 432	CT	Tetrahedral

3D sketches

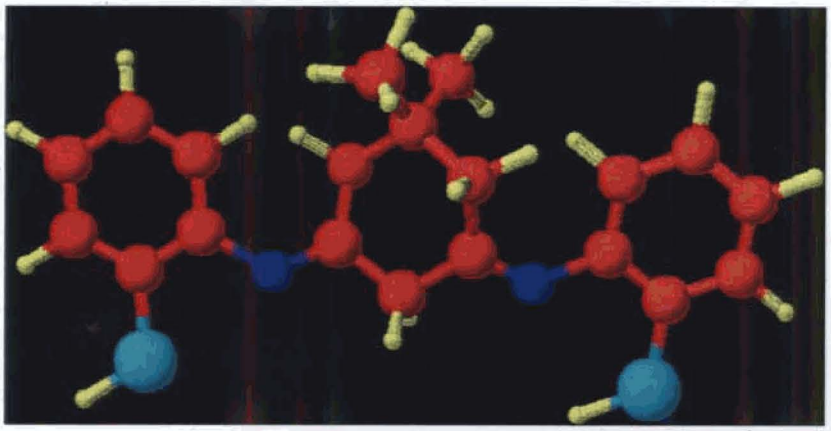

2,2'-[(5,5-Dimethylcyclohexane-1,3-Diylidene)Dinitrilo]Dibenzenethiol H_2DATP

2,2'-[(5,5-Dimethylcyclohexane-1,3-Diylidene)Dinitrilo]Diphenol H_2DAP

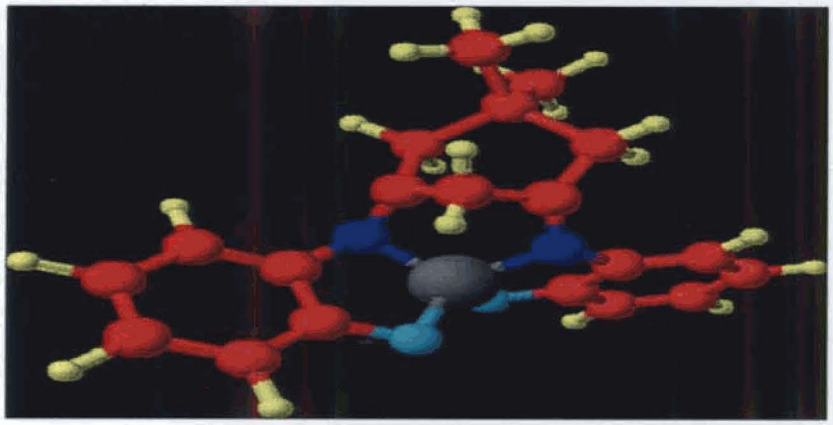

TETRAHEDRAL COMPLEXES OF H_2DAP/H_2DATP

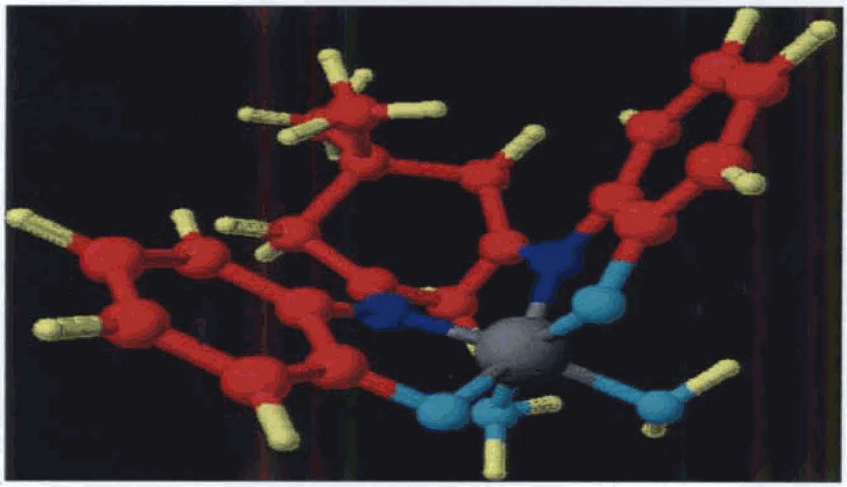

OCTAHEDRAL COMPLEXES OF H_2DAP/H_2DATP

Yellow = Hydrogen; Red = Carbon; blue= Nitrogen; Cyan= oxygen/ sulphur
Gray = metal

The 3D structures and naming ligand are based the on the drawings of ACD soft ware Which follows the norms of Journal of American Chemical Society. The Stereochemistry of the molecules is only an approximation

CHAPTER 5

Studies on Mn(II),Co(II),Ni(II),Cu(II),Zn(II) and Cd(II) Complexes of Cyclohexanone-2- Amino phenol(HCAP) and Cyclohexanone-2- Aminothiophenol (HCATP)

The properties and reactivity of cyclic ketones attract a keen attention to several chemists. Numerous of their derivatives are biologically active compounds, some of which have found practical application. For example diketone derivatives are used in the synthesis of prostaglandins, antibiotics, and alkaloids. In addition, cyclic β-diketones are convenient model compounds for studying the effect of cyclic structure on the properties of the methylene and carbonyl groups and tautomeric equilibria [105-107]. The present study describes the synthesis of new bidentate Schiff base ligands developed from the cyclic ketone. Cyclohexanone-2-aminophenol(HCAP) and Cyclohexanone-2- aminothiophenol (HCATP) have been synthesized for the first time. These ligands produce various complexes with different transition metal ions. Literature survey reveals that no work has been done on the Schiff base complexes derived from the ligands HCAP and HCATP.

Here HCAP can act as bi dentate anionic ligand containing the potential donor group ON while HCATP can also act as a bi dentate anionic ligand containing the SN donor group. It is highly scopefull to synthesize and characterize the complexes of HCAP and HCATP and to conduct detailed investigation about the structure, magnetic property, thermal stabilities, decomposition patterns and biological activities of these complexes.

A . Experimental

1 . Materials and methods

Detailed procedure and specification of reagents, which are useful for the characterization and purification of ligands are explained in chapter II.

2. Preparations of ligands

A hot ethanolic solution of cyclohexanone (0.01mole) was added drop wise to a stirred solution of 2- aminophenol (.01mole) dissolved in ethanol. The mixture was refluxed for about nearly 1 hour and then cooled. The pale pink precipitate formed was filtered , washed with alcohol then dried. Melting point is 121° C. To obtain HCATP the same procedure adopted for HCAP is used . Melting point is 134° C.

3. Synthesis of complexes

The complexes were prepared by adding slowly a hot aqueous solution of the metal acetate to a refluxing ethanolic solution containing the ligand until the metal ligand ratio reached 1:2 .The reaction mixture was refluxed for 30` minutes and the complexes precipitated were separated. It was washed with water followed by ethanol, and dried over anhydrous Ca Cl_2.

B. Results and discussions

UV and IR ,NMR spectral data, magnetic studies, conductance measurements and the thermal data are used for the characterization of the ligands and the complexes.

1.Characterization of ligands

TLC, CHN and IR data are used for establishing purity and homogeneity of ligands.

2. Formula and general properties of complexes

All complexes are colored hygroscopic and stable they are soluble in DMSO. They are non-conducting in DMSO. The complexes were analyzed for metal by using atomic absorption spectroscopy and carbon , hydrogen and nitrogen estimated by standard micro analytic methods. The analytical data of the complexes corresponds to the formulae $ML_2(H_2O)_2$ where M= Mn (II), Co (II), Ni (II), Cu (II), and ML_2 where M=Zn (II) and Cd (II). Results are given the Table I.5.1- I.5.6.

3. Magnetic behavior

Summary of the magnetic moments of the different metal complexes of HCAP and HCATP are given in the Table. I.5.1 and I.5.4. In the case of Mn (II) complexes of HCAP and HCATP the magnetic moment values are about 6.02 and 5.98 which show an octahedral geometry [19] . The cobalt (II) complexes possess magnetic moment values of 5.19 and 5.06 BM as expected[18,19] for octahedral geometry. The complexes of Ni have magnetic moment value 3.1 BM for HCAP and 3.2 BM for HCATP which are in accordance[18,19] with octahedral complexes. The magnetic moment values of Cu (II) are 2.0 BM and 1.86 B.M as expected[21] for octahedral geometry. The reference and the method for theoretical prediction are already explained in the chapter III .The Zn(II) and Cd(II) complexes are found to be diamagnetic

4. IR spectra

The ligand HCATP shows bands at 1579 cm^{-1} and 2655 cm^{-1} which are due to C=N stretching and S-H stretching[104] respectively. The band at 698 cm^{-1} is probably due to C-S streching[104] . The IR spectra of the complexes are compared with that of the free ligand to assign the changes that might have taken

place during the complexation. The band at 1579 cm^{-1} is characteristic of the azomethine nitrogen atom present in the free ligand. The lowering of bands to the frequency region (1572 – 1560 cm^{-1}), observed in all the complexes, indicates the involvement of the azomethine nitrogen atom in coordination [85,86] . The band at 698$cm^{-1}$is characteristic of the C-S in the free ligand. The shifting of this frequency region, observed in all the complexes, indicates that S-H group is ionized and co-coordinated[51,104]. The bands at 418 cm^{-1} -436 cm^{-1} are due to the formation of M–N bonds. In the case of complexes of Mn(II) ,Ni(II) ,Co(II) and Cu (II) the presence of OH frequency at 922 cm^{-1} - 936 cm^{-1} further confirms [51,104] the presence of coordinated water. The characteristic frequency of free acetate ion at 1560 cm^{-1} and 1415 cm^{-1} are absent in all the complexes but the non-conducting nature and stoichiometry of this complex indicate that acetate ion is not present.

IR spectra HCAP shows bands at 1605 cm^{-1} and 3450 cm^{-1} which are due to C=N stretching and O-H stretching respectively. The band at 1226 cm^{-1} is probably due to C-O stretching. The IR spectra of the complexes are compared with that of the free ligand to determine the changes that might have taken place during the complexation. The band at 1605 cm^{-1} is characteristic of the azomethine nitrogen atom present in the free ligand. The lowering of this band to the region (1599 - 1565cm^{-1}), observed in all the complexes, indicates the involvement of the azomethine nitrogen atom in coordination [85,86] . The band at 1226$cm^{-1}$is characteristic of the C-O in the free ligand. The shifting of this frequency region, observed in all the complexes, indicates O-H group is ionized and coordinated. The bands at 523-506 cm^{-1} and 432- cm^{-1} – 418cm^{-1} which are due to the formation of M–N and M–O bonds respectively.[84,88] In the case of Co

(II), Mn(II),Ni (II),Cu (II) the presence of OH frequency at 931 cm^{-1} -935 cm^{-1} further confirms [51,104] the presence of coordinated water. The non-conducting nature and stochiometry of this complex indicate that acetate ion is not present.

5) Electronic spectra

The electronic spectra of all the complexes of HCAP and HCATP are recorded in DMSO The important spectral bands of the complexes and their probable assignments are given in the Table, I.5.3, I.5.6.

In the present investigation Mn (II) complex of HCAP and HCATP shows weak bands at 401 nm, 420 nm may be due to charge transfer spectra. Pale pink color also proves the existence of octahedral geometry [91].

Co(II) complex of HCATP shows absorptions which can be assigned to the $^4T_{1g}(F) \rightarrow {}^4A_{2g}(F)$ transition of octahedral geometry as given in the Table . Low intensity of bands supports octahedral geometry.

HCAP complexes of Co (II) shows absorptions which can be assigned to $^4T_1g(F) \rightarrow {}^4A_{2g}(F)$, $^4T_1g(F) \rightarrow {}^4T_2g(F)$ transitions of octahedral geometry low intensity of bands supports octahedral geometry.

Ni (II) complex of HCAP shows bands at 634 nm and 1010nm ,that of HCATP shows bands at 1152nm and 548nm which are assigned to octahedral stereochemistry [96] as given in the Table.

Cu (II) complexes of HCAP and HCATP show absorption bands at 576nm and 636nm which assigned to the d-d transition in octahedral geometry [100,101] ,with transition $^2E_g \rightarrow 2T_{2g}$ the color of the complex also supports this geometry .

6.NMR spectra

In the case of H_2 CAP, complexes, the proton NMR spectra of diamagnetic complexes were compared with free ligand. The OH singlets 11.1* and 10.1* which

* δ Values

is present in the free ligand disappears in Zn (II) and Cd (II) complexes. The above results clearly indicating the participation of the OH group in chelation [51].

Similarly, in the case of H_2 CATP complexes, the proton NMR spectra of diamagnetic complexes were compared with free ligand. The SH singlets 3.1* and 3.8* which is present in the free ligand disappears in Zn (II) and Cd (II) complexes , which indicate that SH proton is removed by chelation. [51]

7. Conclusion

The coordination compounds of Cu (II) , Mn (II) , Ni(II) , Co(II) ,Zn (II) and Cd(II) with HCAP and HCATP are synthesized The physico chemical properties of all the complexes were studied . The complexes have the general formula $[M(L)_2(H_2O)_2]$ where M= Mn(II) Co(II)) Ni(II) Cu(II) and HL =HCAP or HCATP. The other complexes have been assigned the formula $[ML_2]$ where M=, Zn (II) or Cd(II) and HL =HCAP, HCATP.

8.Structure of Ligands and complexes

By considering the analytical data the structure of the ligand HCAP and HCATP and its Mn(II),Co(II), Ni(II),Cu(II),Zn(II),Cd(II) are drawn . The proposed structure is given in Fig I.5.1-I.5.6.

Ligand- HCAP

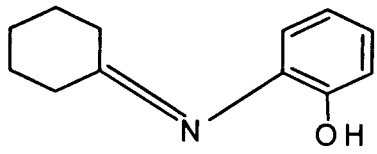

Figure I.5.1

Octahedral Complexes

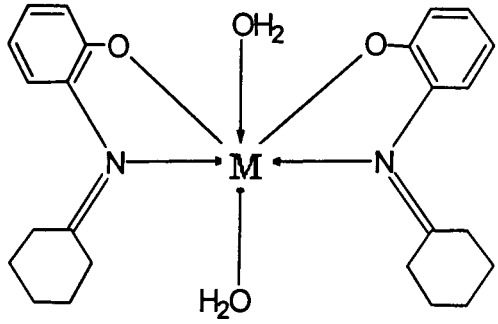

Figure I.5.2
Complexes of HCAP where M = Mn(II),Co,(II),Ni(II) and Cu(II).

Tetrahedral complexes

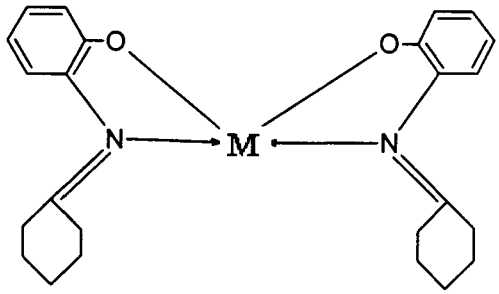

Figure I.5.3
Complexes of HCAP where M = Zn (II),Cd(II)

Ligand –HCATP

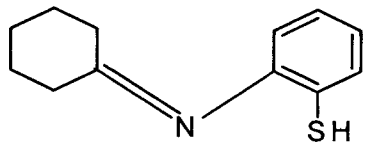

Figure I.5.4

Octahedral complexes

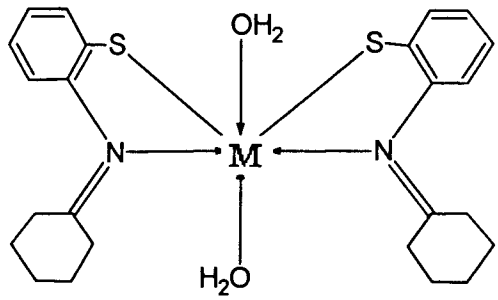

Figure I.5.5
Complexes of HCATP where M = Mn (II),Co,(II),Ni(II) and Cu(II).

Tetrahedral complexes

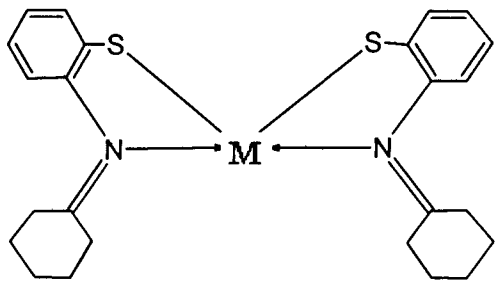

Figure I.5.6
Complexes of HCATP where M = Zn (II) and Cd(II)

Table I. 5.1
Micro analytical, magnetic and Conductance data of transition metal chelates of Cyclohexanone-2- amino phenol (HCAP) complexes

Compound	Molecular formula	Conductance Ohm^{-1}cm^{2}mol^{-1}	μ_{eff} BM	Found (calculated)%			
				Metal	C	H	N
HCAP(Ligand)	$C_{12}H_{15}ON$				75.8 (76.2)	7.01 (7.9)	7.29 (7.40)
$[MnL_2(H_2O)_2]$	$MnC_{24}H_{32}O_4N_2$	13	6.02	11.1 (11.76)	61.00 (61.67)	6.3 (6.85)	5.82 (5.99)
$[CoL_2(H_2O)_2]$	$CoC_{24}H_{32}O_4N_2$	11	5.19	12.4 (12.50)	61.3 (61.15)	6.1 (6.79)	5.2 (5.94)
$[NiL_2(H_2O)_2]$	$NiC_{24}H_{32}O_4N_2$	21	3.1	12.6 (12.47)	61.08 (61.18)	6.02 (6.79)	5.09 (5.94)
$[CuL_2(H_2O)_2]$	$CuC_{24}H_{32}O_4N_2$	13	2	12.4 (13.36)	60.1 (60.56)	5.9 (6.72)	5.11 (5.88)
$[ZnL_2]$	Zn $C_{24}H_{28}O_2N_2$	12	D	14.2 (14.80)	64.9 (65.24)	5.99 (6.34)	6.3 (6.34)
$[CdL_2]$	Cd $C_{24}H_{28}O_2N_2$	13	D	22.9 (23.01)	58.2 (58.96)	5.77 (5.73)	5.70 (5.73)

D=diamagnetic

Table I.5.2
Characteristic Infrared absorption frequencies (cm^{-1})of the of HCAP complexes

Compounds	υ (>C=N-)	υ (-C-O)	γ -OH (H2O)	υ (M- N)	υ (M-O)
Ligand	1605s	1226m	----	----	----
$[MnL_2(H_2O)_2]$	1584s	1203m	931m	517m	418w
$[CoL_2(H_2O)_2]$	1599s	1221m	931m	507m	418w
$[NiL_2(H_2O)_2]$	1565m	1198m	934m	506w	432w
$[CuL_2(H_2O)_2]$	1599s	1211m	935m	523w	418w
$[ZnL_2]$	1565s	1128m		523w	423w
$[CdL_2]$	1587s	1203m		519w	420w

Strong = s, Medium= m, Weak=w broad =br

Table I.5. 3

Characteristic ultraviolet frequencies
And probable assignment of transition
with geometry of HCAP complexes

Complex	Band nm	Assignment	Geometry
$[MnL_2(H_2O)_2]$	401	CT	Octahedral
$[CoL_2(H_2O)_2]$	544 1079	$^4T_1g(F) \rightarrow {}^4A_2g(F)$ $^4T_1g(F) \rightarrow {}^4T_2g(F)$	Octahedral
$[NiL_2(H_2O)_2]$	634 1010	$^3A_2g(F) \rightarrow {}^3T_1g(F)$ $^3A_2g \rightarrow {}^3T_2g$	Octahedral
$[CuL_2(H_2O)_2]$	576	$^2Eg \rightarrow {}^2T_2g$	Octahedral
$[ZnL_2]$	420	CT	Tetrahedral
$[CdL_2]$	360 529	CT	Tetrahedral

Table I. 5.4
Micro analytical, data of transition metal chelates of Cyclohexanone-2- aminothaiophenol (HCATP) complexes

Compound	Molecular formula	Conductance $Ohm^{-1}cm^2mol^{-1}$	μ_{eff} BM	Found (calculated)%			
				Metal	C	H	N
HCATP (Ligand)	$C_{12}H_{15}SN$				69.8 (70.24)	7.1 (7.31)	6.2 (6.82)
$[MnL_2(H_2O)_2]$	$MnC_{24}H_{32}S_2O_2N_2$	13	5.98	10.7 (11.01)	56.89 (57.72)	6.2 (6.41)	5.1 (5.6)
$[CoL_2(H_2O)_2]$	$Co\ C_{24}H_{32}S_2O_2N_2$	11	5.06	11.0 (11.71)	58.1 (57.26)	6.31 (6.36)	5.57 (5.56)
$[NiL_2(H_2O)_2]$	$Ni\ C_{24}H_{32}S_2O_2N_2$	21	3.20	11.62 (11.67)	57.08 (57.29)	6.32 (6.36)	5.34 (5.56)
$[CuL_2(H_2O)_2]$	$Cu\ C_{24}H_{32}S_2O_2N_2$	13	1.86	12.11 (12.52)	56.1 (56.74)	6.1 (6.30)	5.05 (5.51)
$[ZnL_2]$	$Zn\ C_{24}H_{28}S_2N_2$	12	D	13.2 (13.81)	59.7 (60.83)	5.99 (5.91)	5.6 (5.91)
$[CdL_2]$	$Cd\ H_{24}H_{28}S_2N_2$	18	D	21.0 (21.59)	55.0 (55.34)	6.01 (5.38)	5.98 (5.38)

D= diamagnetic

Table I.5.5
Characteristic Infrared absorption frequencies (cm^{-1}) of transition metal chelates of HCATP

Compounds	υ (>C=N-)	γ (OH)	υ (-C-S)	υ (M-N)
HCATP -ligand	1579s	----	698m	----
$[MnL_2(H_2O)_2]$	1569s	936w	681m	432w
$[CoL_2(H_2O)_2]$	1560s	935w	689m	418w
$[NiL_2(H_2O)_2]$	1569m	922w	676m	418w
$[CuL_2(H_2O)_2]$	1572s	928w	669w	435w
$[ZnL_2]$	1564	----	673w	432w
$[CdL_2]$	1569s	----	686w	436w

Strong = s, Medium= m, Weak=w broad =br

Table I. 5.6
Characteristic ultraviolet frequencies
And probable assignment of transition
with geometry of HCATP complexes

Complex	Band (nm)	Assignment	Geometry
$[MnL_2(H_2O)_2]$	420	CT	Octahedral
$[CoL_2(H_2O)_2]$	570	$^4T_1g\,(F) \rightarrow {}^4A_2g\,(F)$	Octahedral
$[NiL_2(H_2O)_2]$	1152 548	$^3A_{2g}(F) \rightarrow {}^3T_{2g}(F)$ $^3A_{2g}(F) \rightarrow {}^3T_{1g}(F)$	Octahedral
$[CuL_2(H_2O)_2]$	636	$^2E_g \rightarrow {}^2T_{2g}$	Octahedral
$[ZnL_2]$	336	CT	Tetrahedral
$[CdL_2]$	345	CT	Tetrahedral

3D sketches

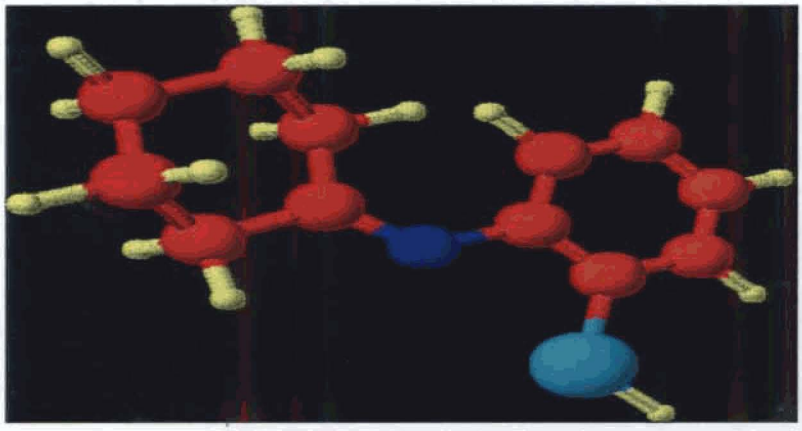

2-(Cyclohexylideneamino)Phenol (HCAP)
2-(Cyclohexylideneamino)Benzenethiol (HCATP)

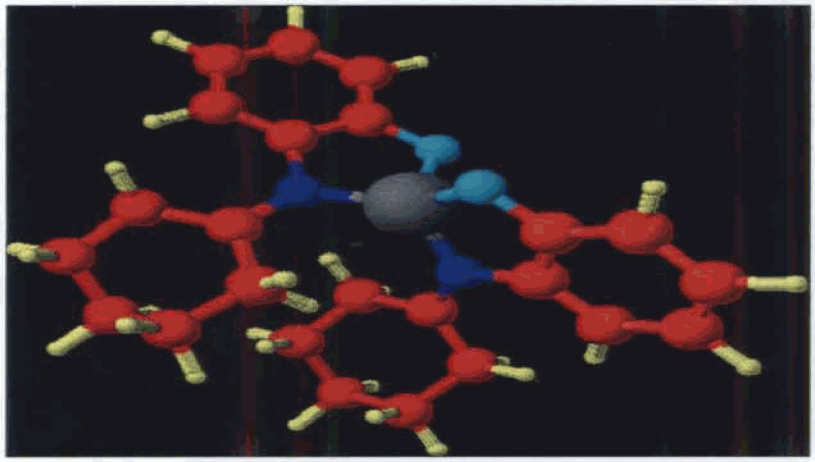

TETRAHEDRAL COMPLEXES OF HCAP/HCATP

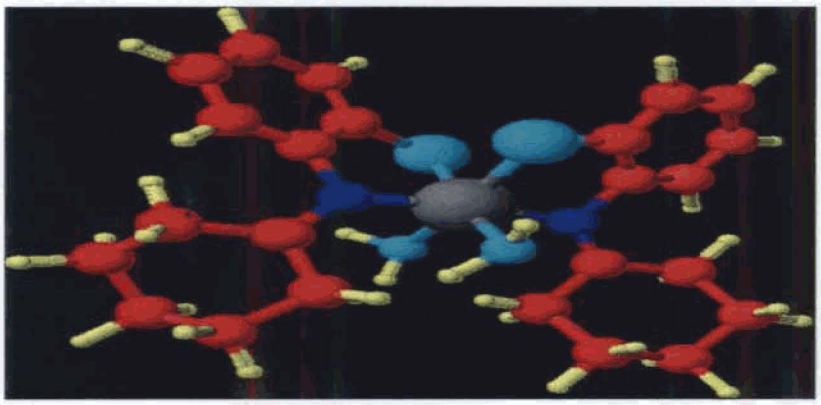

OCTAHEDRAL COMPLEXES OF HCAP/HCATP

Yellow = Hydrogen; Red = Carbon; blue= Nitrogen; Cyan= oxygen/ sulphur
Gray = metal

The 3D structures and naming ligand are based the on the drawings of ACD soft ware which follows on *Journal of American Chemical Society* and the stereochemistry of the molecules is only an approximation

CHAPTER 6

Studies on Mn (II), Co (II), Ni (II), Cu (II), Zn (II) and Cd (II) Complexes of Pyrolidone-2- aminophenol (HPAP) and Pyrolidone -2-aminothiophenol (HPATP)

Two bidentate Schiff base ligands pyrolidone-2- aminophenol (HPAP) and pyrolidone -2-aminthiophenol (HPATP) have been synthesized for the first time. These ligands produce various complexes with different transition metal ions. Studies show that no work has been done on the complexes of pyrolidone and aminophenol or aminothiophenol.

Here HPAP can act as a bidentate ligand containing the ON donor group while. HPATP, can act as a bidentate ligand containing the SN donor group. So it is interesting to synthesize and characterize the complexes of HPAP and HPATP and to conduct detailed investigation about structure, magnetic property, thermal stabilities, decomposition patterns and biological activities of these complexes .

A. Experimental

1) Materials and methods

Details regarding the reagents used, procedure adopted for the characterization of the ligand and complexes are given in chapter II.

2) Preparations of ligands

A hot ethanolic solution of pyrolidone (0.01mol) was added drop wise to a stirred solution (.01mol) of 2 aminophenol dissolved in ethanol . The mixture was refluxed for about 20 minutes and then cooled. The precipitate formed was filtered, washed with alcohol and then dried. Melting point is 138^0C yield 91% . To obtain

HPATP the same procedure is used for synthesizing the ligand HPAP adopted. Melting point. 151^{0}C . Yield 87%.

3) Synthesis of complexes

The complexes were prepared by adding slowly a hot aqueous solution of the metal acetate to a refluxing ethanolic solution of the ligand until the metal ligand ratio reached 1:2. The reaction mixture was refluxed for 20 minutes and the complexes precipitated were separated. It was washed with water followed by ethanol and dried over anhydrous Ca Cl_2.

B. Results and discussions

The complexes were characterized on the basis of elemental analysis ,UV ,IR spectral data, magnetic studies, conductance measurements and the thermal data as given in the Tables ; I.6.1- I.6.6.

1.Characterization of ligands

The ligands were characterized using TLC,CHN and IR spectral data .The assigned structure for the ligands are given in the figures ; I.6.1 and I.6.4.

2. Formula and general properties of complexes

All the complexes are colored, photostable and non hygroscopic. They have low solubility in organic solvents but high solubility in DMF and DMSO.The values of electrical conductivity of the complexes in DMSO show that they are non-electrolytic compounds. The complexes were analyzed for metal, carbon, hydrogen, and nitrogen, by atomic absorption spectroscopy and standard micro analytical methods. Results are given in the Tables ; I.6.1- I.6.6.

3. Magnetic behavior

In the case of HPAP and HPATP complexes of Mn (II) the observed magnetic moment values are 5.96 BM and 5.89 BM which proves the existence of

octahedral geometry. The Co (II) complexes of HPAP and HPATP possess magnetic moment values of 4.8 and 4.9 BM as expected for octahedral geometry. The complexes of Ni (II) have magnetic moment values 3.01BM and 3.1 BM which are in accordance with octahedral complexes. The magnetic moment values of Cu(II) complexes possess normal values of 1.92 and 1.82 B.M as expected for octahedral geometry. The Zn (II) and Cd(II) complexes are found to be diamagnetic.

4.IR spectra

HPATP complexes shows band at a 1616 cm^{-1}. This is due to C=N stretching. The lowering of this frequency region (1597 cm^{-1} - 1565 cm^{-1}), observed in all the complexes, indicates the involvement of the azomethine nitrogen atom in coordination [85,86]. The band at 692$cm^{-1}$is characteristic of the C-S in the free ligand. The shifting of this frequency region, observed in all the complexes, indicates that S-H group is ionized and co-coordinated. The bands at 418-430 cm^{-1} which are due to the formation of M–N bonds. Presence of a broad band around 3200 cm^{-1} (except in Zn (II), Cd (II)) may be due to the OH stretching of coordinated water, which further confirmed from –OH bending frequencies .

In the case of HPAP the band at 1605 cm-1 in free ligand is due to the presence of azomethane linkage in free ligand. During the complexation this value is changing into 1598- 1564cm^{-1} .The C-O band in the free ligand is 1226 which is changing to 1138-1194 cm^{-1} in complexes which indicate the participation of phenolic group in the complexation. The bands at 596-536cm^{-1} which are due to M-N bonds and the bands 412-478cm^{-1}indicate M-O bonds. The bands around 3200cm^{-1} proves the presence coordinated water which is further confirmed by bands near 930cm^{-1} except in Zn(II), Cd(II).The characteristic frequency of free

acetate ion at 1560 cm^{-1},1415 cm^{-1} are absent in all the complexes but the non-conducting nature and stoichiometry of this complexes indicate that acetate ion is not present .

5. Electronic spectra

The electronic spectra of all the complexes of HPAP and HPATP are recorded in DMSO. The important spectral bands of the complexes and their probable assignments are given in Tables. I.6.3 and I.6.6.

In the present investigation Mn (II) complex of HPAP and HPATP shows the band appearing below 400nm only which are due to CT bands. The electronic spectrum of Co (II) complex of the ligand HPAP gives two characteristic bands at 442 and 551nm respectively. In the case of Ligand HPATP characteristic band at 482 and 561nm. In both cases the characteristic bands prove the octahedral geometry . Ni (II) complex shows bands at 564nm and 978nm in HPAP and 551 in HPAP assigned as given in the Tables I.6.3 and I.6.6 . Experimentally obtained data supports the octahedral geometry. Color also supports this observation. In the present investigation Co(II) complex shows absorptions which can be assigned to the d-d transitions of octahedral geometry. Low intensity of bands and purple color supports octahedral geometry. In the case of Cu (II) complexes, absorption maximum at about 666 nm and 732nm supports octahedral geometry. The available data of Zn (II),Cd (II) are insufficient predict the geometry of complexes but as they are four coordinated so tetrahedral geometry is the preferred structure for both complexes .

6.NMR spectra

In the case of H_2 PAP, complexes, the proton NMR spectra of diamagnetic complexes [(Zn $(PAP)_2$] and [Cd $(PAP)_2$] were compared with free ligand. The OH

singlet 10.1 ppm and 10.9 ppm which is present in the free ligand disappears in Zn (II) and Cd (II) complexes. The above results clearly indicating the participation of the OH group in chelation [51].

in the case of H_2 CATP complexes, The SH singlets 3.1ppm and 3.0 ppm which is present in the free ligand disappears in Zn (II) and Cd (II) complexes , which indicate that SH proton is removed by chelation. [51]

7. Conclusion.

Mn (II), Co (II), Ni(II), Cu(II), Zn(II) and Cd(II) complexes of HPAP and HPATP were synthesized . The physico chemical properties of all the complexes were studied. The complexes have the general formula $[M(L)_2(H_2O)_2]$ where M= Mn(II),Co (II),Ni (II) and Cu (II)) and L is bi dentate anion obtained from HPAP or HPATP .For the other complexes is the formula $[ML_2]$ is assigned where L is the bi dentate anionic ligand obtained from HPAP or HPATP where M=Zn (II)or Cd(II).

The IR data, NMR , conductance values and stochiometry of the compounds strongly proves this assumption. The data obtained are insufficient to prescribe the exact geometry of Zn(II) and Cd(II) . However in comparison with structure of other complexes and considering common coordination numbers exhibited by these metal ions, a four coordinated tetrahedral geometry may be assigned to them.

8.Structure of ligands and complexes

By considering the analytical data the structure of the ligand, Mn (II),Co (II), Ni (II),Cu (II),Zn (II) and Cd (II) complexes are drawn . The proposed structures are given in Figure I.6.1- I.6.3.

Ligand- HPAP

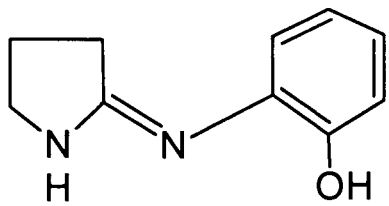

Figure I.6.1

Octahedral Complexes

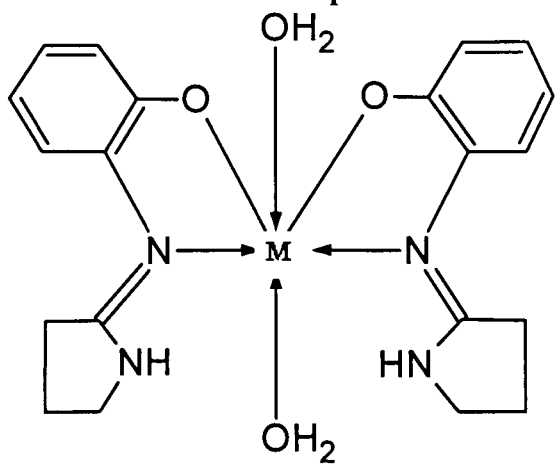

Figure I.6.2
Complexes of HPAP where M = Mn (II),Co,(II),Ni (II) and Cu(II).

Tetrahedral complexes

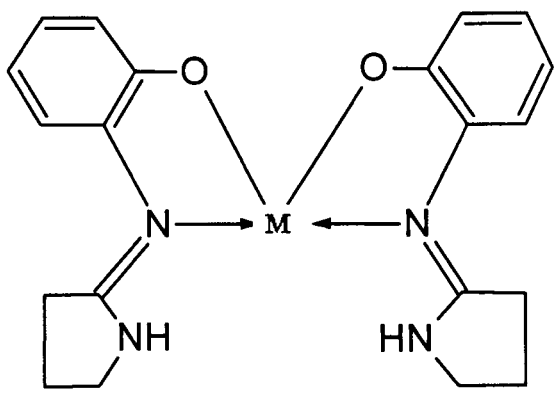

Figure I.6.3
Complexes of HPAP where M = Zn (II),Cd (II)

Ligand –HPATP

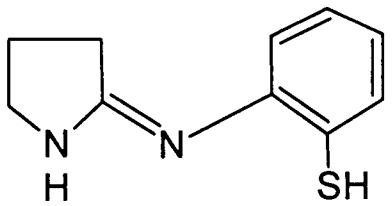

Figure I.6.4

Octahedral complexes

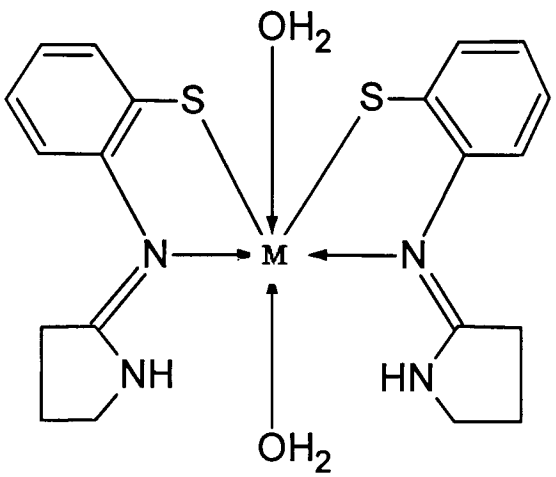

Figure I.6.5
Complexes of HPATP where M = Mn (II),Co,(II),Ni(II) and Cu(II).

Tetrahedral complexes

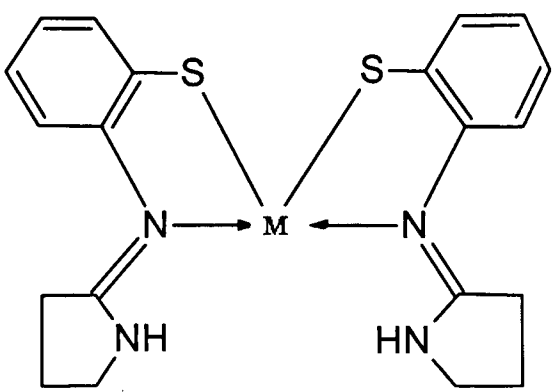

Figure I.6.6
Complexes of HPATP where M = Zn (II), Cd(II)

Table I. 6.1

Micro analytical, Magnetic and Conductance data of transition metal chelates of pyrolidone –2-aminophenol (HPAP) complexes

Compound	Molecular formula	Conductance $ohm^{-1}cm^2mol^{-1}$	μ_{eff} BM	Found (calculated)%			
				Metal	C	H	N
HPAP (ligand)	$C_{10}H_{12}N_2O$				67.9 (68.18)	6.7 (6.818)	14.98 (15.9)
$[MnL_2(H_2O)_2]$	$MnC_{20}H_{26}O_4N_4$	14	5.96	11.9 (12.45)	54.34 (54.42)	5.7 (5.89)	12.2 (12.70)
$[CoL_2(H_2O)_2]$	$CoC_{20}H_{26}O_4N_4$	23	4.8	13.2 (13.23)	53.03 (53.94)	5.82 (5.84)	12.03 (12.58)
$[NiL_2(H_2O)_2]$	$NiC_{20}H_{26}O_4N_4$	8	3.01	12.9 (13.19)	53.8 (53.96)	5.84 (5.84)	12.58 (12.59)
$[CuL_2(H_2O)_2]$	$CuC_{20}H_{26}O_4N_4$	12	1.92	14.36 (14.13)	52.8 (53.38)	5.5 (5.78)	12.1 (12.45)
$[ZnL_2]$	$ZnC_{20}H_{22}O_2N_4$	16	D	15.4 (15.74)	56.9 (57.77)	5.79 (5.29)	13.82 (13.48)
$[CdL_2]$	$ZnC_{20}H_{22}O_2N_4$	12	D	24.36 (24.30)	52.7 (51.90	4.3 (4.75)	12.01 (12.11)

D=diamagnetic

Table I. 6.2
Characteristic Infrared absorption frequencies (cm^{-1})of Transition metal chelates of HPAP

Substance	υ (OH) (H2O)	υ (>C=N-)	υ (-C-O)	γ(O-H) (H2O)	υ (M-N)	υ (M-O)
HPAP -ligand	----	1605s	1226m	----	-----	------
$[MnL_2\{H_2O)]_2$	3246b	1587m	1172m	934m	544w	459m
$[CoL_2\ H_2O]$	3251b	1597m	1138m	932m	540w	447w
$[NiL_2\{H_2O]_2]$	3222b	1564m	1194m	976m	563w	478w
$[CuL_2\ H_2O]$	3210b	1598s	1196m	935m	596w	529m
$[ZnL_2]$	----	1592s	1190m	----	534w	436m
$[CdL_2]$	----	1578s	1194m	----	536w	412w

Strong = s, Medium= m, Weak=w broad =b

Table I.6. 3

Characteristic ultraviolet frequencies and probable assignment of transition with geometry of HPAP complexes

Complex	Band nm	Assignment	Geometry
$[MnL_2(H_2O)_2]$	371	CT	Octahedral
$[CoL\{H_2O]_2]$	442 551	$^4T_1g(F) \rightarrow {}^4T_1g(P)$ $^4T_1g(F) \rightarrow {}^4A_2g(F)$	Octahedral
$[NiL\{H_2O]_2]$	564 978	$^3A_{2g} \rightarrow 3T_{1g}(F)$ $^3A_{2g} \rightarrow 3T_{2g}$	Octahedral
$[CuL_2(H_2O)_2]$	666	$^2Eg \rightarrow {}^2T_2g$	Octahedral
$[ZnL_2]$	420	CT	Tetrahedral
$[CdL_2]$	360	CT	Tetrahedral

Table I. 6.4
Micro analytical, magnetic and Conductance data of transition metal chelates of Pyrolidone-2- aminothiophenol (HPATP) Complexes

Compound	Molecular formula	Conductance $ohm^{-1}cm^2mol^{-1}$	μ_{eff} BM	Found (calculated)%			
				Metal	C	H	N
HPATP	$C_{10}H_{12}N_2S$	----	—	----	61.8 (62.5)	5.9 (6.25)	13.9 (14.58)
$[MnL_2(H_2O)_2]$	$MnC_{20}H_{26}O_2S_2N_4$	12	5.89	10.6 (11.61)	50.3 (50.74)	5.22 (5.49)	11.0 (11.84)
$[CoL_2(H_2O)_2]$	$CoC_{20}H_{26}O_2S_2N_4$	8.0	4.9	12.3 (12.35)	50.34 (50.32)	4.97 (5.46)	11.2 (11.74)
$[NiL_2(H_2O)_2]$	$NiC_{20}H_{26}O_2S_2N_4$	9.0	3.1	11.8 (12.31)	49.9 (50.34)	5.5 (5.45)	11.8 (11.74)
$[CuL_2(H_2O)_2]$	$CuC_{20}H_{26}O_2S_2N_4$	12	1.82	13.01 (13.19)	49.7 (49.83)	5.32 (5.39)	11.06 (11.62)
$[ZnL_2]$	$ZnC_{20}H_{22}S_2N_4$	11	D	14.06 (14.61)	54.2 (53.64)	4.90 (4.91)	12.5 (12.51)
$[CdL_2]$	$CdC_{20}H_{22}S_2N_4$	14	D	22.3 (22.73)	48.2 (48.54)	4.32 (4.44)	11.4 (11.32)

D=diamagnetic

Table I. 6.5.
Characteristic Infrared absorption frequencies (cm^{-1})of transition metal chelates of HPATP

Substance	υ_{OH} (H2O)	υ (>C=N-)	γ_{OH} (H2O)	υ (C-S)	υ (M-N)
HPATP -ligand	----	1616s	----	692m	---
$[MnL_2(H_2O)_2]$	3250b	1597s	925w	679m	430w
$[CoL_2(H_2O)_2]$	3249b	1583s	923w	696w	444w
$[NiL_2(H_2O)_2]$	324b	1597s	943w	688w	418w
$[CuL_2(H_2O)_2]$	322b	1565s	921w	619w	418w
$[ZnL_2]$	----	1585m	----	676w	430w
$[CdL_2]$	---	1569s	---	687w	462w

Strong = s, Medium= m, Weak=w broad =b

Table I. 6.6
Characteristic ultraviolet frequencies and probable assignment of transition with geometry of HPATP complexes

Complex	Band nm	Assignment	Geometry
$[MnL_2(H_2O)_2]$	360 387	CT $^6A_{1g} \rightarrow {}^4T_2g(D)$	Octahedral
$[CoL_2(H_2O)_2]$	482 561	$^4T_1g(F) \rightarrow {}^4T_1g(P)$ $^4T_1g(F) \rightarrow {}^4A_2g(F)$	Octahedral
$[NiL_2\{H_2O]_2]$	551	$3A_2g \rightarrow 3T_1g(F)$	Octahedral
$[CuL_2(H_2O)_2]$	732	$^2Eg \rightarrow {}^2T_2g$	Octahedral
$[ZnL_2]$	565	CT	Tetrahedral
$[CdL_2]$	420	CT	Tetrahedral

3D sketches

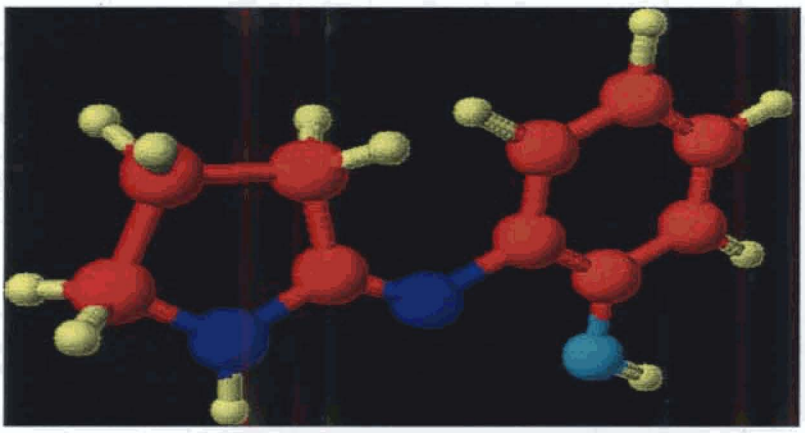

2-[(Pyrrolidin-2-Ylideneamino]Phenol HPAP
2-[Pyrrolidin-2-Ylideneamino]Benzenethiol HPATP

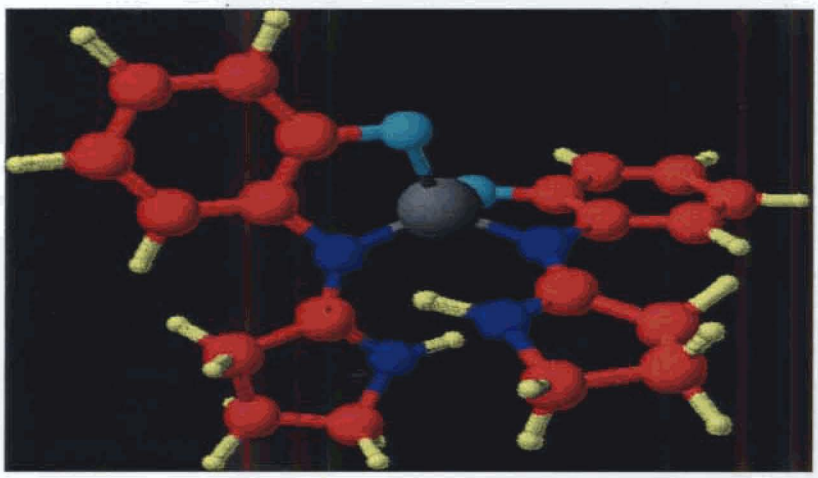

TETRAHEDRAL COMPLEXES OF HPAP/HPATP

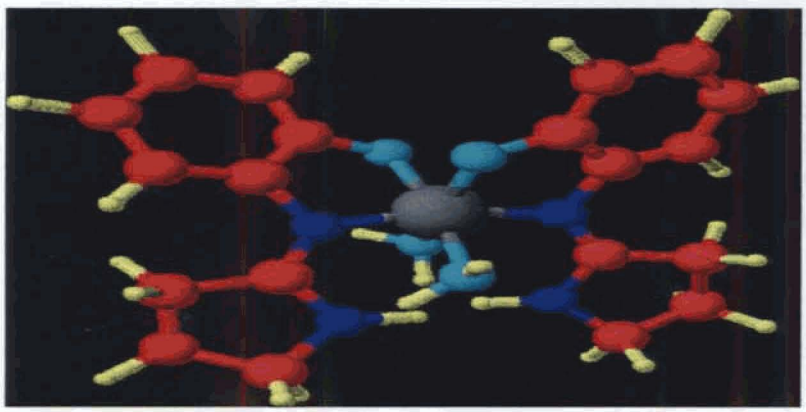

OCTAHEDRAL COMPLEXES OF HPAP/HPATP

Yellow = Hydrogen; Red = Carbon; blue= Nitrogen; Cyan= oxygen/ sulphur
Gray = metal

The 3D structures and naming ligand are based the on the drawings of ACD soft ware which follows on *Journal of American Chemical Society* and the stereochemistry of the molecules is only an approximation

REFERENCES

1) Karno,N.G.; Ratnasamy, S.; Patrick J. W. *Tetrahedron: Asymmetry.* **2001**, 12, 1719–1722.

2) Genet , J.P.; Ferroud , D.; Juge, S.; Montes, J.R. *Tetrahedron Lett.* **1986**, 27, 38, 4573-4576.

3) Chatterjee, D.; Mitra, A.; Shepherd, R. *Inorganica Chimica Acta.* **2004**, 357, 4, 980-990.

4) Lobet, A.; Martell, A. E.; Martinez, M. A. *J. Mol. Catal.* **1998**, 129, 19-26.

5) Erskine, P.T.; Newbold, R.; Roper, J.; Coker, A.; Warren, M.J.; Shoolingin-Jordan, P.M.; Wood, S.P.; Cooper J.B. *Protein Science.***1999**, 8,6, 1250-1256.

6) Nahar, C. T.; Mukhedkar, A. J . *J.Indian Chem.Soc.* **1981**, 58,343-346.

7) Cad,V.T. *Gossypol and its new derivatives*: *Synthesis and study of Biological Activities.* Thesis/PhD. **2002**, Institute of Chemistry of Natural Substances, University of Paris.

8) Verma, M.; Pandeya, S.N.; Singh, K.N.; Stables, J. *Acta Pharm.* **2004**,54,1,49-56.

9) Toshihiko Takeuchi.; Arnd Bottcher. ; Cindy, M.Q.; Melvin, I. S.; Thomas J. M.; Harry B. G. *J. Am. Chem. Soc.* **1998**, 120, 8555-8556.

10) Dashora, R.; Singh, R. V.; Tandon, J. P. *Indian J.Chem,Sect.A.***1986**, 25, 2, 188-190.

11) Nursen, S. *Gazi University Journal of Science.* **2003**,16, 2, 283-8.

12) Zahid H. Chohan.; M. A. Farooq.; Claudiu, T. Supuran. *Metal-Based Drugs.* **2000**, 7 , 171 – 177.

13) Raman, N.; Muthuraj, V.; Ravichandran, S.; Kulandaisamy. *Proc. Indian Acad. Sci. (Chem. Sci.).* **2003**,115, 3, 161–167.

14) Zdena Durackova, M.; Antonia Mendiola, M.; Teresa, S.; Aladar Valent. *Bioelectrochemistry.* **1999**, 48,1,109-116.

15) Iffet, S.; Necla G.; Turgut G.; web article. , *Ankara University*, Science Faculty, Department of Chemistry, 06100,Ankara, Turkey.

16) Susan, S.; Abolfazl , G.; Mohammed Ali, N.; Hashem, S. *Sensors and Actuators B: Chemical.* **2004**, 98, 2-3 , 15, 174-179.

17) Cemal, H.; Kadriye, E.; Berrin, Y.; Engin, C. *Dyes and Pigments* . **2004**, 62, 1 , 35-41.

18) Elif, K.; Esma, K. *Talanta* .**2002**, 58, 4 , 793-802.

19) Papi, S.; Koprivanac, N.; Grabari, Z.; Parac-Osterman. *Dyes and Pigments.* **1994**, 25, 3 , 229-240.

20) Jia-An Gan .;Qun Liang Song .; Xiao Yuan Hou.; Kongchang Chen.;He Tian. *Journal of Photochemistry and Photobiology A: Chemistry.* **2004**, 162, 2-3, 15, 399-406.

21) Dixit, Purnima.; Tandon, J. P. *Indian J.Chem.Sect.A* ,**1988**, 27, 2 ,153-155.

22) Francisco Hueso-Urena.; Antonio L. Peñas-Chamorro.; Miguel N. Moreno-Carretero.;Miguel Quirós-Olozábal.; Juan M.; Salas-Peregrín. *Polyhedron.* **1998**,18, 3-4 , 351-360.

23) Agarwala, B.V.;Hingorani,S. *Inorganica Chimica Acta.* **1990**, 176, 1 , 149-54.

24) Vasile Lozan.; Paul-Gerhard Lassahn.; Cungen Zhang .; Biao Wu.; Christoph Janiak.; Gerd Rheinwald. ; Heinrich Lang. *Z. Naturforsch.* **2003**, 58, 1152 – 1164.

25) Singh, R.V.; Mukta Jain.; Pooja Nagpal. *Main Group Met. Chem.* **2002**, 25,615 – 619.

26) Ferenc Makkay.; Janos Zsako.;Gyorgy Liptay.; Kovacs-Ludescher. *Per. Pol. Chem. Eng.* **1994**,38/3-4, 165-181.

27) Leovac,V.M.; Vojinovi, S. K.; Meszaros Szecsenyi.; Cesljevic,V. I. *J.Serb.Chem.Soc.* **2003**, 68, 12919-929.

28) Jevtovi,V.S.; Jovanovi,S.V.; Leovac,M.; BjelicaL.J. *J.Serb.Chem.Soc.* **2003**, 68, 12,929-942.

29) Pandeya, S. N.; Sriram, D.; Yogeeswari, P.; Stables, J. *Pharmazie.* **2001**,56:11, 875-876.

30) Elzbieta Pomarnacka.; Iwona Kozlarska-Kedra. *Farmaco.* **2003**, 58, 6, 423-429.

31) Salam,M.A.; Bangladesh, J. *J.Acad.Sci.***1992.**

32) Syamal, A.; Kala , K.S. *Ind.J.Chem.***1980** ,19A,5,488.

33) Tez Can, *Chim.Acta.Turc.* **1984**,12,2, 376.

34) Sonabati, A. Z.; Bindary,A.A. *Pol.J.Chem.* **2000**,74,5,621-630.

35) Naik, S et al *J.Indian Counc.Chem.* **1998**,7-9 ,15.

36) Mehtha, B.H.;Desai.;Yogita.*Orient.J.Chem.* **1999**,15,139-142.

37) Adel,S.D.;Mohamed,I.A.;Ramadan. *Transition Met Chem.* **1998**, 23,391-396.

38) Jaya Murthy, J.; Meha ,B.H.*Orient.J.Chem.* **1998**, 14,129-131.

39) Jejukumar,C.R.; Ketan Parikh.*Asian J.Chem.***1997**,9,624-629.

40) Chae.;Hee-Nam.;Choi.;Youg-Kook. *J.Korean Chem.Soc.***1998**,42,422-431.

41) Armin.F.;Oliver.B.; Wolfgang ,B. *ChemBer/*recl.**1998**,130,1467-1473.

42) Mayadevy, S.;Yusuff,K.K . *Synth.React.Inorg.Met-Org.Chem.* **1997**,27,319-319.

43) Syamal,A.;Gupta, B.K. *Acta Ciena.Indica, Chem.* **1985**,11,83-88.

44) Sanchez, G.; Momblona, F.; Serrano, J.L.; Garcia L.; Perez E.; Perez J., Lopez G. *Journal of Coordination Chemistry.* **2002,** 55, 8 ,917-923.

45) Minu, G.B.; Li Kam Wah,H.; Dosieah,A . ; Ridana. M.; Ramalingum , O.;Lacour,D. *Synthesis and Reactivity in Inorganic and Metal-organic Chemistry.***2004**, 34,1-16.

46) Jung-Sook Kim.; Hee-Jung Kim.; Bon-Kweon Koo. *Bull. Korean. Chem. Soc.* **1995** 16, 1,26-29.

47) Salavati-Niasari, M.;Banitaba, S. H. *Journal of Molecular Catalysis*, A: Chemical. **2003**, 201, 43-54.

48) Tayim, H.A.; Salameh A.S.; Meri U. S. I. *Polyhedron* .**1986**, 5, 10 , 1509-1511.

49) Sanchez, G.; Momblona, F.; Serrano, J.L.; Garcia ,L.; Perez ,E.; Perez,J.; Lopez, G. *Coordination Chemistry.* **2002** ,55, 8.

50) Xiaoyuan Chen.; Frank , J. Femia.; John .W. Babich .; Jon Zubieta. *Inorganica Chimica Acta* . **2000,** 308, 1-2 , 80-90.

51) Soliman, A. A .; Linert, W. *Thermochimica Acta.* **1999**, 338, 1-2 , 67-75.

52) Subrata Mandal. ; Rameshwer Shukla.; Parimal,K.Bharadwaj. *Polyhedron* .**1995**, 4 , 15-16 , 2063-2070.

53) Chinnasamy Jayabalakrishnan.; Karuppanannan Natarajan. *Transition Metal Chemistry.* **2002**, 27, 75-79 .

54) Thangaian Daniel Thangadurai.; Karuppanannan Natarajan.; *Transition Metal Chemistry.* **2002**, 27, 5 ,485-489.

55) Kamal, A.R. Salib.; Akila, A. Saleh.; Samy Abu El-Wafa.; Hoda ,F.O. El-Shafiy. *Journal of Coordination Chemistry.* **2003,**56, 4 , 283 – 298.

56) Sergej P. Osinsky.; I. Levitin.; L. Bubnovskaya. A. Sigan.; I. Ganusevich.; V. Michailenko. ; Kovelskaya, T. *6th Internet World Congress for Biomedical Sciences.***1998.**

57) Ahmed A. El-Asmy.;Mohamed Mounir.;*Transition Metal Chemistry.* **1988**,13, 2,143 - 145

58) WangDongmei.;YangRuina.;LiuYingfan.;JinDouman.www.*chemistrymag.org.* **2001** , 3 ,1-4.

59) Kozlov, N. G. *Russian Journal of General Chemistry.* **2002,** 72, 8, 1238- 1242.

60) Casas, J.S. *et al* . *Journal of Chemical Crystallography.* **2001**, 31,329-332 .

61) Agarwal, R. K.; Sharma, S. *Pol. J.Chem.* **1993**, 67: 4, 581-586.

62) Weissburger , A.; Prokaver, E.S.; Riddick, J.A.; Troops, E.E. **1956**, Organic *Solvents*: Interscience, New York , 17.

63) Vogel, A.I. *A text book of qualitative inorganic analysis* (ELBS and Longman, London) , **1978.**

64) Furman,N.H. *Standard Methods of Chemical Analysis:*Dvan Nostrand Co, **1962.**

65) Figgis, B.N.; Lewis, J. *Modern Coordination Chemistry.* Eds. Lewis, J. Wilkins R.G :(Interscience Publishers Inc. New York) , **1963.**

66) Figgis, B.N.; Lewis, J. *Progress in inorganic chemistry*: Interscience Publishers Inc, New York , **1964.**

67) Djebbar, S. S.; Benali, B. O.; Deloume, J. P. *Polyhedron*. **1997**, *16*, 2175-2182.

68) Bhattacharyya, P.; Parr, J.; Ross, A. T. *J.Chem. Soc. Dalton*. **1998**, 3149-3150.

69) He, L.; Gou, S. H.; Shi, Q. F. *J.Chem. Crystallogr*. **1999**, *29*, 207-210.

70) Wu, J. C.; Tang, N.; Liu, W. S.; Tan, M. Y.; Chan, A. S. C. *Chin. Chem. Lett.* **2001**,*12*,757-760.

71) Liu, C. M.; Xiong , R. G.; You, X. Z.; Liu, Y. J.; Cheung , K. K. *Polyhedron*, **1996**,*15*, 4565-4571.

72) Singh, P.; Goel, R .L.; Singh, B. P. *J. Indian Chem. Soc.* **1975,** 52, 958.

73) Mahindra, A .M.; Fisher ,J .M; Rabinovitz. *Nature (London)*. **1983,** 303- 64.

74) Ana, I. M.; Jose M. P.; Paloma.N.; Jose,M.M.; Enrique, C.; Pilar, S. *Journal of Inorganic Biochemistry* . **1999, 76**,*1*,29-37.

75) Djebbar, S. S.; Benali, B. O.; Deloume, J. P. *Transit. Metal. Chem.* **1998**, *23*, 443-447.

76) Hamada, Y. J. *IEEE Trans.Electron Devices*. **1997**, *44*, 1208-1217.

77) Francisco Hueso-Ureña.; Antonio L. Penas-Chamorro.; Miguel N. Moreno-Carretero.; Miguel Quiros-Olozábal .;Juan M. Salas-Peregrín. *Polyhedron.* **1998**,18 ,3-4 , 351-360 .

78) Khuhawar, M. Y.; Mughal ,M. A.; Channar A. H. *European Polymer Journal.* **2004**, 40, 4 , 805-809.

79) Figgis, B.N.; Lewis, J.N. *Progress in inorganic chemistry*: 6th edition ,Eds. Cotton, F.A. Interscience, Newyork. **1964.**

80) Lewis.; Wilkins, R.G . *The magneto Chemistry of complex compounds in coordination* chemistry': New York interscience,**1969.**

81) Figgis, B.N.; Nyholm, R.S. *Journal of American chemical society* .**1958**,4190.

82) Figgis, B.N. *Nature* . **1958**,182, 1568.

83) Goodgame, D.M.L.; Cotton ,F.A . *J.Chem.Soc.* **1961** ,2298.

84) Nakomoto, K . *Spectroscopy and Structure of Metal Chelates Compounds* : New York: John Wiley .**1968.**

85) Dutta, R.L.; Sengupta, G.P. *J.Chemical.Soc* . **1971**, 48,33.

86) Mahapatra, B .; Das ,D. K. *Indian J. Chem.* **1987**, A26, 173.

87) Bellany, L.J. *'The infrared spectra of complex molecules'* :Chapman Hall London .**1975.**

88) Ferrare. R; *Low frequency vibrations of Inorganic and coordination compounds* :Newyork.plenum press.**1971.**

89) Xishi Tai.; Xianhong Yin.; Qiang Chen.; Minyu Tan .*Molecules.* **2003**, *8*, 439-443.

90) Sutton. *Electronic Spectra of Metal Complexes*: Mc graw Hill, London.**1968.**

91) Cotton F.A .;Wilkinson, G : *Advanced Inorganic chemistry* 3rd edition Wiley Eastern ltd **,1979** .

92) Bhara, B.;Chakravarthy. *Indian J Chem*: A. **1971,** 9, 590

93) Barstall, F.H.;Nyholm, R.S. *Journal Chem. Soc.* **1952** ,3570

94) Saaco, A.; Cotton ,F.A. *J.Am.Soc.*,**1962**,84 ,2043.

95) Maki ,G. *J.Chem.Phys.* **1958**, 29,1129.

96) Jorgenson, C.K. *Actad ,chem. Scand.* **1956**,10.

97) Lever, A.B.P. *Inorg electron spectroscopy*: *Elsavior Amstram.***1968**

98) Jhones, C.J. Mc.clevertty, J.A. *J.Che.Soc.***1970**,A.28-29.

99) Jorgenson, C.K. *J.Inorg.Nucl.Chem.***1962**,241,571.

100) Waters, T.N.; Hole D. *J.Chem.Soc.* **1959**,1200.

101) Waters, J.M.; Waters,T.N. *J. Chem. Soc.*, **1964**, 2489.

102) Mary Kutty P .V . PhD Thesis. University of Calicut. **2002**, 163pp.

103) Earnshaw, A. *'Introduction to Magneto Chemistry* ': New York Academic Press, **1968.**

104) Koji Nakanishi.; *Infrared Absorption Spectroscopy*: Holden Day Inc. San Francisco. **1962**

105) Russian Journal of General Chemistry, Vol. 72, No. 8, **2002**, Translated from Zhurnal Obshchei Khimii, **2002** , 1320-1324.

106) Akhrem, A.A., Lakhvich, F.A., Pshenichnyi, V.N.; Lakhvich, O.F. *Dokl. Akad. Nauk SSSR*. **1978,** 240, 3.

107) Ismail, K.A.; El- Tombary, A.A.; Aboulwafa, O.M.; Omar A-Mohsen, M.E.; El-Rewini, S.H. *Arch.Pharm.* **1996**, 329, 10, 437.

PART II
THERMO GRAVIMETRIC ANALYSIS OF SCHIFF BASE COMPLEXES

Abdul Jaleel.U.C "Synthesis, thermal and spectral studies of some transition metal complexes of schiff bases" Thesis. Department of Chemistry , University of Calicut, 2005

Part II

THERMO GRAVIMETRIC ANALYSIS

SCHIFF BASE COMPLEXES OF Cu (II), Ni (II) AND Zn (II)

INTRODUCTION

Among the different analytical methods the thermal studies possess significant use in the structural and kinetic studies of coordination compounds. This analytical method is composed of different techniques such as thermogravimetry (TG), differential thermal analysis (DTA), derivative thermo gravimetry (DTG) and differential scanning calorimetery (DSC).

Thermogravimetry is one of the oldest thermo analytical procedures and has been used extensively in different fields of science .[1,2] It also has wide application in the structural studies of coordination compounds. [3-6.] The technique involves monitoring the weight loss of the sample in a chosen atmosphere (usually nitrogen or air) as a function of temperature. The resulting mass change versus temperature curve provides information concerning the thermal stability and composition of the initial sample. The analytical instrument used is a thermo balance with a furnace programmed for a linear rise of temperature with time.[7]

The derivative thermo gravimetric curve may be obtained either by manual differentiation of the normal thermo gravimetric curve or by suitable instrumentation. It gives the relation ship between the rate of weight change and the temperature .DTG curves have a number of peaks instead of steps . In these curves , the area under the

peaks is proportional to the total change in weight .The usefulness of TGA for analysing complexes was greatly enhanced by the introduction of the ability to record simultaneously the first derivative of the weight loss. This is referred to as derivative thermo gravimetric analysis (DTG).[7,8]

TG is inherently quantitative and therefore an extremely powerful thermal technique, the ability to analyse the volatile products during a weight loss is of great value. The ability of TG to generate fundamental quantitative data from almost any class of materials has led to its widespread use in every field of science and technology.[7, 8]

Many factors influence the form of the TG curve, both sample and instrument related some of which are interactive. The primary factors are heating rate and sample size, an increase in either of which tends to increase the temperature at which sample decomposition occurs and to decrease the resolution between successive mass losses. The particle size of the sample material, the way in which it is packed, the crucible shape and the gas flow rate can also affect the progress of the reaction. Careful attention to consistency in experimental details normally results in good reproducibility. On the other hand studying the effect of deliberate alterations in such factors as the heating rate can give valuable insights into the nature of the observed reactions.[7]

Key application areas of different thermal analysis can be summarized as given below.

Thermal Stability: Related materials can be compared at elevated temperatures under the required atmosphere. The TG curve can help to elucidate decomposition mechanisms.

Kinetic Studies: A variety of methods exist for analysing the kinetic features of all types of weight loss or gain either with a view to predictive studies or to understanding the mechanisms in chemistry.

Material characterization: TG and DTA curves can be used to "fingerprint" materials for identification or quality control. It has obvious uses in the determination of the moisture content of powders, water of hydration and of carbon monoxide and carbon dioxide evolution from carbonates etc.

In Inorganic chemistry the technique has been widely used to study the kinetic and thermal behavior of coordination compounds. The valuable information given by thermo gravimetric analysis of coordination compound includes .

a) Temperature regions of stability

b) Temperature of inception of maximum rate

c) Temperature of the completion of decomposition

On the other hand DTA gives the information like enthalpy changes during the decomposition.

The following authors give much insight to the technical and theoretical aspects of thermal analysis. 1) Brown[7], 2) Duval[8] , 3) Chiang[9], 4) Garn[10], 6) Schulze,[11] 7) Wendlandt[12].

Thermogravimetry, differential thermal analysis and other thermo analytical methods can be used to study the kinetics of a chemical reaction and to determine the basic kinetic constants such as the rate constant, activation energy, order of the reaction and frequency factor. These methods usually measure continuously and automatically a change in some physical properties such as weight enthalpy, length or volume of the given system as a function of temperature .

Kinetic analysis

In kinetic studies which is based on the observation of weight change, two approaches are possible

- Isothermal(static) and
- Non isothermal (dynamic heating)

Non isothermal (dynamic heating)

The non-isothermal method is the determination of the degree of transformation as a function of time during a linear increase of temperature compared with static method .

The fundamental calculation of kinetic data from a TG curve is based on the kinetic equation

$$-dx/dt=kx^n \qquad (1)$$

here **x** is the amount of the sample undergoing reaction, **n** is the order of the reaction and **k** is the specific rate constant.

The temperature dependence of the specific rate constant k is expressed by Arrhenius equation

$$k=A\, e^{-E/RT} \qquad (2)$$

where **A** is the pre exponential factor , **E** is the activation energy, **R** is the universal gas constant and **T** is the absolute temperature

Consider a solid state reaction of the kind

$$\mathbf{A\ (solid) \rightarrow B\ (solid)\ + C\ (gas)}$$

For monitoring the above reaction from mass loss , a dimension less quantity, the fractional decomposition α which at time t is defined as the fraction of **A** the sample decomposed , is employed .

The relation ship of **x** to mass loss w is given by the equation.

$$dx = m_o\, dw/w_\alpha \qquad (3)$$

Where m_o is the initial mass of the sample, and w_α is the maximum mass loss .By integrating the equation with left hand side limit of m_o to **x** and right hand side limit of **zero** to **w** , following equation will be obtained

$$x = m_o (w_\alpha - w)/ w_\alpha \qquad (4)$$

By substituting equation (4) and (2) in equation (1) and by differentiating the logarithmic form, an expression is obtained which is used in the differential method. Integral method is using the integrated form of the equation (1) after the transposition of the mass loss w, in equation (3), (4)

The mathematical treatments of kinetic equation make use of one of the following three methods of evaluation

1 Differential methods

2 Integral methods

3 Approximation methods

Using these approaches number of equations are derived by different authors.[13-15] only one integral method used in the present study and outlined in this chapter.

Coats Redfern method[14]

Integral methods are generally accepted as the most precise among the methods accessible for the determination of kinetic parameters from TG data The disadvantages are prior determination of '**n**' is required and temperature integral has to be approximated in this method.

Consider that in the reaction

$$aA \rightarrow bB + C\ (g)$$

The rate of disappearance of **A** decomposed at a time **t** is give n by

$$d\alpha/dt = k(1-\alpha)^n \qquad (5)$$

Where **n** is the order of reaction and **k** is the rate constant

By combining equations (2) and (5) rearranging and integrating at constant heating rate $\Phi = dT/dt$ we obtain

$$\int_0^{\alpha} d\alpha/(1-\alpha)^n = A/\Phi \int_0^{\infty} \exp(-E/RT)\, dT \qquad (6)$$

The left hand side of this equation has two different solutions depending on the value of n namely

$$1-(1-\alpha)^{1-n}/(1-n)T^2 \text{ for } n=/1 \qquad (7)$$

and

$$-\log(1-\alpha)/T^2 \text{ for } n=1 \qquad (8)$$

In both cases the right hand side of equation has the solution

$$AR/\Phi E(1-2RT/E) \exp(-E/RT) \qquad (9)$$

The following two equations are obtained after taking logarithms

$$\ln [1-(1-\alpha)^{1-n}/(1-n)T^2 \text{ for} = \ln[AR/\Phi E(1-2RT/E]-E/RT \; n=/1 \qquad (10)$$

And

$$\ln(-\log(1-\alpha)/T^2 = \ln [AR/\Phi E(1-2Rt/E]-E/RT \text{ for } n=1 \qquad (11)$$

In ordinary thermal decomposition reactions ln [AR/ΦE(1-2Rt/E] is practically constant and plots of $\ln [1-(1-\alpha)^{1-n}/(1-n)T^2$ vs . 1/T for n =/1 . $\ln(1-(1-\alpha)/T^2$ vs. 1/T for n=1 respectively result in straight line with slope of –E/2.303R for correctly chosen value of '**n**'. Using this value of **n** the kinetic parameters were calculated . The entropy of activation was obtained from the equation

$$A = kTs/h \exp^{(\Delta S/R)} \qquad (12)$$

Where

k =Boltzman constant

h=Planks constant

Ts=Peak temperature

The activation entropy, the activation enthalpy and the free energy of activation were calculated using the following equations

$\Delta S^{\ddagger} = 2.303[\log (Ah/kt)] R (\Delta H^{\ddagger}), (\Delta G^{\ddagger}),$

$\Delta H^{\ddagger}, = E^{\ddagger} - RT$ [16,17]

$\Delta G^{\ddagger} = \Delta H^{\ddagger} - T\Delta S^{\ddagger}$ [16,17]

Where k and h are the Boltzman constant and Plank constant respectively .

Scope of present investigation

In this part the results of kinetic decompositions of Cu (II), Ni (II)and Zn(II)complexes of H_2DAP, H_2DSC, H_2DATP using TG are presented. From the TG curves the temperature regions of stability have been noted. The temperature of inception and decomposition and temperature of maximum rate of decomposition have been noted. The thermal stability and decomposition stages of the complexes have been noted .

The non-isothermal TG curves have been subjected to mathematical analysis using the integral methods of **Coats Redfern** and the activation parameters have been evaluated for all the complexes .

Chapter 2
THERMAL DECOMPOSITION KINETICS OF
Ni (II), Cu (II) and Zn (II)
COMPLEXES OF DIMEDONE BIS SEMICARBAZONE

Several attempts were made to study the thermal behavior of the complexes containing azomethine linkage[18-22]. The early papers which give much insight to this area of study was by Wendlandt etal[24-26]. The thermal studies of these complexes give information about the coordinated water molecules, thermal stability and the coordination number. Schemes of thermal decomposition of the complexes have also been proposed [23]. In the recent papers the determination of enthalpy of activation and free energy of activation have also been made [16].

In this chapter thermo gravimetric analysis (both TG and DTG) of some Schiff base coordination compounds are described in detail. TG and DTG techniques are helpful in establishing the structure of coordination compounds and the studying of kinetics of their decomposition. Coats Red fern equation[14] was applied. The kinetic and thermodynamic parameters like frequency factor (A), order of the reaction (n), activation energy (E), enthalpy of activation ($\Delta H^{\ddagger}$),entropy of activation($\Delta S^{\ddagger}$) and free energy of activation,($\Delta G^{\ddagger}$) were evaluated[16]. Here studies of the thermal decomposition of three representative complexes viz dimedone bis semicarbazone (H_2DSC) of Cu (II) Ni (II) and Zn (II) are described. In this chapter interpretation and mathematical analysis of these thermal decomposition data and evaluation of the order of the reaction, free energy and entropy of activation, enthalpy of activation and pre exponential factor based on the Coats Red fern equation are also described .

Experimental

Preparative procedures for the ligand and the complexes were described in part 1. Thermo gravimetric and differential thermal analysis curves are traced in an atmosphere of the static air at a constant heating rate of $10^0 C min^{-1}$ and a sample of 2-5mg were used for the study. Kinetic and thermo dynamical parameters were calculated by using Coats Red fern equation with a personal system using a Microsoft Excel work sheet .

Treatment of data

The instrumental TG and DTA curves were redrawn using Microsoft Excel worksheet. It is represented in the Fig No.II.2.1--II.2.3. By using Coats Redfern equation the kinetic and thermodynamic parameters for the metal chelates were calculated. The corresponding values of E, A, $\Delta H^{\ddagger}$, $\Delta G^{\ddagger}$, $\Delta S^{\ddagger}$ are given in the Table II .2.1-II.2.6 .

Results and discussion

Thermal decomposition curve of the [CuL $(H_2O)_2$] gives a three-stage decomposition pattern which is supported by the DTG data. The first stage represents loss of $2H_2O$ molecules According to Nikolaev et al [27] water eliminated around 150 ^0C can be considered as coordinated water. The second stage represents the loss of dimedone part and 1 semicarbazone part. In the third stage another semicarbazone moiety is disappearing. The over all stepwise reaction can be represented

$CuL(H_2O)_2 \xrightarrow[\text{dehydration}]{80\text{-}180^\circ C} CuL$

$CuL \xrightarrow[\text{partial decomposition}]{180\text{-}380^\circ C}$ intermediates

Intermediates $\xrightarrow[\text{final decomposition}]{380\text{-}560^\circ C}$ metal oxides

DTG curve gives well-defined peaks in the appropriate region. The over all loss of mass from the curve is 77.5%while the theoretical loss in mass during the

decomposition of the complex is 77.81. The data obtained are given in the Tables.II.2.1and II.2.2.

The negative values of ($\Delta S^{\ddagger}$) for most of the complexes means that the activated complex is more ordered than the reactant and that the reactions are slow. The more ordered nature might be due to polarization of bonds in the activation state, which might happen through charge transfer electronic transitions.[5]

In the case of Ni (II) chelate a three stage decomposition pattern is observed. First decomposition stage in this case is about 9.4 %. It is quite reasonable to assume that it is due to loss of 2 water molecule. The peak temperature is about 120 ^{0}C . The second stage is a partial decomposition due to the loss of 2 semicarbazone part . Third stage is the final decomposition and subsequent formation of corresponding oxide

$NiL(H_2O)_2$ $\xrightarrow[\text{dehydration}]{80\text{-}160^{\circ}C}$ NiL

NiL $\xrightarrow[\text{partial decomposition}]{160\text{-}340^{\circ}C}$ intermediates

Intermediates $\xrightarrow[\text{final decomposition}]{340\text{-}440^{\circ}C}$ metal oxides

The total mass loss 78% is obtained for this decomposition. This value is in accordance with theoretical loss percentage and pyrolysis data given in the Table II.2.3 The kinetic and thermodynamic parameters calculated by using Coats Redfern equation summarized in the Table II.2.4.

The Zn (II) chelate showed a two-stage decomposition pattern. The first stage is loss of dimedone part and I molecule of the semicarbazone part. Second stage decomposition is due to the loss of semicarbazone moiety. At the end of the stage total mass loss is found to be 74.9%, which is very close to the theoretical value and pyrolytic data.

ZnL $\xrightarrow[\text{partial decomposition}]{160\text{-}300^{o}C}$ intermediates

Intermediates $\xrightarrow{\text{final decomposition}}$ $\xrightarrow{300\text{-}450^{o}C}$ metal oxides

The activation energies obtained for the main decomposition stage of these three complexes are also comparable to those of coordination compounds of 3d transition metals having similar structures. The decomposition and kinetic data are given in the Tables II.2.5 and II.2..6.

The initial decomposition and inflation temperature and free energy of activation have been used to determine the thermal stability of the metal chelates. Here in the present investigation based on the observation made by the other studies the relative thermal stabilities of the metal chelates of the dimedone bis semicarbazone can be given as

ZnL > $NiL(H_2O)_2$ > $CuL(H_2O)_2$

Name of the complexes	Initial decomposition temperature ^0C	Inflation temperature ^0C	Free energy of activation ($\Delta G^{\ddagger}$), kJ/mole
ZnL	160	250	150.12
Cu $L(H_2O)$	80	150	118.9
Ni $L(H_2O)$	80	120	110.22

Chapter 3
THERMAL DECOMPOSITION KINETICS OF
Ni (II), Cu (II) and Zn (II)
COMPLEXES OF DIMEDONE BIS –2-AMINOTHIOPHENOL

In this chapter we focus on the study of the thermal activities of the complexes of the ligand, dimedone bis aminothiophenol. In this case TG/DTG were recorded in the static air condition with heating rate of 10^0C /min. Coats Redfern equation is used to calculate the kinetic and thermodynamic parameters like frequency factor (A), order of the reaction (n), activation energy E, enthalpy of activation ($\Delta H^{\ddagger}$), free energy of activation ($\Delta G^{\ddagger}$)and entropy of activation ($\Delta S^{\ddagger}$). Thermo gravimetric analysis is further used for the structural perspective of the above said compounds. Here studies of the thermal decomposition of three representative complexes of dimedone bis aminothiophenol (H_2DATP) of Cu (II) Ni (II) and Zn (II) are described.

Experimental

Preparation and structural analysis of the complexes were described in part 1. TG curves are presented in Fig II.3.1-3.3 Kinetic and thermo dynamical parameters are calculated by using Coats Redfern equation with a personal system using a Microsoft Excel work sheet.

Results and discussion

In the case of copper complex, thermal decomposition curve consists of three stages, which is supported by the DTG data. First stage is due to the loss of $2H_2O$ molecules. These two water molecules can be considered as the coordinated water molecule .The second stage represents the loss of dimedone part. In the third stage

two molecules of aminothiophenol moiety are disappearing. The over all stepwise reaction can be represented

$CuL(H_2O)_2 \xrightarrow{\text{dehydration}} {}^{90\text{-}160^{\circ}C} CuL$

$CuL \xrightarrow{\text{partial decomposition}} {}^{160\text{-}280^{o}C}$ intermediates

Intermediates $\xrightarrow{\text{final decomposition}} {}^{340\text{-}440^{o}C}$ metal oxides

DTG curve gives well-defined peak in the appropriate region. The over all loss of mass from the curve is 83.6% while the theoretical loss in mass during the decomposition of the complex is 81.5. Thermal decomposition data are given in the Table II.3.1.The data obtained by using Coats Redfern equation are given in the Table II.3.2

In the case of Ni (II) chelate a three-stage decomposition pattern is observed First decomposition stage in this case is about 8. 5 %. The theoretical mass loss percentage for the two water molecule is 8.05 % .The peak temperature is about 100 ^{0}C. In this stage peak temperature, free energy of activation ($\Delta G^{\ddagger}$) and initial decomposition temperatures are very low which indicate lesser stability of the molecule. The second stage is a partial decomposition due to the loss of one dimedone part and one ATP moiety. Third stage is the final decomposition which is due to the loss of aminothiophenol moiety and subsequent formation of corresponding oxide

$NiL(H_2O)_2 \xrightarrow{\text{dehydration}} {}^{80\text{-}160^{\circ}C} NiL$

$NiL \xrightarrow{\text{partial decomposition}} {}^{160\text{-}230^{\circ}C}$ intermediates

Intermediates $\xrightarrow{\text{final decomposition}} {}^{230\text{-}300^{\circ}C}$ metal oxides

The total mass loss is the 83.6 % is obtained for this step. This value is in accordance with theoretical loss percentage and pyrolysis data. The various data obtained during the thermal decomposition are given in the Tables. II.3.3 and II.3.4.

Zn(II) complex of H_2DATP showed a two-stage decomposition curve. The first stage is loss of dimedone part and I molecule of the aminothiophenol part. Second stage decomposition is due to the loss of aminothiophenol moiety. At the end of the stage total mass is found to be 80%, where the theoretical percentage is 80.97 as given in the Table II.3.5.

ZnL $\xrightarrow{\text{partial decomposition}}$ $^{160\text{-}370°C}$ intermediates

Intermediates $\xrightarrow{\text{final decomposition}}$ $^{370\text{-}530°C}$ metal oxides

The obtained values of various kinetic and thermodynamic parameters are given in the Table II.3.6 .

The initial decomposition temperature and inflation temperature and free energy of activation ($\Delta G^{\ddagger}$) have been used to determine the thermal stability of the metal chelates. By considering these factors the stability can be predicted as given

ZnL > $CuL(H_2O)_2$ > $NiL(H_2O)_2$

Name of the complexes	Initial decomposition temperature ^0C	Inflation temperature ^0C	Free energy of activation ($\Delta G^{\ddagger}$), (first stage) kJ/mole
Zn L	160	230	146.76
$CuL(H_2O)_2$	90	120	116.47
$NiL(H_2O)_2$	80	100	107.47

Chapter 4

THERMAL DECOMPOSITION KINETICS OF Ni (II), Cu (II), and Zn (II) COMPLEXES OF DIMEDONE BIS 2-AMINOPHENOL

In this chapter study of the thermal activities of the complexes of ligand, dimedone bis aminophenol were conducted. Here also TG/DTG were recorded in the static air condition with heating rate of 10^0C /min. Coats Redfern equation is used to calculate the kinetic and thermodynamic parameters like frequency factor (A), order of the reaction (n), activation energy E, enthalpy of activation ($\Delta H^{\ddagger}$), ($\Delta G^{\ddagger}$), ($\Delta S^{\ddagger}$). Thermo gravimetric analysis is further used for the structural perspective of the above said compounds. Here Studies of the thermal decomposition of three representative complexes of dimedone bis aminothiophenol (H_2DAP) of Cu (II) Ni (II),and Zn (II) are described .

Experimental

Preparation and structural analysis of the complexes were described in part 1. Kinetic and thermo dynamical parameters were calculated by using Coats Redfern equation with a personal system using a Microsoft excel work sheet .

Results and discussion

Thermal decomposition curve of Cu (II) complex consists of three stages which is supported by the DTG data. First stage is due to the loss of two H_2O molecules. These two water molecules can be considered as the coordinate water molecule .The second stage is a sharp fall due to the loss of 1 dimedone molecule. This stage is highly favored by entropy of activation. Due to the very fast reaction the percentage of mass fall was very rapid with maximum rate of reaction . In the third

stage 2 aminophenol moieties are disappearing. The over all stepwise reaction can be represented

$CuL(H_2O)_2 \xrightarrow{\text{dehydration}}{}^{115\text{-}215^{\circ}C} CuL$

$CuL \xrightarrow{\text{partial decomposition}}{}^{215\text{-}245^{\circ}C}$ intermediates

Intermediates $\xrightarrow{\text{final decomposition}}{}^{245\text{-}345^{\circ}C}$ metal oxides

DTG curve gives well-defined peak in the appropriate region. The over all loss of mass from the curve is 82.92%while the theoretical loss in mass during the decomposition of the complex is 81.04. The data obtained are given in the Tables. II.4.1and II.4.2.

In the case of Ni (II) chelates a three-stage decomposition pattern is observed. Mass loss in first decomposition stage in this case is about 10 %. The theoretical mass loss percentage for the two water molecule is 8.6 % The peak temperature is about 105 ^{0}C. In this stage peak temperature, free energy of activation ($\Delta G^{\ddagger}$) and initial decomposition temperatures are very low, which indicate that the lesser stability of the molecule. The second stage is a partial decomposition due to the loss of one dimedone and one aminophenol part. Third stage is the final decomposition which is due to the loss of aminophenol moiety and subsequent formation of corresponding oxide

$NiL(H_2O)_2 \xrightarrow{\text{dehydration}}{}^{65\text{-}125^{\circ}C} NiL$

$NiL \xrightarrow{\text{partial decomposition}}{}^{125\text{-}255^{\circ}C}$ intermediates

Intermediates $\xrightarrow{\text{final decomposition}}{}^{255\text{-}545^{\circ}C}$ metal oxides

The total mass loss is the 81.7% and this value is in accordance with theoretical loss percentage and pyrolysis data. The kinetic and thermodynamic parameters calculated. The data during the decomposition, various known thermodynamic and kinetic parameters are given in the Tables II.4.3 and II.4.4.

Zn (II) complexes of H_2DAP showed a two-stage decomposition curve. The first stage is loss of dimedone part and one aminophenol part. Second stage decomposition is due to the loss of aminophenol moiety. At the end of the stage total mass is found to be 78.0%, where the theoretical percentage is 78.9.

ZnL $\xrightarrow{\text{partial decomposition}}$ $^{165\text{-}295^oC}$ intermediates

Intermediates $\xrightarrow{\text{final decomposition}}$ $^{295\text{-}395^oC}$ metal oxides

The thermodynamic and kinetic parameters during this decomposition are given in the Table II.4.5 and II.4.6.The activation energies obtained for the main decomposition stage of these three complexes are also comparable to those of coordination compounds of 3d transition metals having similar structures.[28]

By considering the initial decomposition temperature and inflation temperature and free energy of activation ($\Delta G^{\ddagger}$), the thermal stability of the metal chelates is as given below

ZnL > $CuL(H_2O)_2$ > $NiL(H_2O)_2$

Decomposition pattern

Name of the complexes	Initial decomposition temperature ^0C	Inflation temperature ^0C	Free energy of activation ($\Delta G^{\ddagger}$), kJ/mole
Zn L	165	215	145.98
Cu L($H_2O)_2$	115	155	123.54
Ni L($H_2O)_2$	65	105	105.37

Table II.2.1

Thermal decomposition data of Cu(II) complex of dimedone bis semicarbazone-$[CuL(H_2O)_2]$

Complex	Stage	Temp range in TG	Peak temp	Loss of mass %			Assignments
		^0C	^0C	From TG	Theoretical		
$[CuL(H_2O)_2]$	I	80-180	150	9.9	10.2	=======	Loss of 2 H_2O
	II	180-380	360	52.1	51.4	=======	Loss of Dimedone+ Semicarbazone part
	III	380-560	400	15.5	16.21	=======	Loss of Semicarbazone part and subsequent formation of oxide
				77.5	77.81	77.4	$[CuL(H_2O)_2] \rightarrow CuO$

TableII.2.2
Kinetic parameters of the decomposition of Cu(II) complex of dimedone bis semicarbazone-$[CuL(H_2O)_2]$

STAGE	E (kJ/K)	A sec -1	$\Delta S^{\ddagger}$(J/K)	$\Delta H^{\ddagger}$(kJ)	$\Delta G^{\ddagger}$(kJ)	γ	n
I	47.522	$4.9*10^3$	-177.07	44.00	118.90	-0.9748	0.74
II	70.671	$6.21*10^3$	-178.47	65.40	178.38	-0.9753	0.82
III	62.27	$6.04*10^1$	-217.57	56.68	203.11	-0.9824	0.63

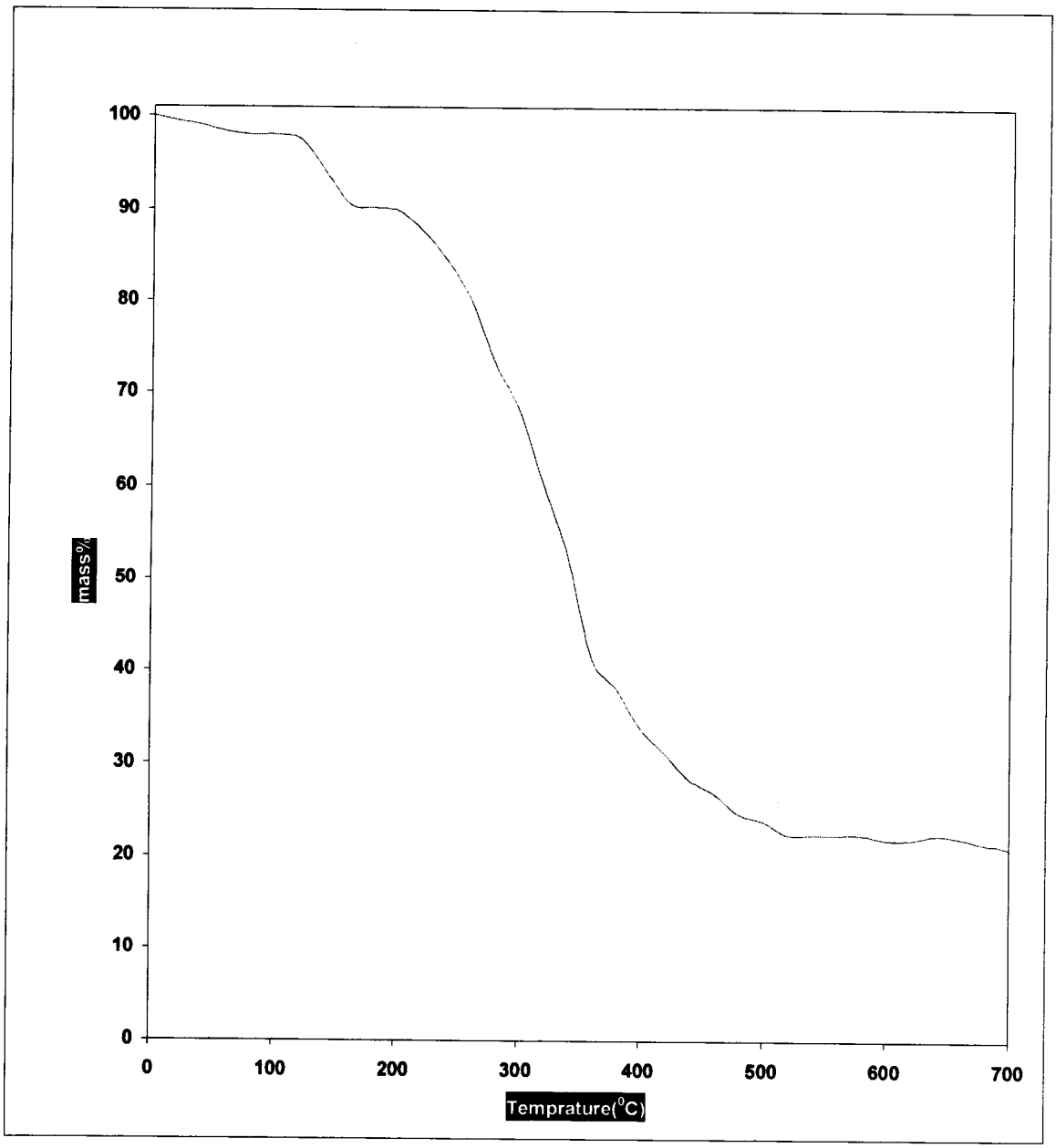

Figure II. 2.1 TG trace Cu DSC$(H2O)_2$

Table.II.2.3

Thermal decomposition data of Ni(II) complex of dimedone bis semicarbazone-$[NiL(H_2O)_2]$

Complex	Stage	Temp range in TG	Peak temp	Loss of mass %			Assignments
		^0C	^0C	From TG	Theoretical	Pyrolysis	
$[NiL(H_2O)_2]$	I	80-160	120	09.40	10.38		Loss of 2 H_2O
	II	160-340	280	40.60	42.11		Loss of 2 Semicarbazone part
	III	340-440	380	28.00	26.53		Loss of 1dimedone part and addition due to oxide formation
				78.00	79.03	78.90	$[NiL(H_2O)_2] \rightarrow NiO$

Table.II.2.4.

Kinetic parameters of the decomposition of Ni(II) complex of dimedone bis semicarbazone-$[NiL(H_2O)_2]$

STAGE	E (kJ/K)	A sec -1	$\Delta S^{\ddagger}$(J/K)	$\Delta H^{\ddagger}$(kJ)	$\Delta G^{\ddagger}$(kJ)	γ	n
I	47.58	1.43+E4	-168.29	44.32	110.22	-0.9721	1
II	74.27	4.72+E4	-160.56	69.67	158.46	-0.9684	0.87
III	307.200.	2.62E+22	177.75	301.77	185.69	-0.9536	0.99

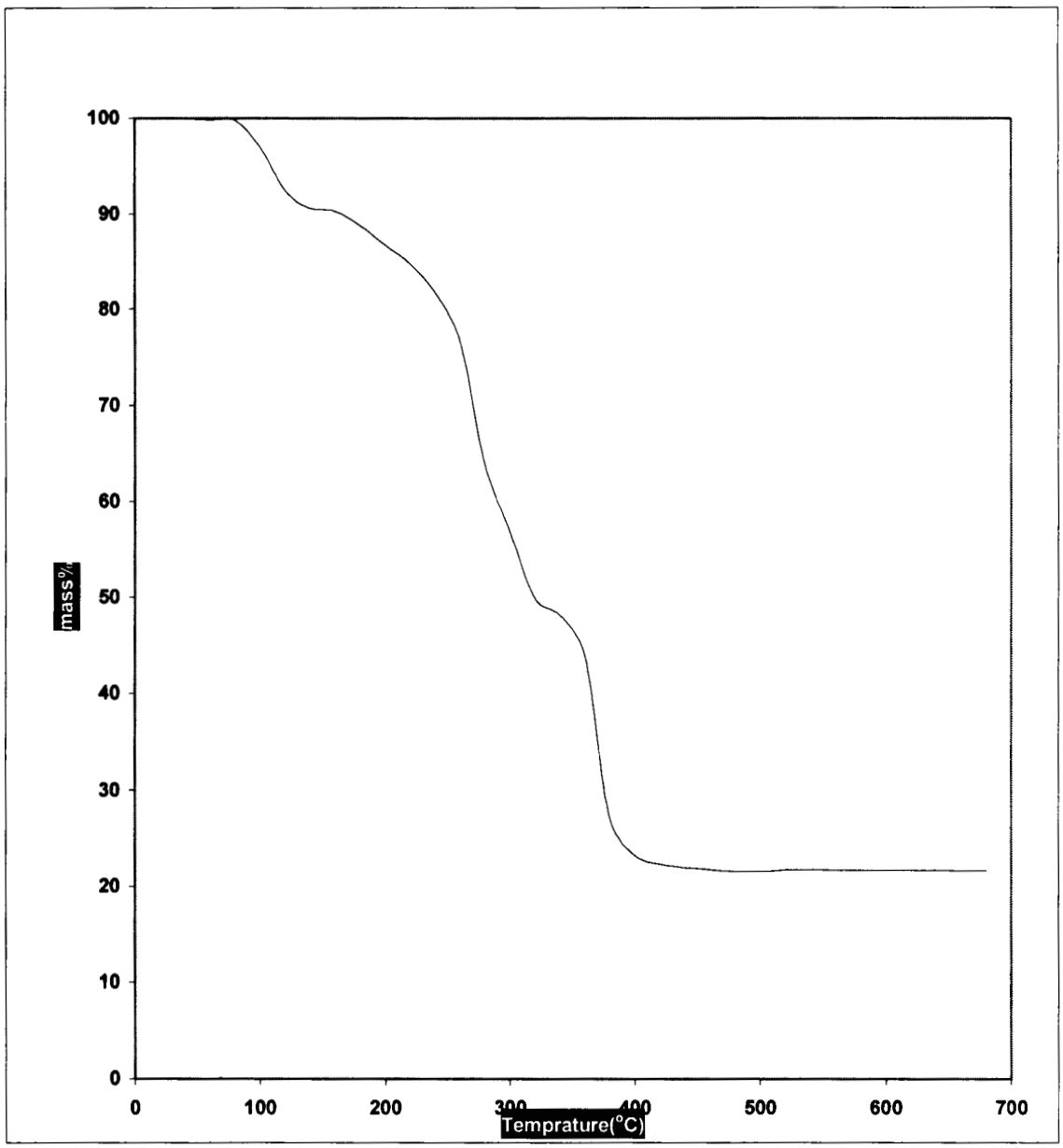

Figure II. 2.2 TG trace of Ni DSC$(H2O)_2$

TableII.2.5

Thermal decomposition data of Zn(II) complex of dimedone bis semicarbazone-[ZnL]

Complex	Stage	Temp range in TG	Peak temp	Loss of mass %			Assignments
		^{0}C	^{0}C	From TG	Theoretical		
[ZnL]	I	160-300	250	55.9	57		Loss of dimedone part+ one semicarbazone part
	II	300-450	425	19	18		Loss of second semicarbazone part and addition due to oxide formation
				74.90	74.99	74.96	[ZnL] → ZnO

Table II.2.6
Kinetic parameters of the decomposition of Zn(II) complex of dimedone bis semicarbazone-[ZnL]

STAGE	E (kJ/K)	A sec -1	$\Delta S^{\ddagger}$(J/K)	$\Delta H^{\ddagger}$(kJ)	$\Delta G^{\ddagger}$(kJ)	γ	n
I	46.81	1.92+E2	-205.84	42.47	150.12	-0.9687	0.47
II	148.258	8.21+E8	-81.32	142.45	199.22	-0.9758	0.33

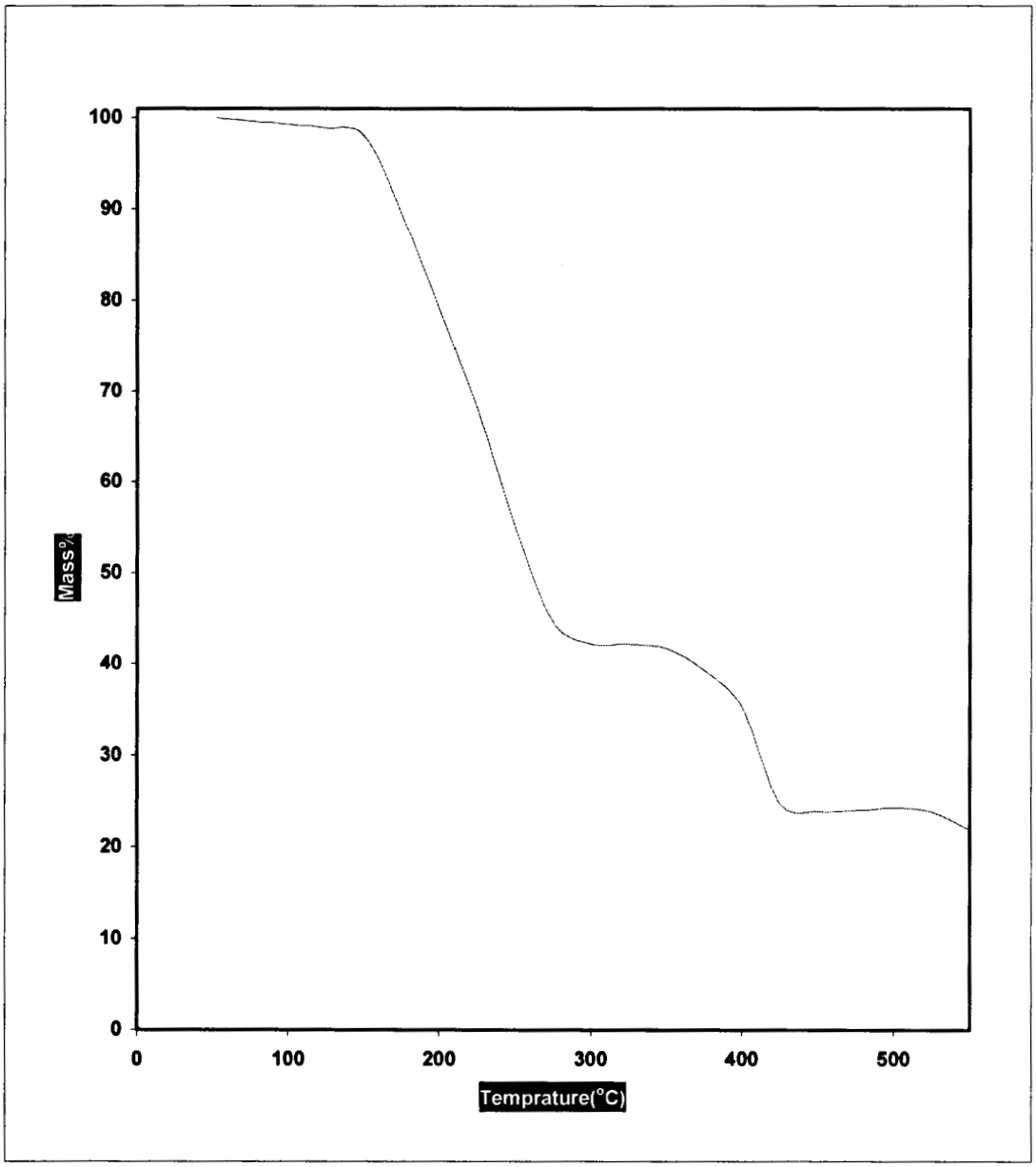

Figure II. 2.3 TG trace of ZnDSC

Table II.3.1
Thermal decomposition data of Cu(II) complex of dimedone bis –2-aminothiophenol-[$CuL(H_2O)_2$]

Complex	Stage	Temp range in TG	Peak temp	Loss of mass %			Assignments
		^0C	^0C	From TG	Theoretical		
$[CuL(H_2O)_2]$	I	90-160	120	7.7	7.97		Loss of 2 molecules of water
	II	160-280	240	23.1	23.9		Loss of 1 molecules of dimedone
	III	340-440	400	52.8	50.49		Loss of 2 molecules of aminothiophenol + and addition due to oxide formation
				83.6	81.49	83.22	$[CuL(H_2O)_2] \rightarrow CuO$

Table II.3.2
Kinetic parameters of the decomposition of Cu(II) complex of dimedone bis –2-aminothiophenol-[$CuL(H_2O)_2$]

STAGE	E (kJ/K)	A sec -1	$\Delta S^{\ddagger}$(J/K)	$\Delta H^{\ddagger}$(kJ)	$\Delta G^{\ddagger}$(kJ)	γ	n
I	14.48	8.3E-2	-267.82	11.22.	116.47	-0.9806	0
II	106.45	7.2E+08	-79.81	102.19	143.13	-0.9648	1
III	321.43	3.9E+26	257.41	315.84	142.60	-0.9955	0.9

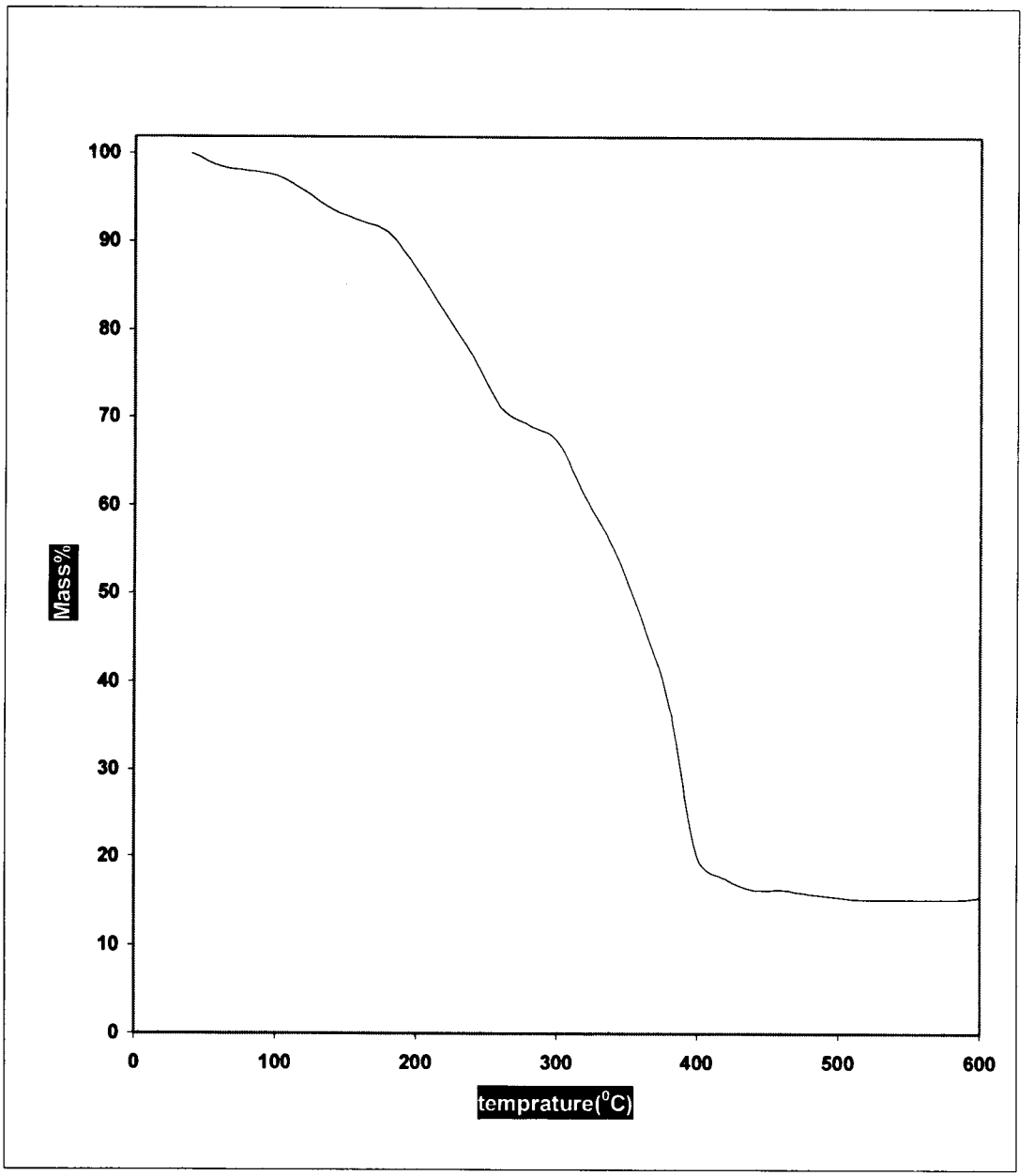

Figure II. 3.2 TG trace of $[CuDATP(H_2O)_2]$

Table II.3.3

Thermal decomposition data of Ni(II) complex of dimedone bis-2-aminothiophenol-[NiL(H_2O)$_2$]

Complex	Stage	Temp range in TG	Peak temp	Loss of mass %			Assignments
		^{0}C	^{0}C	From TG	Theoretical		
[NiL(H_2O)$_2$]	I	80-160	100	8.5	8.05		Loss of 2 molecules of water
	II	160-230	210	51.9	51.48		Loss of 1 molecule of dimedone and 1 ATP part
	III	230-300	260	23.2	23.72		**Loss** of 1 ATP and formation of oxide
				83.6	83.72	84.21	[NiL(H_2O)$_2$]→NiO

Table II.3.4

Kinetic parameters of the decomposition of Ni(II) complex of dimedone bis –2-aminothiophenol-[NiL(H_2O)$_2$]

STAGE	E (kJ/K)	A sec -1	$\Delta S^{\ddagger}$(J/K)	$\Delta H^{\ddagger}$(kJ)	$\Delta G^{\ddagger}$(kJ)	γ	n
I	40.11	1.052*E3	-188.91	37.01	107.47	-0.9882	0.76
II	209.318	5E+20	146.58	205.30	134.50	-0.9806	0.82
III	258.69	1E+23	193.57	254.68	161.18	-0.9633	0.97

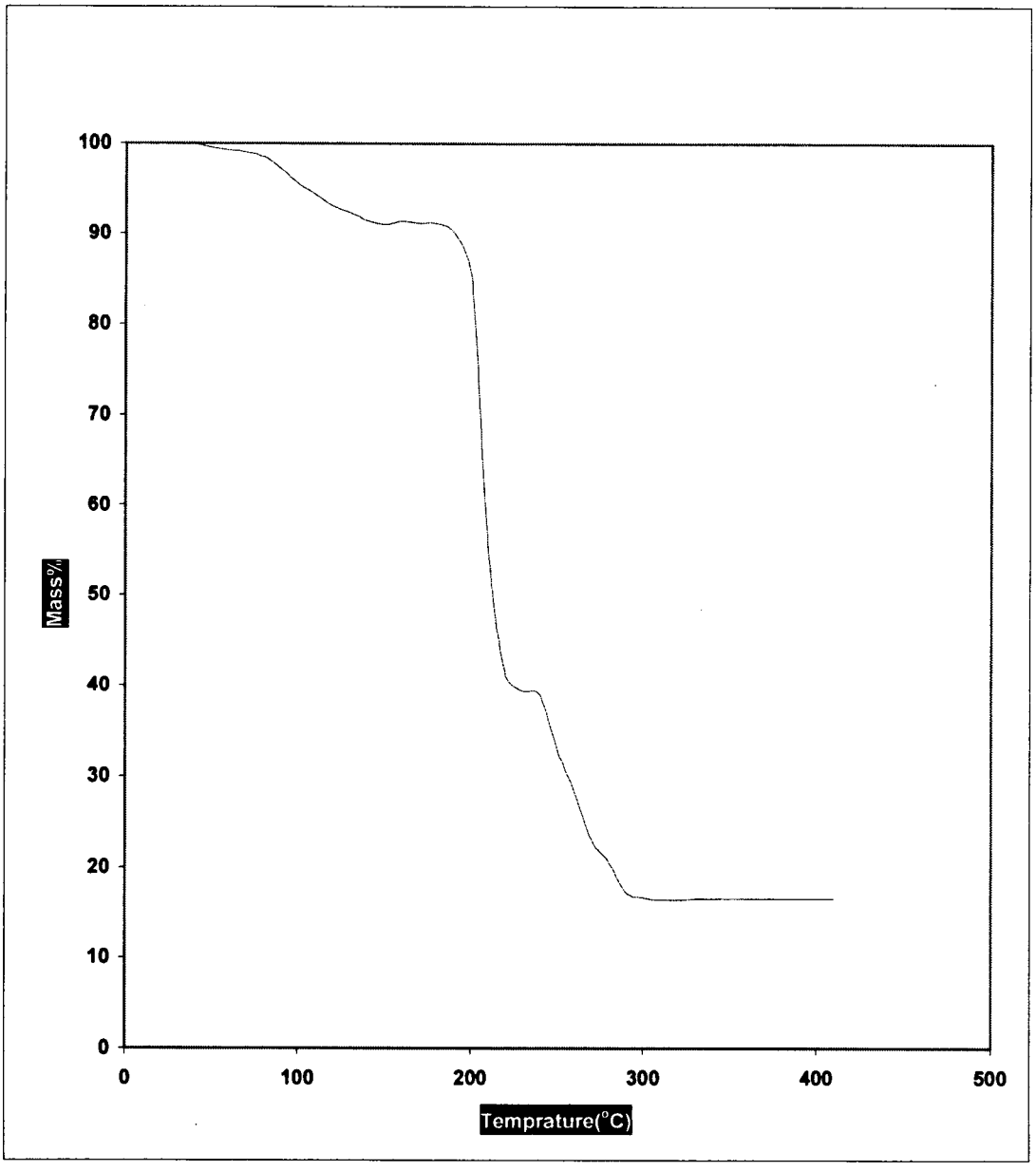

Figure II. 3.2 TG trace of [NiDATP(H_2O)$_2$]

Table II.3.5
Thermal decomposition data of Zn(II) complexes of dimedone bis-2-aminothiophenol-[ZnL]

Complex	Stage	Temp range in TG	Peak temp	Loss of mass %			Assignments
		^{0}C	^{0}C	From TG	Theoretical		
[ZnL]	I	160-370	230	56.20	55.10		Loss of 1 molecule of dimedone And 1 molecule ATP molecules
	II	370-530	490	23.80	25.87		Loss of 1 molecule of ATP and formation of oxide
				80.00	80.97	81.27	[ZnL] → ZnO

Table II.2.3.6
Kinetic parameters of the decomposition of Zn(II) complexes of dimedone bis –2-aminothiophenol-[ZnL]

STAGE	E (kJ/K)	A sec -1	$\Delta S^{\ddagger}$(J/K)	$\Delta H^{\ddagger}$(kJ)	$\Delta G^{\ddagger}$(kJ)	γ	n
I	45.71	4.4+E1	-217.42	41.74	146.76	-0.9812	0.8
II	178.41	2E+10	-53.86	172.06	213.16	-0.9786	0.93

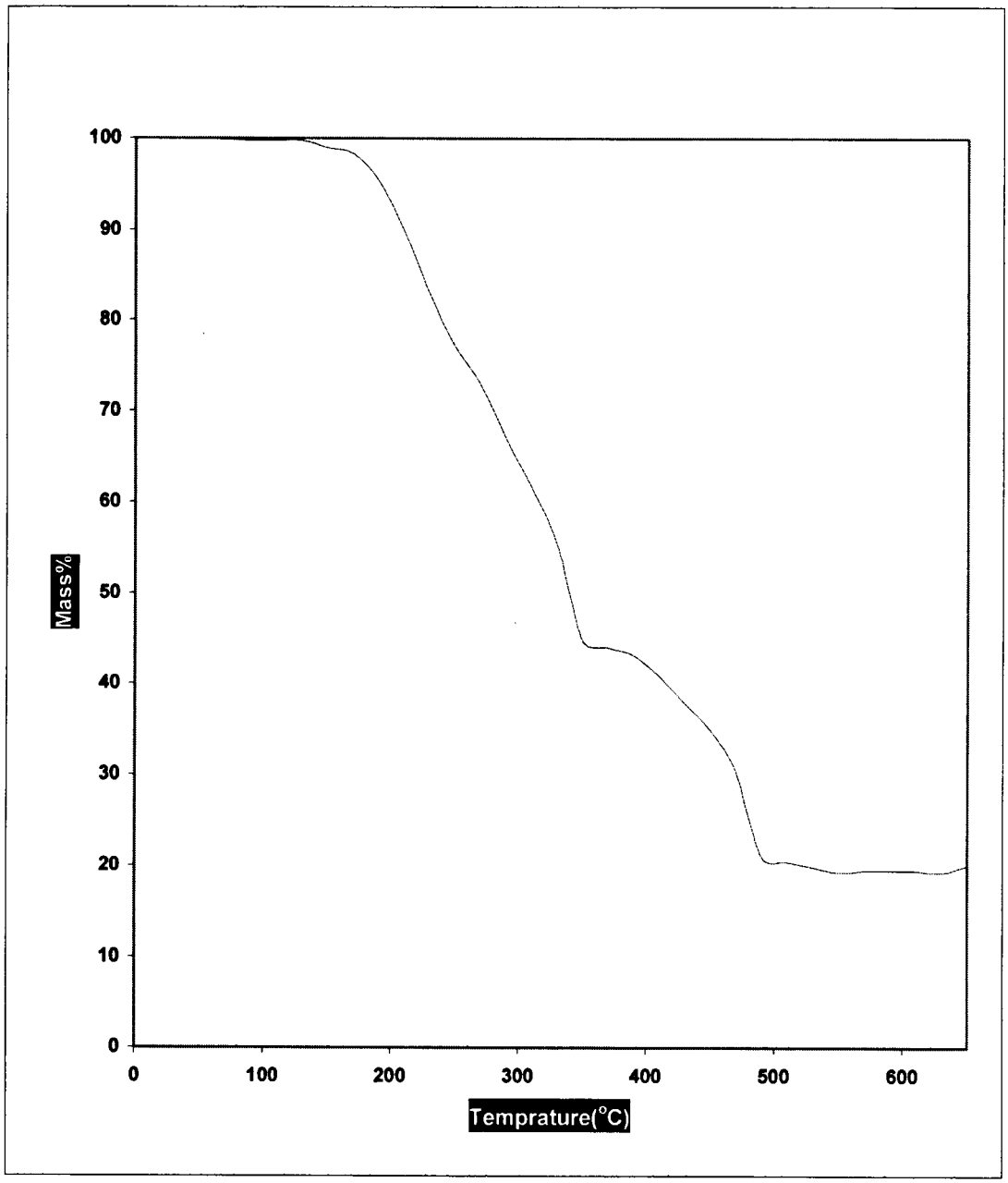

Figure II. 3.3 TG trace of [ZnDATP]

Table II.4.1
Thermal decomposition data of Cu(II) complex of dimedone bis-2-aminophenol-[$CuL(H_2O)_2$]

Complex	Stage	Temp range in TG	Peak temp	Loss of mass %			Assignments
		^0C	^0C	From TG	Theoretical		
$[CuL(H_2O)_2]$	I	115-215	155	9.4	8.58		Loss of 2 molecules of water
	II	215-245	235	24.3	25.74		Loss of 1 molecules of dimedone
	III	245-345	295	49.22	46.71		Loss of 2 molecules of aminophenol and oxide formation
				82.92	81.04	79.99	$[CuL(H_2O)_2] \rightarrow CuO$

Table.II.4.2
Kinetic parameters of the decomposition of Cu(II) complex of dimedone bis –2-aminophenol-[$CuL(H_2O)_2$]

STAGE	E (kJ/K)	A sec -1	$\Delta S^{\ddagger}$(J/K)	$\Delta H^{\ddagger}$(kJ)	$\Delta G^{\ddagger}$(kJ)	γ	n
I	61.123	7.9+E4	-154.15	57.56	123.54	-0.9798	0.82
II	490.43	4.78E+48	682.56	486.21	139.47	-0.9839	0.98
III	114.06	16+E8	-93.00.	109.34	162.16	-0.9862	1

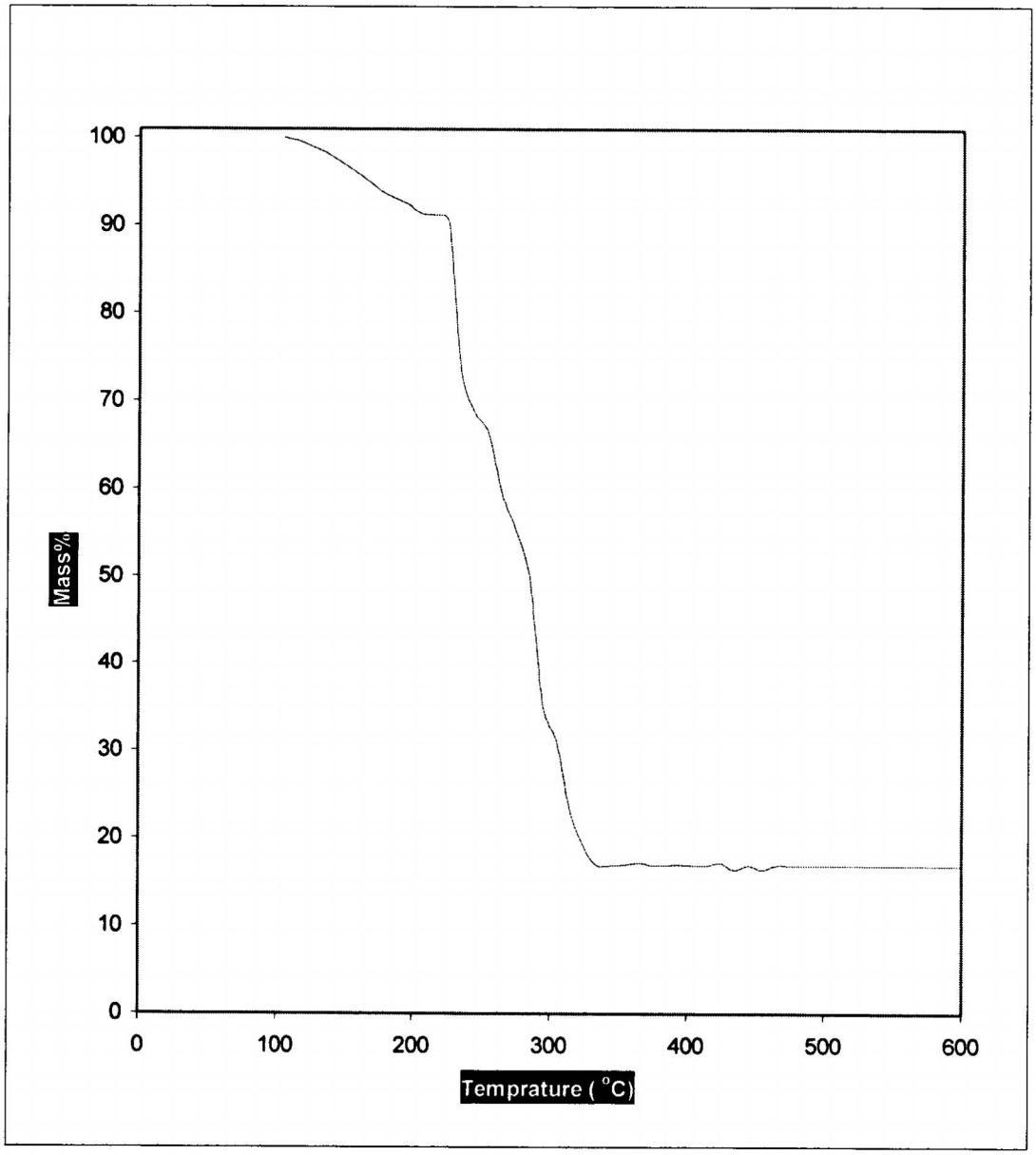

Figure II. 4.1 TG trace of [CuDAP(H_2O)$_2$]

Table II.4.3
Thermal decomposition data of Ni(II) complex of dimedone bis-2-aminophenol-[$NiL(H_2O)_2$]

Complex	Stage	Temp range in TG	Peak temp	Loss of mass %			Assignments
		^0C	^0C	From TG	Theoretical		
$[NiL(H_2O)_2]$	I	65-125	105	10	8.68		Loss of 2 molecules of water
	II	125-255	205	49.4	51.60		Loss of 1 molecules of dimedone part+1molecule Aminophenol part
	III	255-545	263	20.6	21.70		1 molecules of aminophenol and oxide formation
				81.7	81.98	81.64	$[NiL(H_2O)_2] \rightarrow NiO$

Table II.4.4
Kinetic parameters of the decomposition of Ni(II) complex of dimedone bis –2-aminophenol-[$NiL(H_2O)_2$]

STAGE	E (kJ/K)	A sec -1	$\Delta S^{\ddagger}$(J/K)	$\Delta H^{\ddagger}$(kJ)	$\Delta G^{\ddagger}$(kJ)	γ	n
I	56.73	5.6+E5	-136.78	53.59	105.30	-0.9955	0.65
II	601.62	3.99E+60	910.78	597.39	134.71	-0.9882	0.95
III	394.83	5.83E+35	434.89	390.38	157.27	-0.9284	0.99

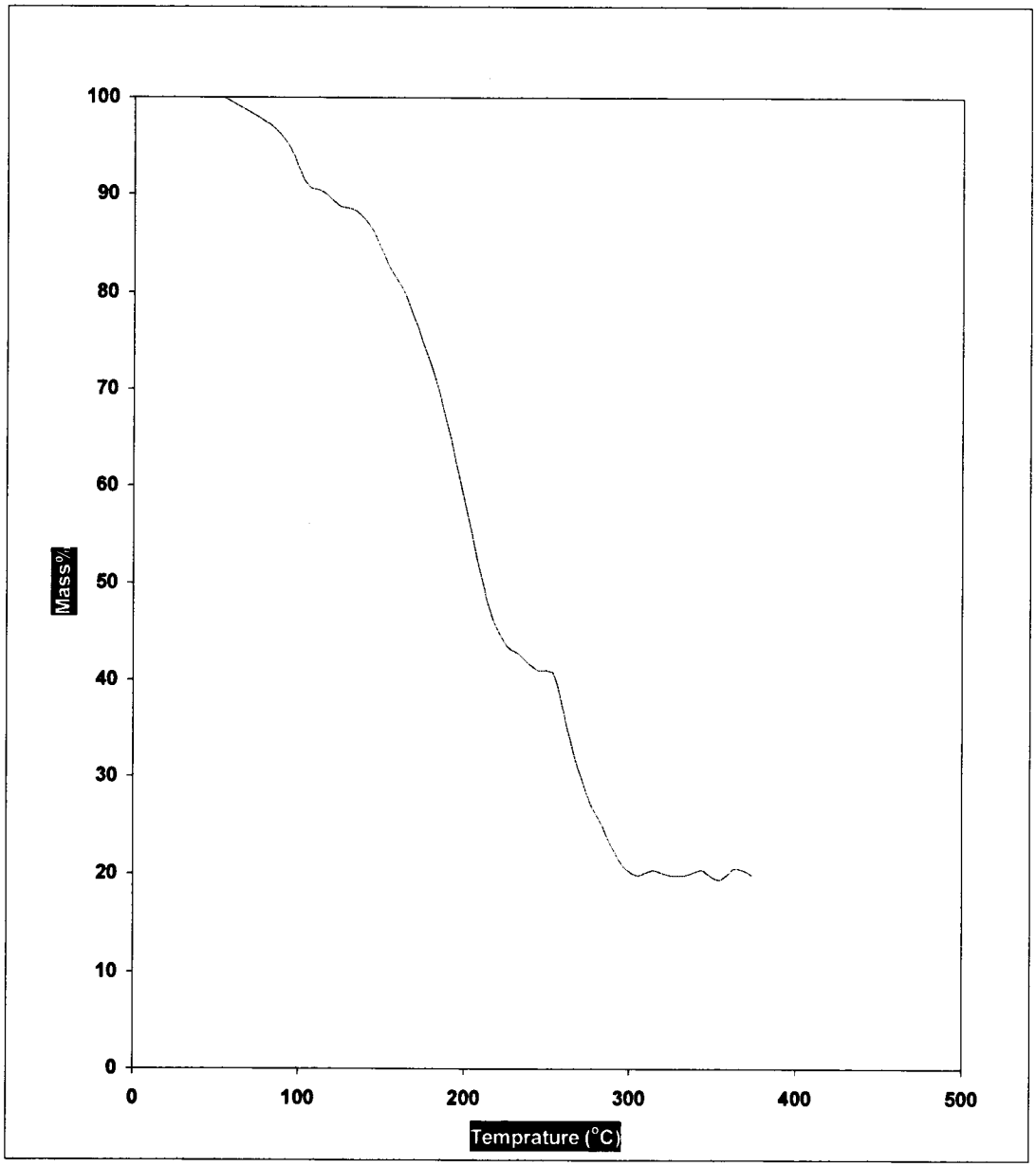

Figure II. 4.2 TG trace of [NiDAP(H_2O)$_2$]

Table II.4.5
Thermal decomposition data of Zn(II) complex of dimedone bis-2-aminophenol [ZnL]

Complex	Stage	Temp range in TG	Peak temp	Loss of mass %			Assignments
		^{0}C	^{0}C	From TG	Theoretical		
[ZnL]	I	165-295	215	55.7	55.52		Loss of 1 dimedone part and 1 aminophenol part
	II	295-395	355	22.3	23.4		1 aminophenol part and formation of oxide
				78.0	78.9	79.86	[ZnL] → ZnO

Table II.4.6
Kinetic parameters of the decomposition of Zn(II) complex of dimedone bis –2-aminophenol-[ZnL]

STAGE	E (kJ/K)	A sec -1	$\Delta S^{\ddagger}$(J/K)	$\Delta H^{\ddagger}$(kJ)	$\Delta G^{\ddagger}$(kJ)	γ	n
I	124.32	1.80E+10	-52.70	120.26	145.98	-0.9848	0.91
II	210.08	1.37E+16	57.82	205.65	169.33	-0.8775	0.99

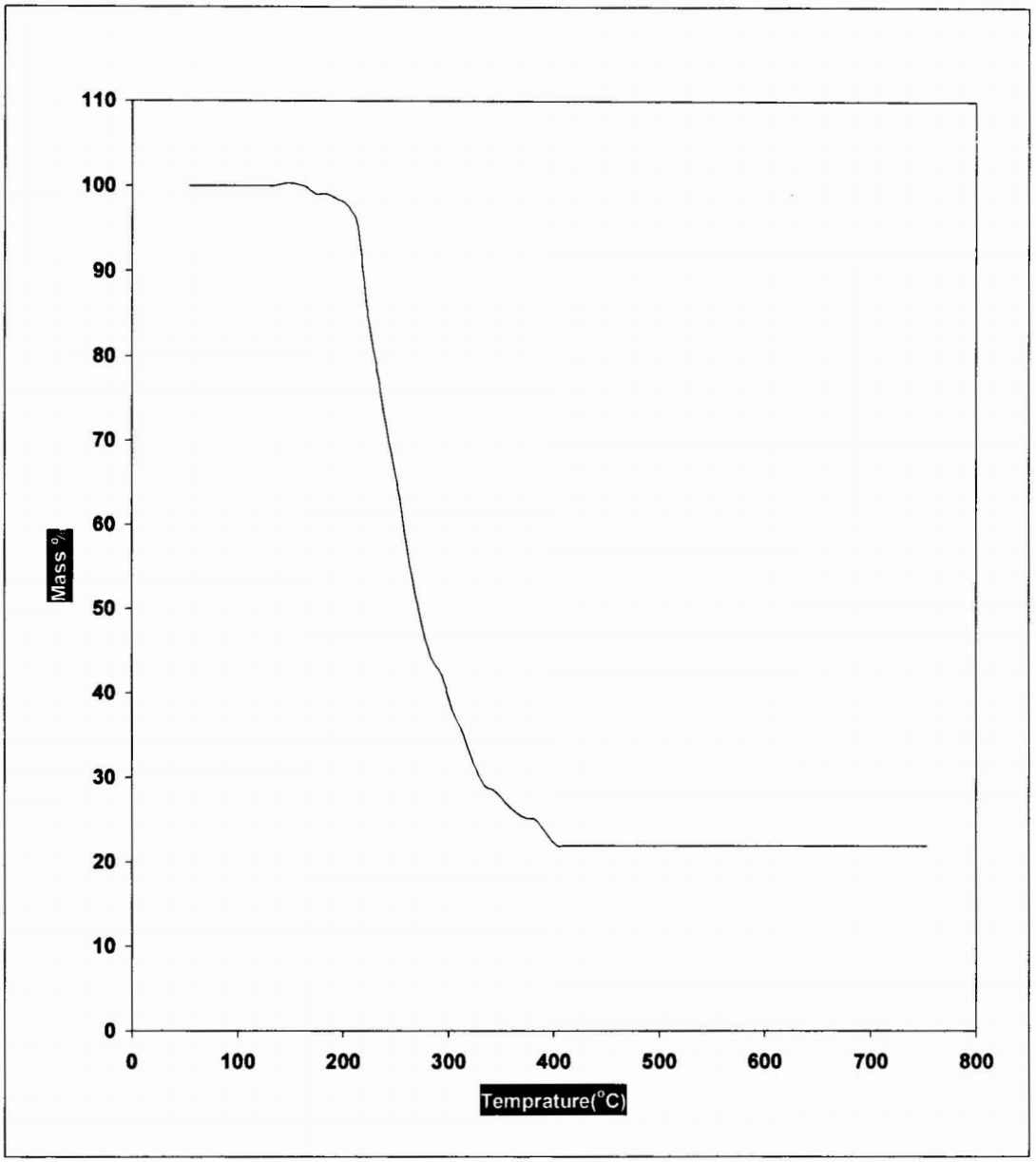

Figure II. 4.3. TG trace of [ZnDAP]

References

1) Christian,S.*Soil Sci. Soc. Am. J.* **2004**, 68,1656–1661.

2) Vadim, M.; Serge, B.; Michel, L. B.; Sophie, D.; Jaroslav, S. Phys. *Chem. Chem. Phys.* **2000**, 2, 4708-4716.

3) Yilmaz.I.; Cukurovali, A. *Polish J. Chem.* **2004,** 78, 663–672.

4) Marisa ,S. C.; Clovis A. R.; Valentina, C. M. G.; Henrique, E. Z.*Quimica Nova.* **1999,** 22.

5) Osman ,A.H.; Aly,A.A.M.; El-Mottaleb,M.A.; Gouda G. A. H., *Bull. Korean Chem. Soc.* **2004**, 25, 1.

6) Iffet Sakyan.; Gunduz,N.; Gunduz,T. Ankara University, Science Faculty, Department of Chemistry, Ankara, Turkey . www.ankara.edu.tr .**2004.**

7) Brown, M.E. *Introduction to Thermal Analysis Techniques and Applications Series*; Hot Topics in Thermal Analysis and Calorimetry, **2002** , 1 , 280 pp.

8) Duval , C. *Inorganic Thermogravimtric Analysis* ;New york. Elsevier,**1963.**

9) Smoothers, W.J.; Yaochiang, M.S. *Hand book of differential thermal analysis* : Newyork, chemical publishing co, **1966.**

10) Garn,P.D. T*hermo analytical methods of analysis* ; New York: Interscience, **1964**.

11) Schulze, D. Differential thermal analyzer, Berlin, **1969.**

12) Wendlandt, W.W. *Inorg.Nucl.chem.* **1963**, 25 ,545.

13) Horowitz, H . H.; Metzger, G. *J. Anal. Chem.* **1963** ,35, 1464.

14) Coats, A.W.; Redfern, J.P. *Nature.* **1964**. 201, 68.

15) Maccallum, J.R .; Tanner, J. *Europian.polym.j.* **1970** ,61,1033.

16) Soliman, A.A.; Linert,W. *Thermochimica Acta.* **1999**,338, 67,75.

17) Atkins .P.W. *Physical chemistry* ;Oxford university press, 1075 pp .

18) Sadeek ,S.A.; Refat, M.S.; Teleb, S.M. *Bulletin of the Chemical Society of Ethiopia*. **2004**, 18, 2, 149-156.

19) Jeong,B.G etal. *Bull. Korean. Chem. Soc.* **1996** ,17, 173 - 179 .

20) Parra, M.etal. *j. Chil. Chem. Soc.* **2003**,48 ,1 .

21) Rao,N.S.;Reddy ,M.G. *Biol Met.* **1990**,3,1,19-23.

22) Friscic, T.; Lough, A. J. ; Ferguson, G.; Kaitner, B. *Acta Cryst.* **2002**, C58, 313-315 .

23) Al-Shihri,A. S. M.; Abdel-Fattah, H. M. *Journal of Thermal Analysis and Calorimetry.* **2003** ,71, 2 , 643 - 649 .

24) Ascenzo ,G.D.; Wendlandt,W.W. *Anal.Chem.Acta.* **1970**,50,75.

25) Chang,F.C.;Wendlandt, W.W. *Thermochim.Acta.* **1971**,293.

26) Perry. D.L.; Vaz ,W. C.; Wendlandt, W .W. *Thermochim.acta.* **1974**, 9,76.

27) Nikolaev, A.V.; logvinenko V.A.; Myachina, L.I. *Thermal analysis* ; New York: Academic Press, **1969**,779.

28) Vatsala, S.; Parameswaran, G. *J. Them. Anal.* **1986**,31,883.

29) Sheshadri Naidu, R .;Ragavanaidu.R. *Indian J. Chem.* **1967**, 15A ,65.

PART III
ANTIFUNGAL ACTIVITIES OF SCHIFF BASE COMPLEXES

Abdul Jaleel.U.C "Synthesis, thermal and spectral studies of some transition metal complexes of schiff bases" Thesis. Department of Chemistry , University of Calicut, 2005

PART III

Antifungal activities of Schiff base complexes

Chapter. 1

INTRODUCTION

Damages due to diseases play a major role in limiting black pepper (*Piper nigrum* L.) production in India. Several diseases caused by fungi, virus and mycoplasma affect black pepper, besides nutritional disorders. Foot rot is the major disease of black pepper in India. It is popularly known as quick wilt and is caused by he fungus *Phytophthora capsici.* This disease is prevalent during southwest monsoon in all black pepper growing tracts of south India and is characterized by leaf infection with characteristic fimbriate margin and foot rot[1-5]. Crop losses due to foot rot disease in Kerala is estimated to be 10% of the total production [6].

Phytophthora as plant pathogen

Fungi are a group of spore bearing organisms lacking chlorophyll. They are heterotrophic in their nutrition. They either infect living organisms as parasite or utilize dead organic matter as saprophytes to obtain their food. The thallus or body of the fungus is called as mycelium that consists of a large number of branched tubular, hyaline structures each of which is individually called as hypha. Many fungi are parasitic on plants causing severe diseases and crop loss [7, 8] . *Phytophthora* is a oomycetous fungus which cause severe diseases in many horticultural crops worldwide [9].

Phytophthora species cause severe diseases on various crops[2].Many of the plantation and spices crops in India are affected by *Phytophthora* and resulting in economic crop loss. They affect rubber, coconut, arecanut, black pepper, cardamom, vanilla etc. Therefore the study of their biology and control is highly significant. Ribeiro described various procedures for the study of *Phytophthora* [10].

Biology of *Phytophthora*

Phytophthora is oomycetous fungus, which is a group of mycelial organisms and represents a unique evolutionary line. In addition to being dispersed via zoospores and generating thick walled sexual oospore, they posses features such as cellulose (β → 1, 4 glucans) in their cell wall, vegetative diploidy, heterokont flagella [11-14] , tubular mitochondrial cristae[15]. *Phytophthora* species do not synthesise sterols but require an exogenous source of β hydroxy sterols [16].

Phytophthora reproduce by vegetative, asexual and sexual methods. Vegetative growth of *Phytophthora* depends upon the nutrient status. The asexual method of reproduction is by sporangium or more specifically a zoosporangium, which means a vessel containing zoospore. Sporangia are born on long stalks called sporangiophores. In some species new sporangiophores emerge through the base of the old sporangium from which uninucleate zoospores have been released. In other species new sporangiophores arise just beneath the base of the old sporangium, i.e. they are sympodial and produce more sporangia successively. It varies in size and shape [9,10].

Sporangium germinates in aqueous solutions or in agar media by the production of germ tube that usually emerges from the tip of the sporangium (direct germination). In aqueous medium sporangium produces uninucleate biflagellate

zoospores that are released into the water (indirect germination). The zoospores are renyform in shape with two heterocont flagella emerging from the concave side. In *Phytophthora* a long whiplash characterize one of the flagella and shorter tinsel the other [9,11].

Zoospores swim for hours and eventually cease to swim, round up and within minutes develop a cell wall. At this stage the spore is called a cyst. Encystment can be induced by agitation either produced artificially by shaking zoospore in a flask or naturally by their bumbing against solid surface. Eventually their flagella are shed and cysts germinate by producing germ tubes. Occasionally another zoospore may form within the cyst and be released. Zoospores are considered to be the major infectious propagules [9,10]. The chlamydospores are spherical to oval. It is hyaline or brown and has either thin or thick wall. Chlamydospores may form terminally at the tips of hyphae or may be intercalary (between the tip and base of hyphae) [9,10].

Phytophthora reproduce by sexual spores under suitable environmental conditions. The sexual structure of *Phytophthora* is composed of an antheridium (male component) and an oogonium (female component). The oogonia are usually globose or subglobose but are occasionally pyriform. The oogonium is delimited from the hyphae by septum; the antheridium is delimited by a septum that attaches to the oogonial incept. Oogonial incept grows through the antheridial incept. This type of antheridium is classified as amphigynous (surrounding the female). In some species antheridium attaches to the oogonium by contact to the lower hemisphere side of the oogonium and is called paragynous (beside the female). Reduction division or meiosis of the nucleus occurs in the coenocytic antheridia and oogonia. A fertilization tube from the antheridium ruptures the oogonial wall and deposits the antheridial nucleus. The haploid nuclei from the antheridium and the oogonium are

fused to form the diploid nucleus. A nucleus presumed to be the fusion nucleus remains along oogonial cytoplasm. The single egg that forms within the oogonium is globose and characteristically develops a thick inner wall composed largely of β →1-3 glucans. The diploid oospore germinates under suitable conditions by the production of single or multiple germ tubes at the tips. Some species of *Phytophthora* are homothallic where as others are heterothallic. *P. Capsici* is heterothallic ,however only one mating types is present in India and therefore sexual reproduction is not reported [9].

Foot rot of black pepper caused by *Phytophthora capsici*

Phytophthora capsici is a devastating soil born pathogen that affects all parts of the black pepper plant. Infection of the under ground portion remain undetected until symptoms appear on the aerial portion. This renders the control measures taken after noticing the symptoms ineffective. Its infection on under ground parts like roots and collar (foot) result in the root rot and foot rot respectively. Aerial infections on leaves, spikes and stems also occur and spread rapidly under favourable conditions causing yellowing and wilting of leaves followed by defoliation.[17,]

Phytophthora capsici occur both in the nursery as well as in the main field. The fungus survives in the infected plants and soil for a period of more than a year. The pathogen spreads mainly through rain and water splashes. High rainfall, high relative humidity, low temperature and shorter duration of sunshine are the factors that favour the spread of the disease in black pepper plantation. Climatic conditions influence the life cycle of *Phytophthora*, its pathogenicity and the epidemic it causes. Fungus remains dormant in the form of resting spores during unfavorable seasons[18] .

Sporangia are predominantly tapered at the base and are caducous with long pedicels varying in length. Sporangia are extremely variable in shape and

dimension. Black pepper isolates of *Phytophthora* produce sporangia on sporangiophores that are characteristically umbellate. *Phytophthora capsici* is predominantly heterothallic and antheridia are amphigynous. Oogonia are spherical or sub spherical and hyaline to brown in colour. Dimension of oogonia from different host vary from 23-50 μm[9,10]. *Phytophthora capsici* has four different phases of growth, which are mycelial growth, sporangial formation, zoospore liberation and zoospore germination. A compound inhibiting one of these phases could be useful as an antifungal agent [19].

Biological control

Although chemical control is feasible against *Phytophthora,* owing to the health hazardous nature of chemical fungicides, biological control has emerged as an alternative to chemical control [20]. *Gliocladium virens, Trichoderma* spp, vesicular arbuscular mycorrhizae and *Pseudomonas fluorescens* etc are used against *Phytophthora capsici. Trichoderma* spp inhibited mycelial growth and production of sporangial production in *P. capsici* [21].

Biocontrol agents produce enzymes and secondary metabolites, which inhibit plant pathogens. It has been reported that application of nitrogenous organic substance suppresses *Phytophthora* population in the soil [21]. Extract of garlic has been reported to be effective against *Phytophthora* sp [22].

Chemical control

During the past two decades many chemicals having selective toxicity to fungi were developed and some of them are used as fungicide in commercial scale. Fungicides are compounds that destroy a fungus or inhibit, suppress its growth. For control of *Phytophthora* infections, a number of fungicides are being used. They are often classified as contact and systemic fungicides [9].

The contact fungicides used are copper compounds especially Bordeaux mixture, Copper oxychloride and Cuprous oxide [23], Organotin compounds, Dithiocarbamates (Zineb, Maneb, Mancozeb), Chlorothalonil and phthalimides (captan, captofol and folpet)[24]. Organotin compounds are particularly effective antisporulant fungicides [25]. Ziram and Ferbam are dialkyldithiocarbamates while Nabam, Zineb and Maneb are dialkyl bis dithiocarbamates. The dithiocarbamates are ideal to copper fungicides because they are much less phytotoxic. Chlorothalonil has greater persistence in rainy weather than other contact fungicides [26].

Another class of fungicide is systemic fungicides. These are the compounds, which can be taken up through roots, stems and leaves. Comparing with protective fungicides, systemic fungicides are less subject to loss by rainfall and can suppress the pathogen even after the infection. The systemic fungicides effective against *Phytophthora* are classified into several groups. These include the carbamates (Prothicarb and Propamocarb) [27,28] isoxazoles (Hymexazol), cyanoacetamide oximes (Cymoxanil), ethyl phosphonates (Fosetyl Al) and phenyl amides (Metalaxyl and several related compounds) [26 , 29].

Metalaxyl (DL-methyl – N- (2,dimethyl – phenyl)- N (2-methoxyacetyl) alaninate)-a phenyl amide- was the most effective fungicide on mycelial growth of *Phytophthora capsici*. Metalaxyl was also found to be compatible with Furadan and Phorate. Among the fungicides Metalaxyl-Ziram or a similar combination has been proposed as a major component in the integrated management of *Phytophthora* infections in black pepper [30].

Even thorough several chemical controls are available in commercial scale, scientists and farmers are facing major hindrances like phytotoxicity, environmental pollutions due to this compounds. The possible means for the solving this intricacy is

the improvement of biological control or development of chemical control with lesser hazardness. On this context search for a new chemical control will be highly justifiable. Such a development will be an added advantage in the drug research against the oomycete pathogen like *Phytophthora capsici.*

Coordination compounds

Coordination compounds in general and derived from Schiff base in particular has played an important role in the development of anti fungal agents. The biological activities of some transition metal complexes with Schiff bases have been reported. Schiff base complexes of Copper (II), Nickel (II), Vanadium (IV) and Uranium (VI) derived from phenyl butazone and 2-amino phenol shows antibacterial activity against *E. coli*[31].

Among the Schiff base complexes of first transition series Nickel complex of N-benzoyl – N' – (2 – aminophenyl) thiocarbamide has been shown to exhibit antifungal activity. The organism, *Pyricularia oryzae* which cause rice blast and *Helminthosporium oryza* which cause brown leaf spot can be controlled with Ni (II) complexes of 1– phenyl-3–methyl–4–nitroso–2–pyrazolin–5–one and 3–methyl–4–nitroso–2– pyrozolin–5–one[32].

Copper complexes of the ligands N-benzoyl-N'- (2-aminophenyl) thiocarbamide is found to be effective compounds for *Aspergillus niger, Fusarium oxysporum* and *Helminthosporium oryzae* [32]. Copper complexes are reported to be more active fungicides than similar Iron, Cobalt and Nickel complexes. The complexes were found to be more effective than the free ligands[33]. This findings turn out to be another hope in the tackling of plant and animal diseases. So coordination compound have a wide possibility in the exploration of new antifungal, antibacterial, antiviral agents.

Mechanism of antifungal activity

The study of the fungicide is now bound for the development of mode of action of drugs in a more precise way. This can be achieved by studying the percentage of inhibition by different compounds on a trial and error method., and subsequent determination of mode of action by choosing the most effective drug[34]. Specific determination of the mechanism of antifungal activity may lead to the better development of extra apposite antifungal agents.

Coyle Barry *et al.*, studied the mode of antifungal activity of 1,10 phenanthroline and its Cu (II), Mn (II) and Ag (I) complexes against the pathogenic yeast *Candida albicans* and showed that all the complexes promote reduction in the levels of cytochromes b and c in the cells, while the Ag (1) complex lowers the amount of cytochromes aa_3. They damage mitochondria function and uncouple respiration [34]. Similar studies in *Phytophthora capsici* will create way for the development of antifungal agents.

Scope of present investigation

In spite of the popular trend for completely organic and pesticide free farming, the diseases like foot rot of black pepper will probably never be completely controlled without fungicides since the pathogen spreads rapidly under favorable conditions. But the hazardness of the presently using fungicides /pesticides creates much anxiety among the public. So the pursue for a hazardous free chemical control is the next pragmatic way out in the warfare against fungi. The developments of antifungal agents look for a special attention in molecular and genetical level also. So the studying and revealing the exact mode of the anti fungal activity of different compounds will further help the above said search in the new direction

In view of this, a group of ligands and their metal complexes were tested against the mycelial growth of *Phytophthora capsici*. Based on the lead from the preliminary study a detailed study was under taken to find out the inhibitory effect of these ligands and metal complexes of Copper, Cobalt, Nickel on the various stages of the growth of *Phytophthora capsici* viz. mycelial growth sporangial production, zoospore liberation and zoospore germination.

CHAPTER. 2

MATERIALS AND METHODS

In this chapter anti fungal activity of transition metal complexes of dimedone - bis -2-aminophenol (H_2DAP), Cyclohexanone -2-aminophenol (HCAP), pyrolidone -2-aminophenol (HPAP), dimedone bis -2-aminothiophenol (H_2DATP) are described. The details of preparation and characterization of the above-mentioned complexes are presented in Part I. It was found that all complexes were soluble in DMSO. Standard solutions of complexes were prepared in DMSO and diluted to the required concentration using sterile distilled water. The complexes in required quantity were incorporated with carrot agar medium to study its effect on various growth stages of *Phytophthora capsici* infecting black pepper.

CULTURE MEDIA

Carrot agar was used as the culture media to grow *P. capsici.* The materials required for the preparation of 1 liter of carrot agar are,

Carrot – 200g

Agar – 20 g

Distilled water – 1 liter

The 200 g of carrot was pealed and cut into small pieces. The carrot was grinded and about one liter of juice was obtained. The carrot juice was then boiled and 20g of agar was added while stirring. This was distributed in to conical flasks and sterilized by autoclaving at 121°C (15lb) for 15 minutes.

ISOLATION OF *Phytophthora capsici*

. Infected roots of diseased plants were collected and brought to the laboratory. It was washed several times with sterilized water and small pieces were cut from

advancing margins of lesions. It was then sterilized in 0.1% $HgCl_2$ for 30 seconds and washed with three charges of sterile distilled water and blot dried. These bits were placed on Carrot Agar media containing PVPH and incubated at 24^0C for 48- 72 hours. The *Phytophthora* was sub cultured into carrot agar slants for further studies.

BIOASSAY

The thermo labile nature of the complexes was noted and it was found that except Co (II) all other complexes were thermo stable. Ligand was found to be thermo labile. Hence, all further studies were conducted by adding the solutions of these complexes to carrot agar media before sterilization for thermo stable complexes. For thermo labile complexes, it was added just before pouring the media into plates. The effect of these complexes on mycelial growth, sporulation (sporangial production), zoospore release and zoospore germination of *Phytophthora capsici* was studied by incorporating the complexes into Carrot Agar media as specified.

The complexes and ligands were dissolved in DMSO-water mixture (1:40 ratio) to form a stock solution of 2000ppm. From the stock solution, different dilutions were made.

IN-VITRO* EFFECT OF COMPLEXES ON VARIOUS STAGES OF *PHYTOPHTHORA CAPSICI

Mycelial growth

Poisoned food technique was used for the mycelial growth study [19]. The test solutions were mixed with carrot agar to obtain concentrations ranging from 250 to 1000 ppm so as to form a final volume of 50ml medium. The amended medium was poured into petriplates (90mm) @20ml per plate. Inoculum plug of *Phytophthora capsici*, 5mm in diameter, were taken from the periphery of 48-hour-old culture and placed in the centre of the petriplates. Three replications were maintained. Carrot

Agar plates without test solutions and inoculated with culture disc were used as the control. The plates were incubated at 25 ± 1^0C in dark and growth of the colony was measured after 72 hours of inoculation. The radial growth of colony was measured from three sides of the plate and the mean of these three readings were taken as the radius of the colony. The growth of the colony in the control sets were compared with that of various treatments and the percentage of inhibition was calculated using the formula, ((C-T) / C) X 100 Where 'C' is the radial growth in the control, 'T' is the radial growth in the complex solutions.

Sporangial production

For studying the effect of metal complexes on sporulation, the *Phytophthora capsici* was grown on carrot agar in dark for 48 hour at 25^0C. Few discs of 5mm size taken from the edge of 48hr old culture were placed in sterile petriplates containing 10ml test solutions of different concentrations and incubated under fluorescent light for 24 hour. In control, the discs were placed in 10ml of sterile distilled water. Number of sporangia produced per microscopic field (20 X) was counted and the average number of sporangia per field was calculated and compared with that of control [10]. The percentage inhibition over control was calculated using the formula

((C-T) / C) X 100

Where 'C' is the number of sporangia in the control, 'T' is the number of sporangia in the complex solutions.

Zoospore Release/ Indirect Germination of Sporangia

To study the effect of complexes on zoospore release (indirect germination of sporangia), 5mm discs cut from the periphery of 48hour old culture was allowed to sporulate as described above. Cold shock treatment was given by keeping the

petriplates in the freezer at 4^0C for 10 minutes. These plates were then taken and incubated at laboratory temperature for 30 minutes before observation. Distilled water instead of test solution was used in control. Zoospores from sporangia were released after the cold shock. The number of sporangia released are counted per microscopic field. Also noted was the number of sporangia do not opened[10]. Percentage inhibition of zoospore release was calculated by using the formula ((C-T) / C) X 100 Where 'C' is the number of sporangia opened in the control, 'T' is the number of sporangia opened in the complex solutions.

Zoospore germination

The effect of test solutions on germination of zoospores was studied. The zoospores were produced by following the above procedure and collected in vials. The zoospore settled at the bottom were collected and placed in clean cavity slides containing 50µl of test solution. The zoospores were taken in cavity slides containing different concentration of test solution ranging from 250-1000ppm concentrations and incubated for 12 hours at 24^0C. Replicates were also kept for all the concentrations. In each slide, 5 microscopic fields were observed for counting the number of zoospores germinated [10]. Percentage inhibition of zoospore germination was calculated using the formula ((C-T) / C) X 100, where 'C' is the number of zoospores germinated in the control, 'T' is the number of zoospores germinated in the complex solutions.

In order to understand the level of difference in the percentage of inhibition of complexes and their corresponding metal salts, a detailed study about the extent of inhibition were conducted on *Phytophthora capsici* by using the corresponding metal acetates.

Chapter 3

ANTI FUNGAL STUDIES OF

Co (II), Ni (II), Cu (II), Zn (II) COMPLEXES

It is well known that the elements of first transition series form biologically important complexes. Among them compounds of Cu (II) and Zn (II) found application in large number of fungicides. So the study of the antifungal activity of the complexes of Co (II), Ni (II), Cu (II), and Zn (II) are highly relevant. A report on the inhibitory effect of H_2DAP, H_2DATP HCAP, HPAP, complexes of these metals on the four stages of growth of *Phytophthora capsici* is presented here.

Mycelial growth

The Mycelial growths at different concentrations of the all complexes are presented in the Fig.III.3.1-III.3.4. The data of inhibition of mycelial growth of *Phytophthora capsici* on carrot agar with different concentrations of complexes are presented in Table III.3.1-III.3.4. The data showed that, among the complexes Cu(II), Ni(II), Co(II) complexes are found to be more effective against the *Phytophthora capsici*. In the case of H_2DAP complexes, those of Cu(II),Co(II) show more than 50% inhibition at 1000ppm concentration. In the case of HPAP, Co(II), Cu(II) and Ni(II) complexes show more than 50% inhibition at 750ppm. The copper complex is highly active and it shows more than 50% inhibition at 500ppm. Ni(II), Cu(II) complexes of H_2DATP are highly active and showed more than 50% inhibition at 1000ppm. Among them the Cu(II) complex is most active and it showed more than 50% inhibition at 250ppm.

The HCAP complexes showed comparatively lower inhibition at lower concentrations. But all complexes showed more than 50% inhibition at 1000ppm Generally the complexes showed greater activity compared to the ligands. Among the metal complexes of Cu(II) complexes are more active than those of others. Zn(II) complexes are generally less active. No regular trend is found among them.

Comparison of the activity of the ligands showed that PAP is more active at 1000ppm. H_2DATP also showed considerable inhibition.

Sporangial production

The Sporangiogenesis at different concentrations of the all complexes are presented in the Table III.3.6-III.3.9. All the complexes tested were found to be very effective in inhibiting the sporangial production. All the complexes are showed more than 50%inhibition at 250 ppm. Complexes of H_2DAP and H_2DATP are the most effective in the inhibition of sporangial production compared to the HPAP. This trend is just opposite to the trends happened in mycelial growth. Among the ligands H_2DATP showed more inhibition.

Zoospore Release

Inhibitions of zoospore release by complexes at various concentrations are presented in the Table III.3.10-III.3.13. Among DAP complexes, Co(II),Cu(II) and Ni(II) showed more than 50% inhibition at 1000ppm. But in HPAP complexes and H_2DATP complexes all the three complexes were showed an inhibition of 80% at 1000ppm. When comparing the complexes of different metals, Cu(II) complexes showed maximum inhibition. Among the ligands maximum inhibition was shown by H_2DATP and HPAP. But in every case the complexes show a better inhibition than its own Ligand.

Zoospore Germination

Inhibition shown by the complexes on the zoospore germination of *Phytophthora capsici* is given in the III.3.14-III.3.17. The results of H_2 DAP, H_2DATP and HPAP complexes of Co(II), Ni(II) and Cu(II) showed very high percentage of inhibition at 1000 ppm. At this stage all the complexes showed approximately similar behavior in inhibition. The most varied behavior observed at this stage is the almost total inhibition by copper complexes on the germination of *Phytophthora capsici.* Among the ligands PAP is showing maximum inhibitory effect.

From the above data it is clear that some of these complexes are inhibitory to all the four stages of *Phytophthora capsici.* Among the four stages the inhibition is more pronounced in the zoosporangial production and zoospore release.

Discussion

The major conclusions we can draw from the results are given. Antifungal activity is increasing during the complexation. These results are in accordance with the activity of complexes of the ligand benzoyl-N-(2-amino phenyl) thiocarbamide [32]. Antifungal activity is very pronounced in copper complexes. Ni(II), Co(II) complexes are showing very high percentage of inhibition. Zn(II) complexes showed lesser activity. Early studies showed that the trace elements Zinc, Iron, Manganese clearly promotes growth of *Phytophthora* at lower concentration [35]. The results are in accordance with the reference. These drugs are effective in the final stages of the reproduction. (Zoospore release and zoospore germination) which may be due to easiness of inhibition of certain pathways at this stage.This result is indicating that mode antifungal activity to be studied with a special reference to the final stages of reproduction.

In all types of complexes the drugs are not uniformly active suggests their bioactivity has a degree of metal-ion dependency, which indicated the metal dependency of antifungal activity.

In General, the study on chemical control of *Phytophthora capsici* is to be diverted in such manner to elucidate the mechanism of antifungal action at various stages of growth. Even though several mechanism put forwarded about the inhibition and possible way of anti fungal activity the study made by the Coyle Barry *et al.*, is very prominent[34]. They studied the mode of action of the anti-fungal compounds, 1,10-phenanthroline (phen),$[Cu(phen)_2(mal)]2H_2O$,$[Mn(phen)_2(mal)]2H_2O]$ ($malH_2$ = malonic acid), using the pathogenic yeast *Candia albicans*. All of the drugs promote reductions in the levels of cytochromes b and c in the cells, whilst the Ag (I) complex also lowers the amount of cytochrome aa_3. Cells treated with phen and the Cu (II) and Ag (I) species show reduced levels of ergo sterol whilst the Mn (II) complex induces an increase in the sterol concentration. The general conclusion is that the drugs damage mitochondrial function and uncouple respiration. This finding is useful to understand the possible mechanism of action of the drugs (coordination compounds) on the different growth stages of *Phytophthora capsici*.

Another possible way for explaining the inhibitory effects of complexes is on the basis of chelation [36,37]. Chelation theory suggested that due to chelation, the charge of the metal ion reduces because of partial sharing of positive charge with the donor groups and possible π electron delocalisation over the whole chelate ring. Due to chelation the lipophilic character [38,39] of the metal complexes increases that favors its permeation through lipid layers of cell membrane.

These observations and conclusions may open up new avenues in the quest for tackling the problem of 'Foot rot' a devastating disease that affects black pepper.

Table III.3.1
MYCELIAL GROWTH
% of inhibition by H_2DAP complexes

Compound	L=H_2DAP	CoL$(H_2O)_2$	Ni L$(H_2O)_2$	Cu L$(H_2O)_2$	Zn L
250ppm	10.34	26.67	24.14	29.66	10.34
500ppm	16.21	40.00	31.03	40.69	20.00
750ppm	20.69	46.67	32.41	46.21	31.03
1000ppm	28.28	53.33	40.69	62.76	33.79

Figure III.3.1
MYCELIAL GROWTH
Comparison of % of inhibition of Ligand (H_2DAP) and its complexes

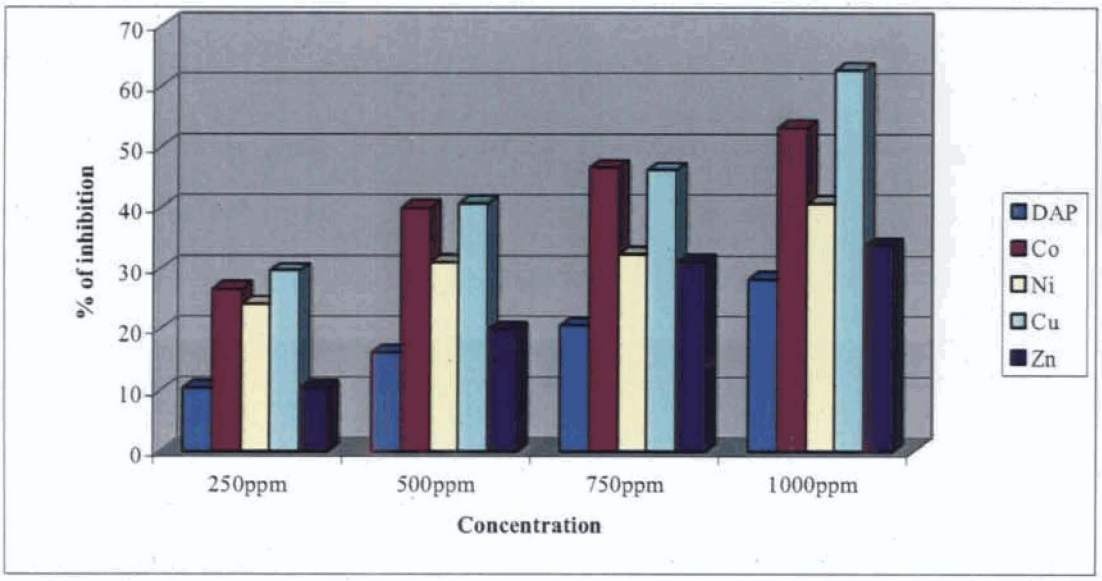

DAP=H_2DAP , Co=[CoL $(H_2O)_2$], Cu=[CuL $(H_2O)_2$], Ni=[NiL$(H_2O)_2$]

Zn=[ZnL]

Table III. 3.2
MYCELIAL GROWTH
% of inhibition by H_2DATP complexes

Compound	L=H_2DATP	CoL(H_2O)$_2$	Ni L(H_2O)$_2$	Cu L(H_2O)$_2$	Zn L
250ppm	18.62	28.48	26.90	58.62	21.38
500ppm	25.52	36.42	33.79	61.38	31.03
750ppm	32.41	47.02	37.93	71.03	33.79
1000ppm	39.31	49.67	58.62	72.41	44.83

Figure III.3.2
MYCELIAL GROWTH
Comparison of % of inhibition of Ligand (H_2DATP) and its complexes

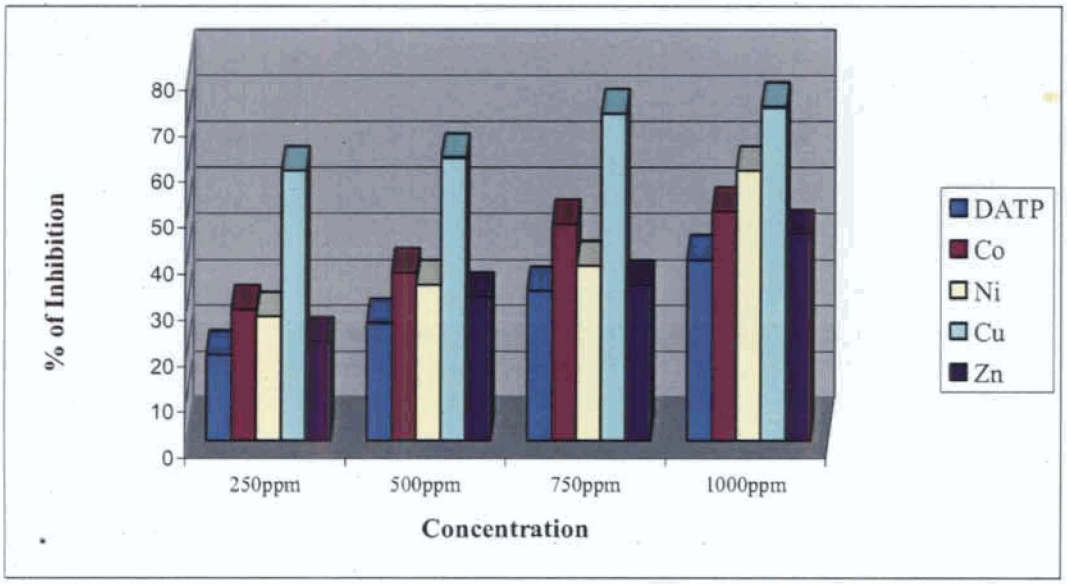

DATP=H_2DATP , Co=[CoL (H_2O)$_2$], Cu=[CuL (H_2O)$_2$], Ni=[NiL(H_2O)$_2$]

TABLE III.3.3
MYCELIAL GROWTH
% of inhibition by HPAP complexes

Compound	L=HPAP	$CoL_2(H_2O)_2$	$Ni\ L_2(H_2O)_2$	$Cu\ L_2(H_2O)_2$	$Zn\ L_2$
250ppm	15.86	33.33	26.90	47.59	17.24
500ppm	25.24	46.67	31.03	54.48	29.66
750ppm	32.69	60.00	51.72	68.28	31.03
1000ppm	62.76	72.00	72.41	73.79	32.41

Figure III.3.3
MYCELIAL GROWTH
Comparison of % of inhibition of Ligand (HPAP) and its complexes

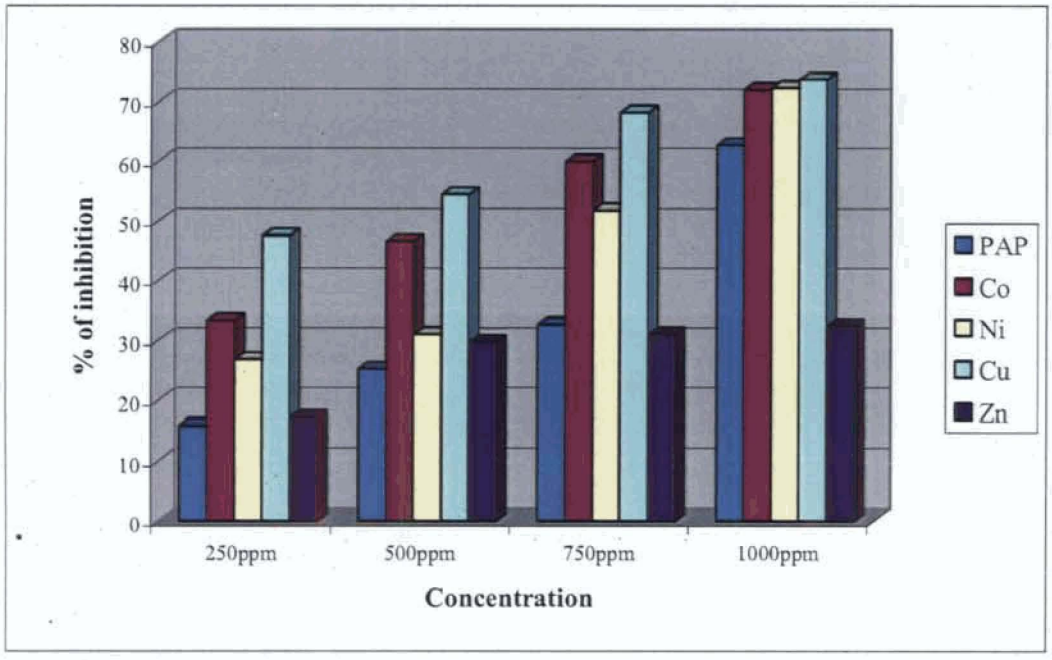

PAP=HPAP , Co=[$CoL_2(H_2O)_2$], Cu=[$CuL_2(H_2O)_2$], Ni=[$NiL_2(H_2O)_2$]

Zn=[ZnL_2]

TABLE III.3.4
MYCELIAL GROWTH
% of inhibition by HCAP complexes

Compound	L=HCAP	$CoL_2(H_2O)_2$	$Ni\ L_2(H_2O)_2$	$Cu\ L_2(H_2O)_2$	$Zn\ L_2$
250ppm	10.34	33.33	29.66	47.59	10.34
500ppm	17.24	40.00	39.31	51.72	17.24
750ppm	22.76	46.67	48.97	71.03	24.14
1000ppm	32.41	60.00	58.62	72.41	50.34

Figure III.3.4
MYCELIAL GROWTH
Comparison of % of inhibition of Ligand (HCAP) and its complexes

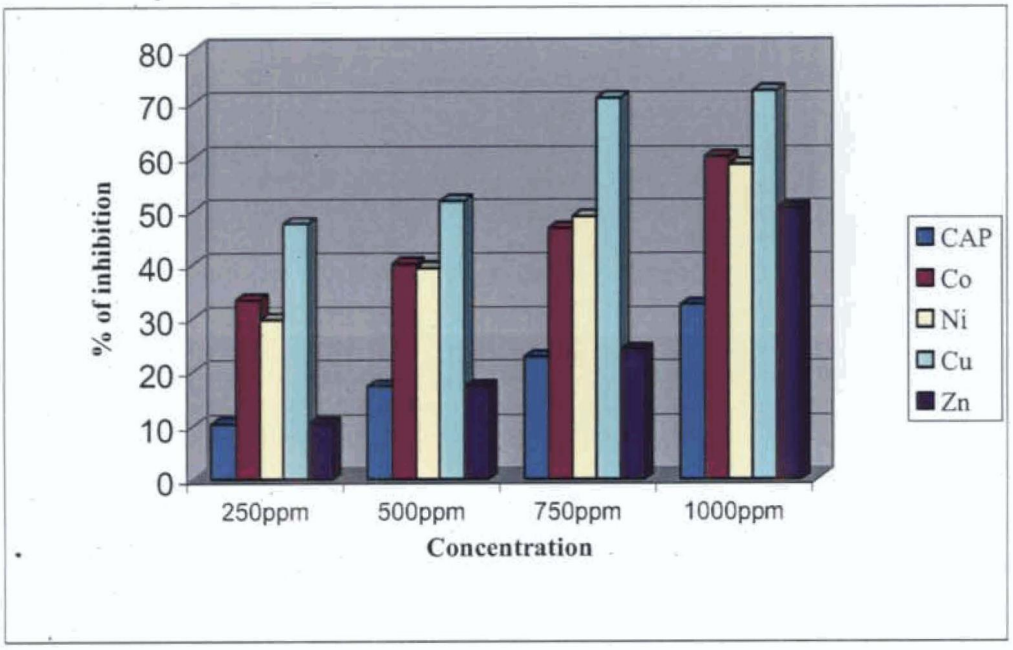

CAP=HCAP , Co=$[CoL_2(H_2O)_2]$, Cu=$[CuL_2(H_2O)_2]$, Ni=$[NiL_2(H_2O)_2]$

Zn=$[ZnL_2]$

Table III.3.5
Comparison of % of inhibition of mycelial growth by different ligands

Ligand	H_2DAP	H_2DATP	HPAP	HCAP
250ppm	10.34	18.62	15.86	10.34
500ppm	16.21	25.52	25.24	17.24
750ppm	20.69	32.41	32.69	22.76
1000ppm	28.28	39.31	62.76	32.41

FigureIII.3.5
Comparison of % of inhibition of mycelial growth by different ligands

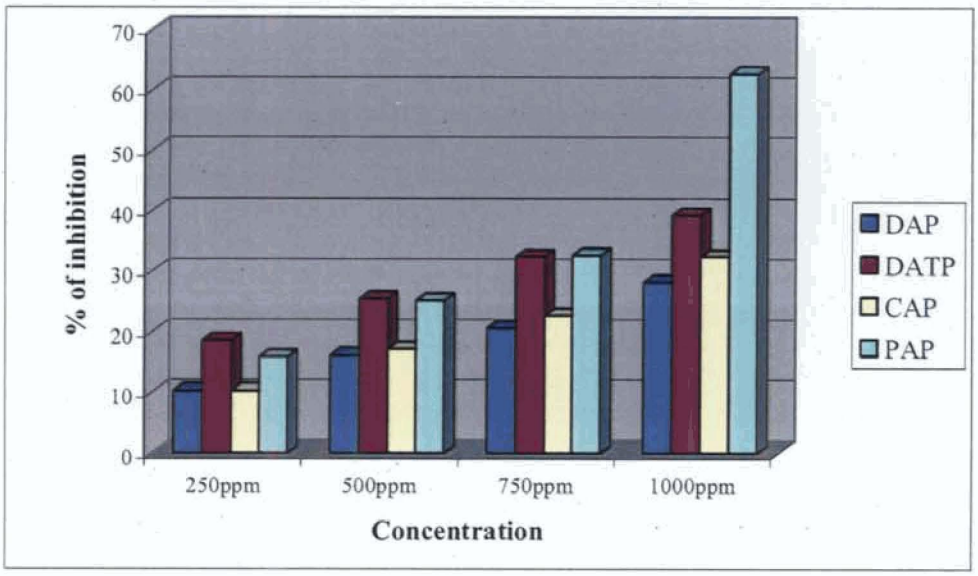

DAP=H_2DAP, DATP=H_2DATP, PAP=HPAP ,CAP=HCAP

Table. III.3.6
% of inhibition of sporangial production by H_2DAP complexes

Compound		L=H_2DAP	$CoL(H_2O)_2$	$Ni\ L(H_2O)_2$	$Cu\ L(H_2O)_2$	Control
250ppm	No of sporangia/field	27	22	23	17	61
	% Inhibition	55.73	63.93	62.29	72.13	
500ppm	No of sporangia/field	23	21	19	12	61
	% Inhibition	62.29	65.57	68.85	80.32	
750ppm	No of sporangia/field	19	14	16	11	61
	% Inhibition	68.85	77.04	73.77	81.96	
1000ppm	No of sporangia/field	15	12	10	5	61
	% Inhibition	75.40	80.32	83.60	91.80	

Figure. III.3.6
% of inhibition of sporangial production by H_2DAP complexes

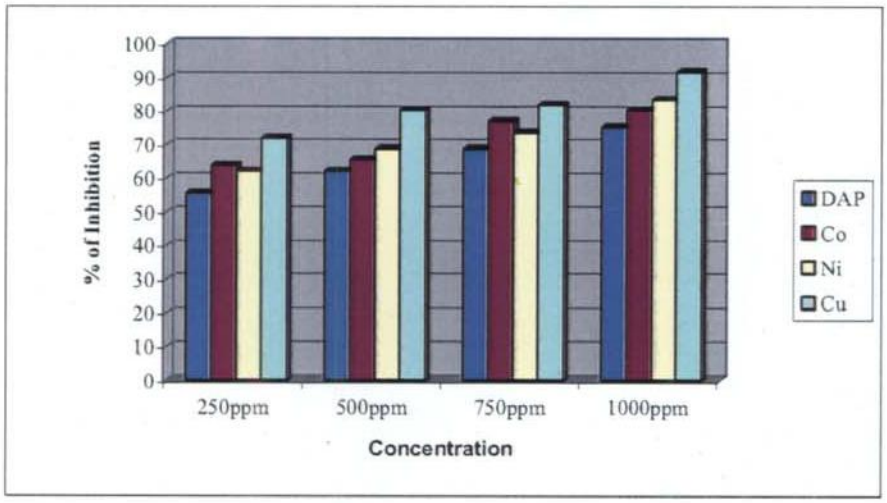

DAP=H_2DAP , Co=$[CoL(H_2O)_2]$, Cu=$[CuL(H_2O)_2]$, Ni=$[NiL(H_2O)_2]$

Table. III.3.7
% of inhibition of sporangial production by H_2DATP complexes

Compound		L=H_2DATP	CoL $(H_2O)_2$	Ni L$(H_2O)_2$	Cu L$(H_2O)_2$	Control
250ppm	No of sporangia/field	20	14	16	15	61
	% Inhibition	67.21	77.04	73.77	75.40	
500ppm	No of sporangia/field	19	12	12	11	61
	% Inhibition	68.85	80.32	80.32	81.96	
750ppm	No of sporangia/field	13	10	15	9	61
	% Inhibition	78.68	83.60	75.40	85.24	
1000ppm	No of sporangia/field	12	7	11	6	61
	% Inhibition	80.32	88.52	81.96	90.16	

Figure. III.3.7
% of inhibition of sporangial production by H_2DATP complexes

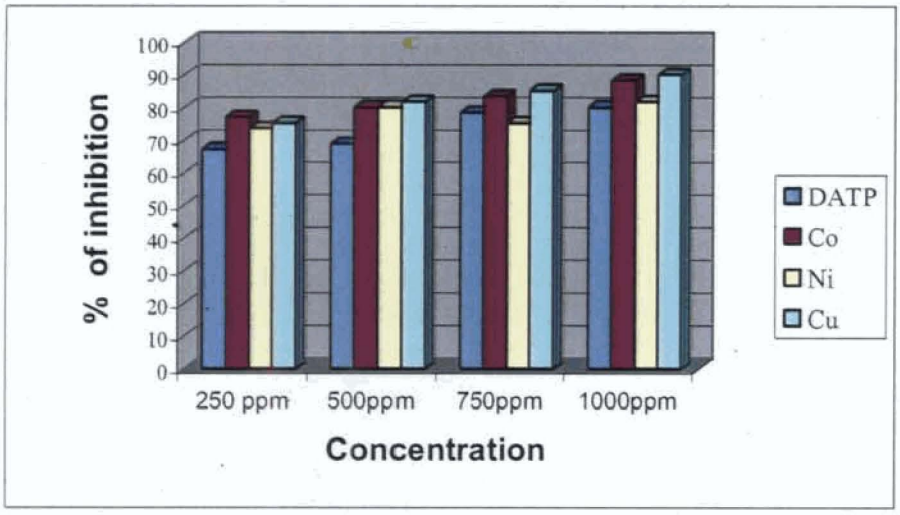

DATP=H_2DATP , Co=[CoL$(H_2O)_2$], Cu=[CuL$(H_2O)_2$], Ni=[NiL$(H_2O)_2$]

Table. III.3.8
% of inhibition of sporangial production by HPAP complexes

Compound		L=HPAP	$CoL_2(H_2O)_2$	$Ni\ L_2(H_2O)_2$	$Cu\ L_2(H_2O)_2$	Control
250ppm	No of sporangia/field	31	29	26	16	61
	% Inhibition	49.18	52.45	57.37	73.77	
500ppm	No of sporangia/field	27	27	20	12	61
	% Inhibition	55.73	55.73	67.21	80.32	
750ppm	No of sporangia/field	25	26	18	9	61
	% Inhibition	59.01	57.37	70.49	85.24	
1000ppm	No of sporangia/field	22	22	16	7	61
	% Inhibition	63.93	63.93	73.77	88.52	

Figure .III.3.8
% of inhibition of sporangial production by HPAP complexes

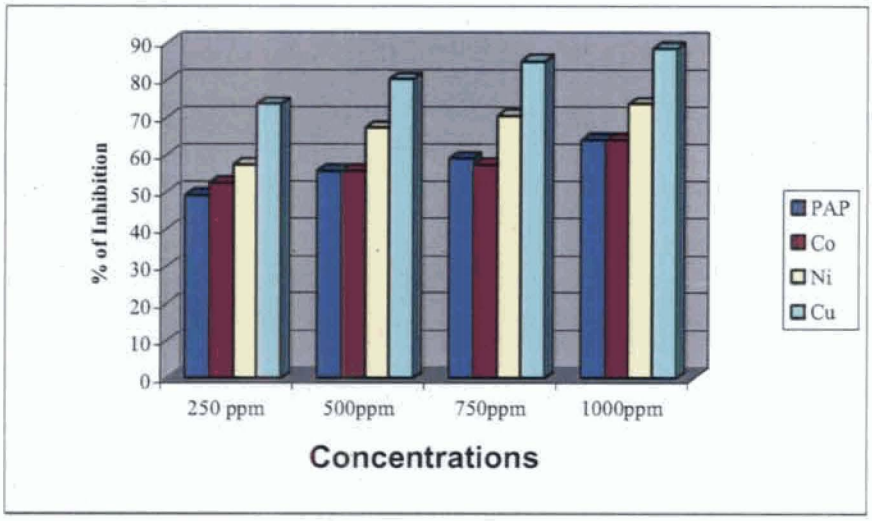

PAP=HPAP , Co=$[CoL_2(H_2O)_2]$, Cu=$[CuL_2(H_2O)_2]$, Ni=$[NiL_2(H_2O)_2]$

Table .III.3.9
Comparison of % of inhibition of Sporangial production by different ligands

Ligand	H_2DAP	H_2DATP	HPAP
250 ppm	55.73	67.21	49.18
500ppm	62.29	68.85	55.73
750ppm	68.85	78.68	59.01
1000ppm	75.40	80.32	63.93

Figure. III.3.9
Comparison of % of inhibition of Sporangial production by different ligands

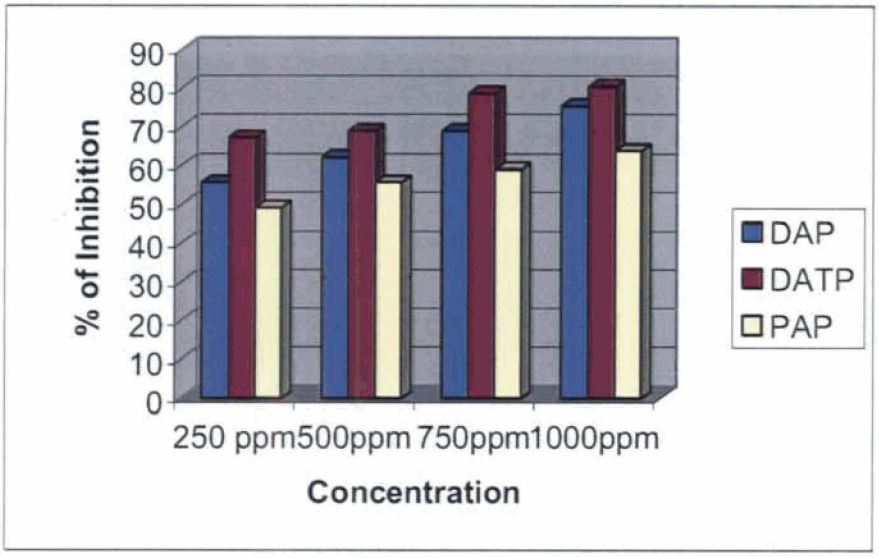

DAP=H_2DAP, DATP=H_2DATP, PAP=HPAP

Table III.3.10.
Zoospore release
% of inhibition by H_2DAP complexes

Compound		L=H_2DAP	CoL $(H_2O)_2$	Ni L $(H_2O)_2$	Cu $L(H_2O)_2$	Control
250ppm	%Zoospore release	43	40	37	19	47
	% Inhibition	8.51	14.89	21.27	59.57	
500ppm	%Zoospore release	40	33	30	18	47
	% Inhibition	14.89	29.78	36.17	61.70	
750ppm	%Zoospore release	37	27	20	17	47
	% Inhibition	21.27	42.55	57.44	63.82	
1000ppm	%Zoospore release	30	18	16	14	47
	% Inhibition	36.17	61.70	65.95	70.21	

Figure. III.3.10.
Zoospore release
% of inhibition by H_2DAP complexes

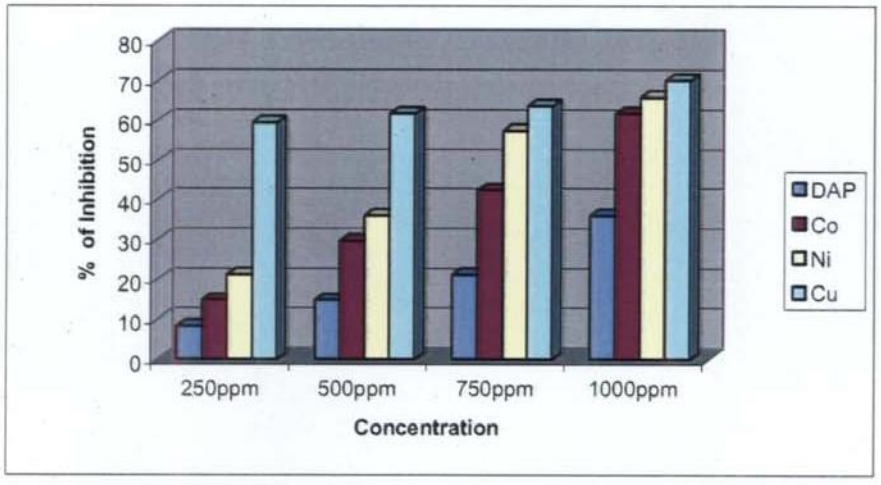

DAP=H_2DAP , Co=[$CoL(H_2O)_2$], Cu=[$CuL(H_2O)_2$], Ni=[$NiL(H_2O)_2$]

Table III.3.11
Zoospore release
% of inhibition by H_2DATP complexes

Compound		L=H_2DATP	CoL $(H_2O)_2$	Ni L $(H_2O)_2$	Cu L $(H_2O)_2$	Control
250ppm	%Zoospore release	32	27	22	14	47
	% Inhibition	31.91	42.55	53.19	70.21	
500ppm	%Zoospore release	27	16	16	6	47
	% Inhibition	42.55	65.95	65.95	87.23	
750ppm	%Zoospore release	21	10	12	0	47
	% Inhibition	55.31	78.72	74.46	100	
1000ppm	%Zoospore release	14	8	8	0	47
	% Inhibition	70.21	82.97	82.97	100	

Figure III.3.11
Zoospore release
% of inhibition by H_2DATP complexes

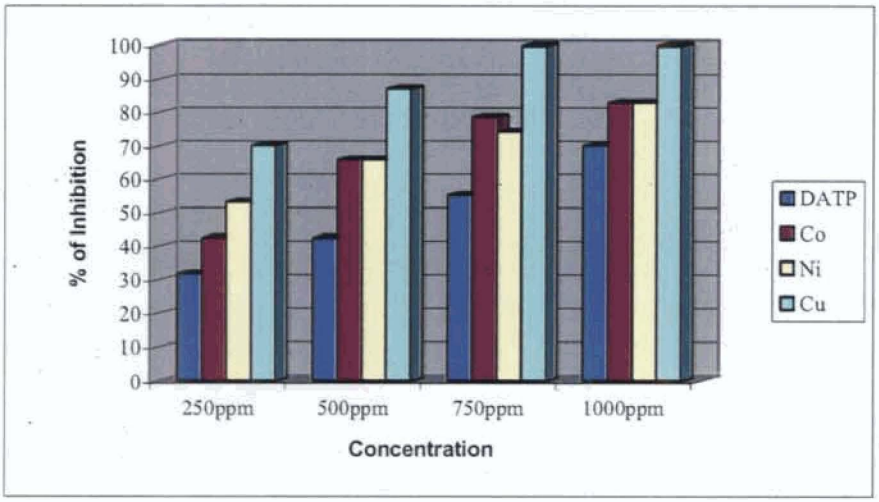

DATP=H_2DATP , Co=[CoL$(H_2O)_2$], Cu=[CuL$(H_2O)_2$], Ni=[NiL$(H_2O)_2$]

Table III.3.12
Zoospore release
% of inhibition by HPAP complexes

Compound		L=HPAP	$CoL_2(H_2O)_2$	$Ni\ L_2(H_2O)_2$	$Cu\ L_2(H_2O)_2$	Control
250ppm	%Zoospore release	27	32	31	34	47
	% Inhibition	42.55	31.91	34.04	27.65	
500ppm	%Zoospore release	24	21	21	9	47
	% Inhibition	48.93	55.31	55.31	80.85	
750ppm	%Zoospore release	12	11	7	0	47
	% Inhibition	74.46	76.59	85.10	100	
1000ppm	%Zoospore release	5	5	3	0	47
	% Inhibition	89.36	89.36	93.61	100	

Figure III.3.12
Zoospore release
% of inhibition by HPAP complexes

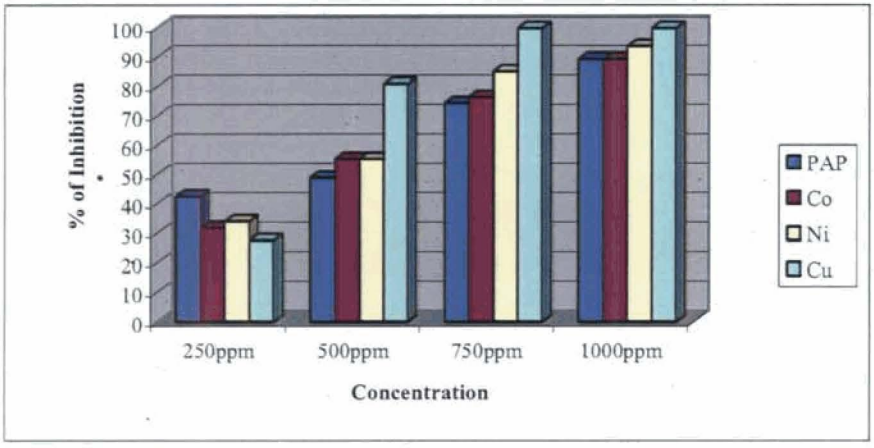

AP=HPAP , Co=$[CoL_2(H_2O)_2]$, Cu=$[CuL_2(H_2O)_2]$, Ni=$[NiL_2(H_2O)_2]$

Table III.3.13
Zoospore release
% of inhibition by Different ligands

Ligand	H_2DAP	HPAP	H_2DATP
250ppm	8.51	31.91	42.55
500ppm	14.89	42.55	48.93
750ppm	21.27	55.31	74.46
1000ppm	36.17	70.21	89.36

FIgure III.3.13
Zoospore release
% of inhibition by Different ligands

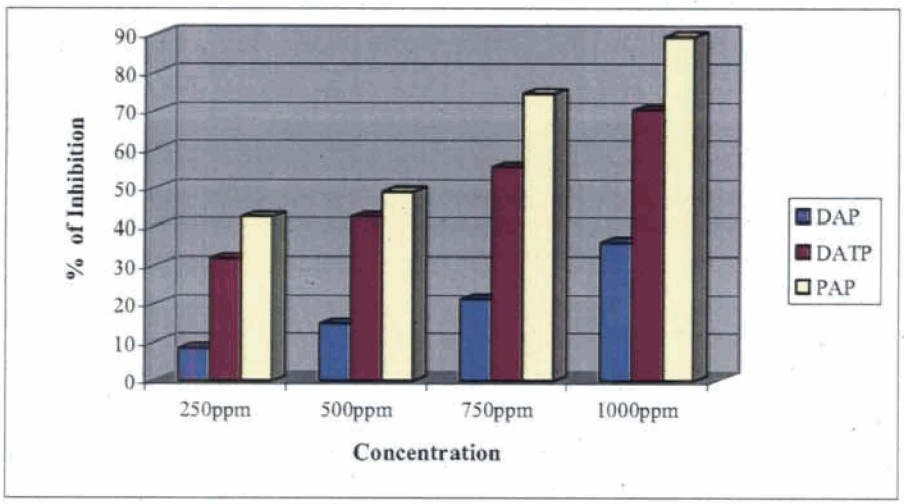

DAP= H_2DAP, DATP= H_2DATP, PAP= HPAP

Table III.3.14
Zoospore germination
% of inhibition by H_2DAP complexes

Compound		L=H_2DAP	Co L$(H_2O)_2$	Ni L$(H_2O)_2$	Cu L$(H_2O)_2$	Control
250ppm	%Zoospore germination	62	60	59	58	74
	% Inhibition	16.21	18.91	20.27	21.62	
500ppm	%Zoospore germination	58	56	50	47	74
	% Inhibition	21.62	24.32	32.43	36.48	
750ppm	%Zoospore germination	51	47	38	36	74
	% Inhibition	31.08	36.48	48.64	51.35	
1000ppm	%Zoospore germination	47	43	33	31	74
	% Inhibition	36.48	41.89	55.40	58.10	

Figure. III.3.14
Zoospore germination
% of inhibition by H_2DAP complexes

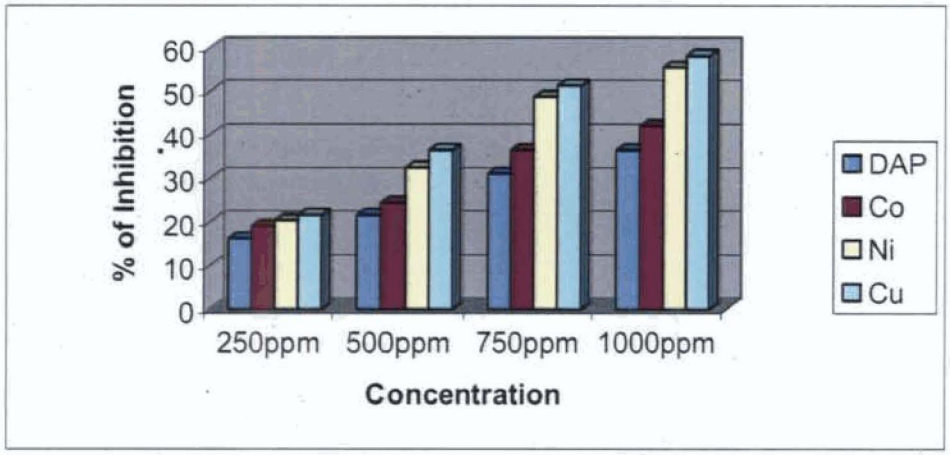

DAP=H_2DAP , Co=[$CoL(H_2O)_2$], Cu=[$CuL(H_2O)_2$], Ni=[$NiL(H_2O)_2$]

Table III.3.15
Zoospore germination
% of inhibition by H_2DATP complexes

Compound		L=H_2DATP	$CoL(H_2O)_2$	Ni $L(H_2O)_2$	Cu $L(H_2O)_2$	control
250ppm	%Zoospore germination	44	42	27	23	74
	% Inhibition	40.54	43.24	63.51	68.91	
500ppm	%Zoospore germination	32	31	13	14	74
	% Inhibition	56.75	58.10	82.43	81.08	
750ppm	%Zoospore germination	27	23	11	8	74
	% Inhibition	63.51	68.91	85.13	89.18	
1000ppm	%Zoospore germination	20	18	9	8	74
	% Inhibition	72.97	75.67	87.83	89.18	

Figure III.3.15
Zoospore germination
% of inhibition by H_2DATP complexes

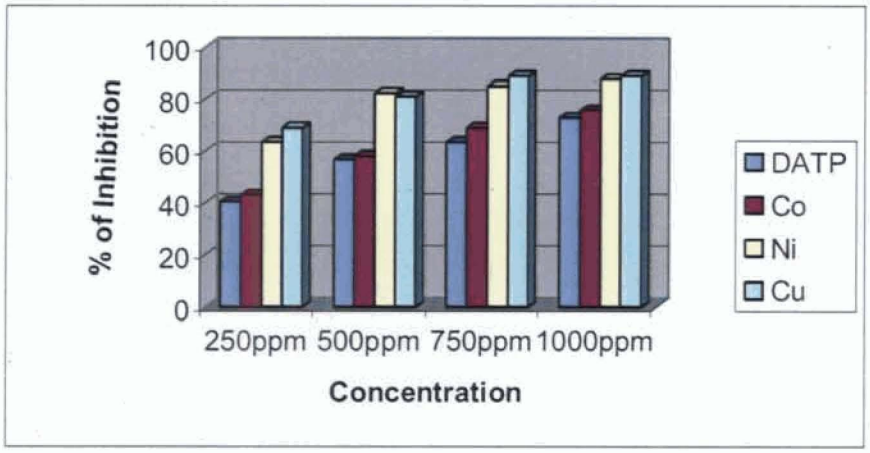

DATP=H_2DATP , Co=[$CoL(H_2O)_2$], Cu=[$CuL(H_2O)_2$], Ni=[$NiL(H_2O)_2$]

Table III.3.16
Zoospore germination
% of inhibition by HPAP complexes

Compound		L=HPAP	$CoL_2(H_2O)_2$	$Ni\ L_2(H_2O)_2$	$Cu\ L_2(H_2O)_2$	Control
250ppm	%Zoospore germination	43	33	21	17	74
	% Inhibition	41.89	55.40	71.62	77.02	
500ppm	%Zoospore germination	33	22	14	14	74
	% Inhibition	55.40	70.27	81.08	81.0	
750ppm	%Zoospore germination	26	17	11	6	74
	% Inhibition	64.86	77.02	85.13	91.89	
1000ppm	%Zoospore germination	20	11	6	4	74
	% Inhibition	72.97	85.13	91.89	94.59	

Figure III.3.16
Zoospore germination
% of inhibition by HPAP complexes

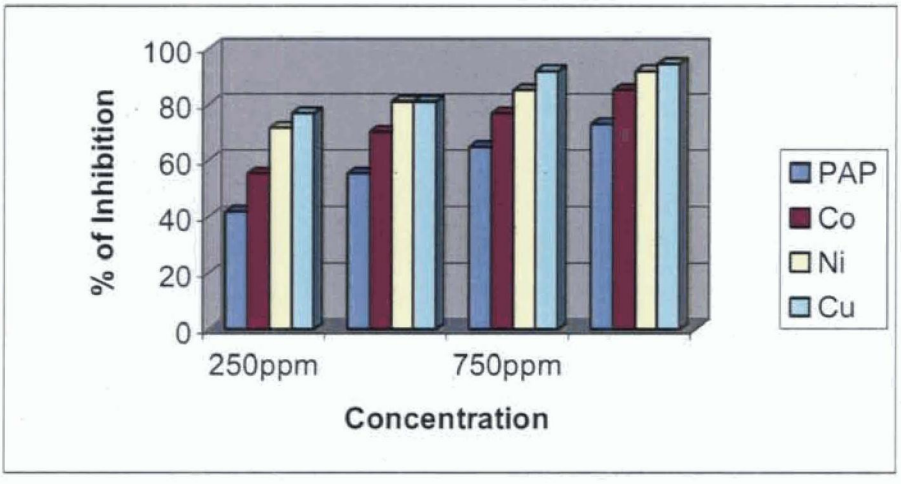

PAP=HPAP , Co=$[CoL_2(H_2O)_2]$, Cu=$[CuL_2(H_2O)_2]$, Ni=$[NiL_2(H_2O)_2]$

Table III.3.17
% of inhibition
Comparison of ligands
ZOOSPORE GERMINATION

Ligand	H_2DAP	H_2DATP	HPAP
250ppm	16.21	40.54	41.89
500ppm	21.62	56.75	55.40
750ppm	31.08	63.51	64.86
1000ppm	36.48	72.97	72.97

Figure III.3.17
% of inhibition
Comparison of ligands
ZOOSPORE GERMINATION

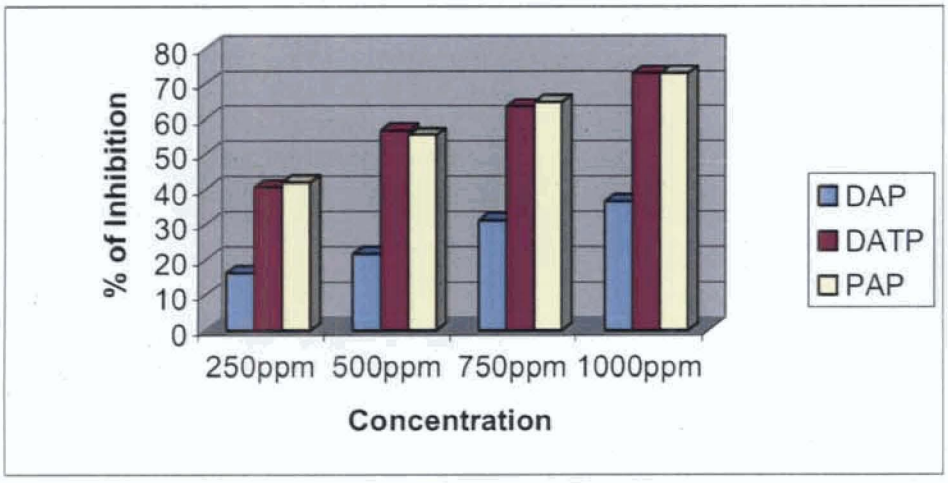

DAP=H_2DAP , DATP=H_2DATP PAP=HPAP

Photo.1
BLACK PEPPER GROWING IN THE HEALTHY ATMOSPHERE

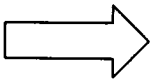

Photo.2
BLACK PEPPER - AFTER PHYTOPHTHORA INFECTION

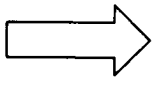

1730

10

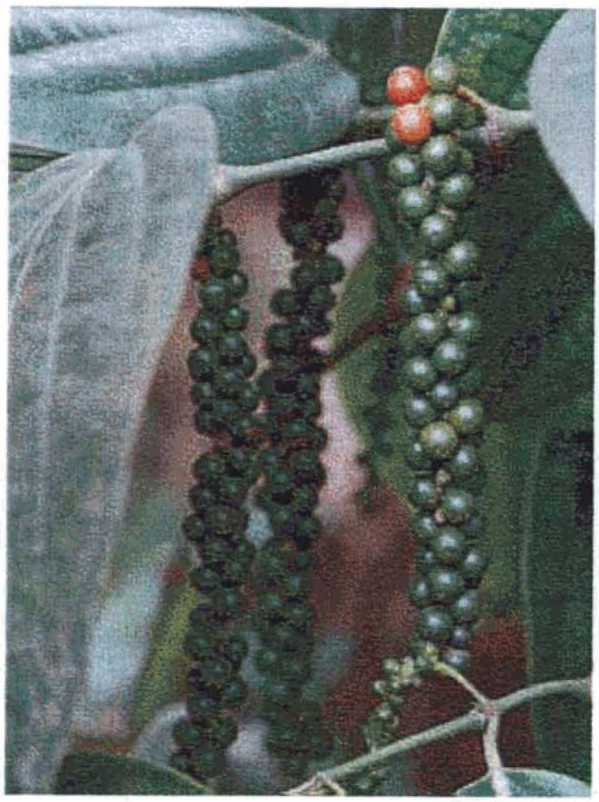

10

Photo.3
Effect of [Co $(CAP)_2$ $(H_2O)_2$]
On mycelial growth of *Phytophthora capsici*

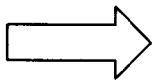

Photo.4
Effect of [Co (DATP) $(H_2O)_2$]
On mycelial growth of *Phytophthora capsici*

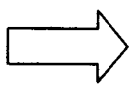

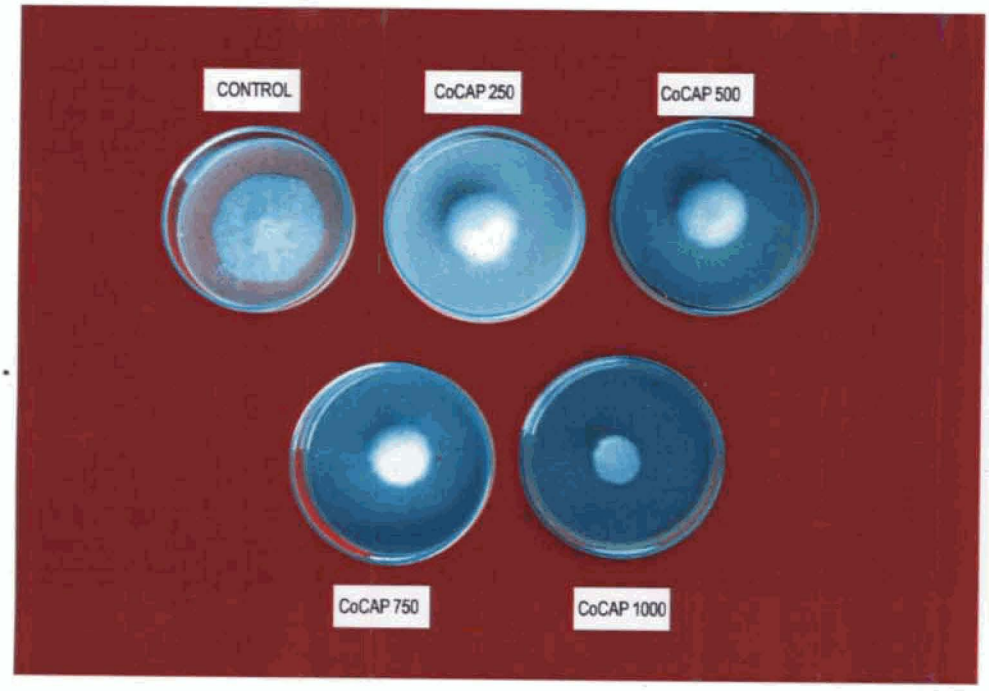
CONTROL
CoCAP 250
CoCAP 500
CoCAP 750
CoCAP 1000

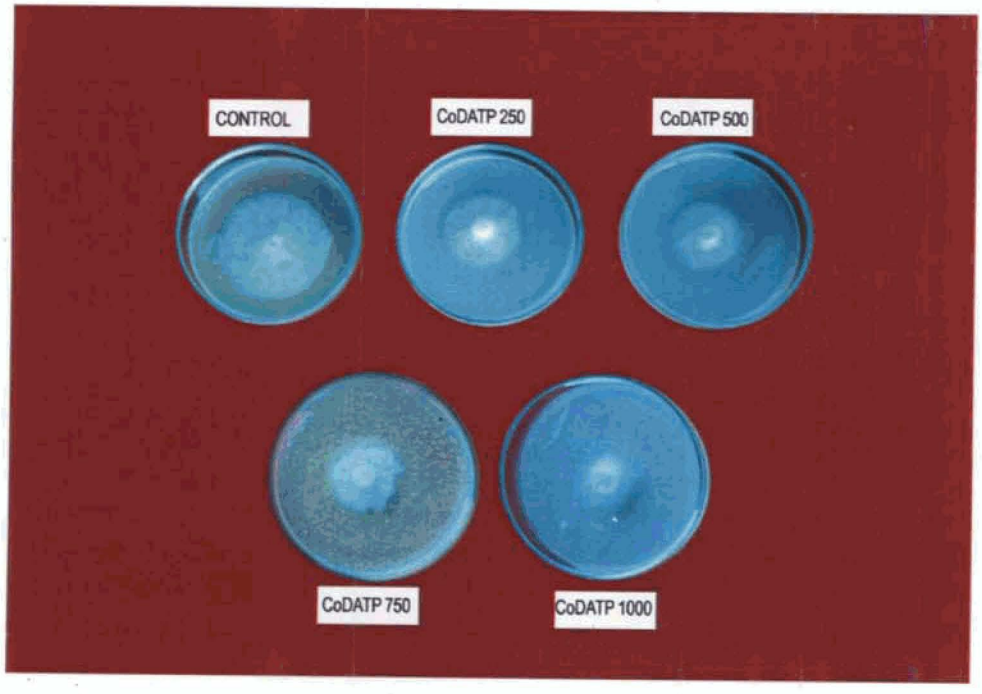
CONTROL
CoDATP 250
CoDATP 500
CoDATP 750
CoDATP 1000

Photo.5
Effect of [Co $(PAP)_2$ $(H_2O)_2$]
On mycelial growth of *Phytophthora capsici*

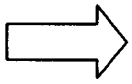

Photo.6
Effect of [Co (DAP) $(H_2O)_2$]
On mycelial growth of *Phytophthora capsici*

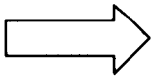

1750

12

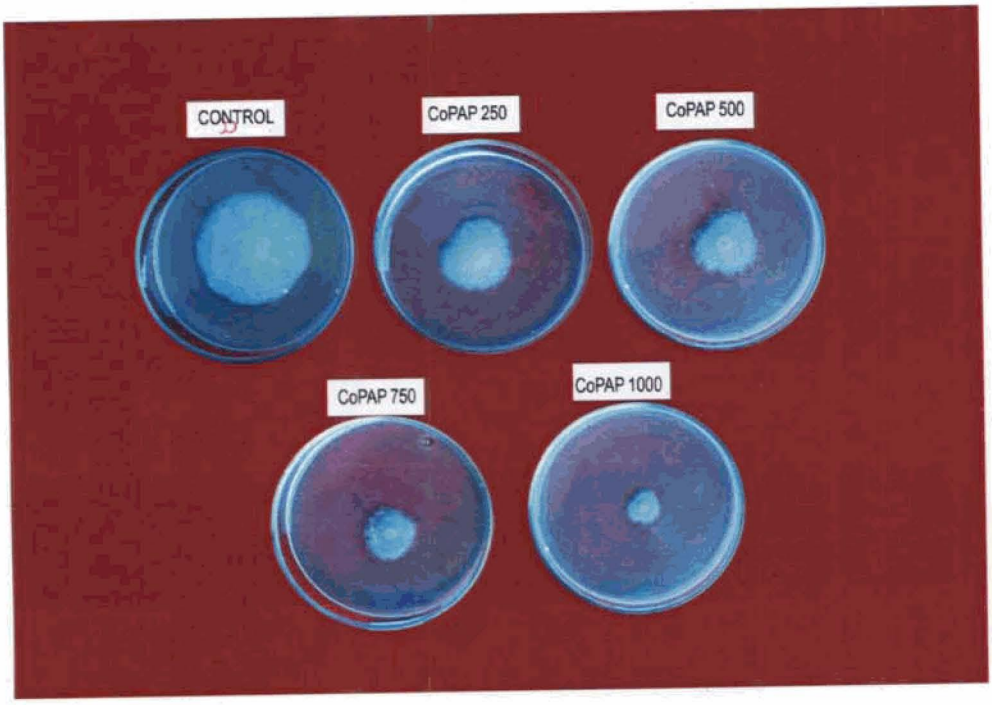
CONTROL
CoPAP 250
CoPAP 500
CoPAP 750
CoPAP 1000

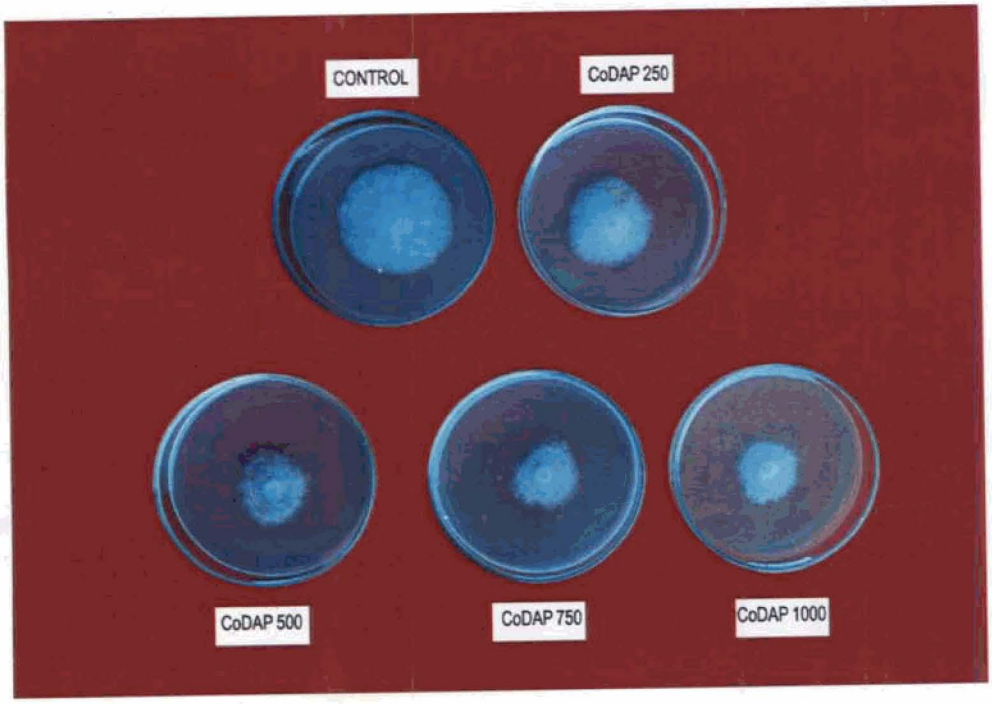
CONTROL
CoDAP 250
CoDAP 500
CoDAP 750
CoDAP 1000

Photo.7
Effect of [Ni (DAP) $(H_2O)_2$]
On mycelial growth of *Phytophthora capsici*

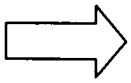

Photo.8
Effect of [Ni (DATP) $(H_2O)_2$]
On mycelial growth of *Phytophthora capsici*

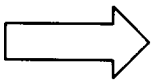

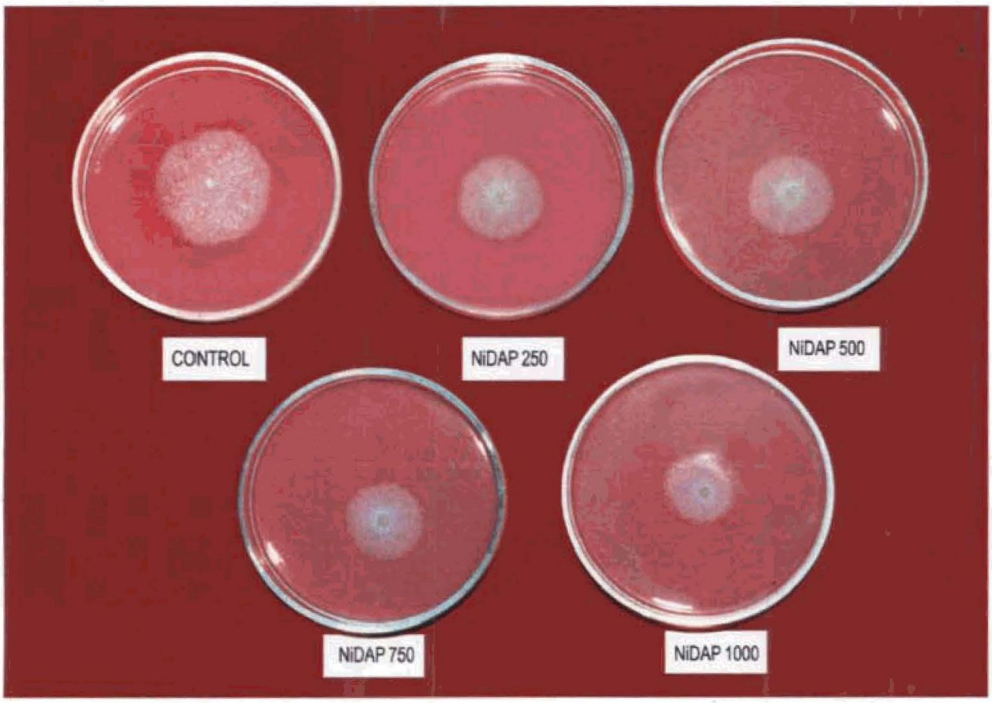
CONTROL
NiDAP 250
NiDAP 500
NiDAP 750
NiDAP 1000

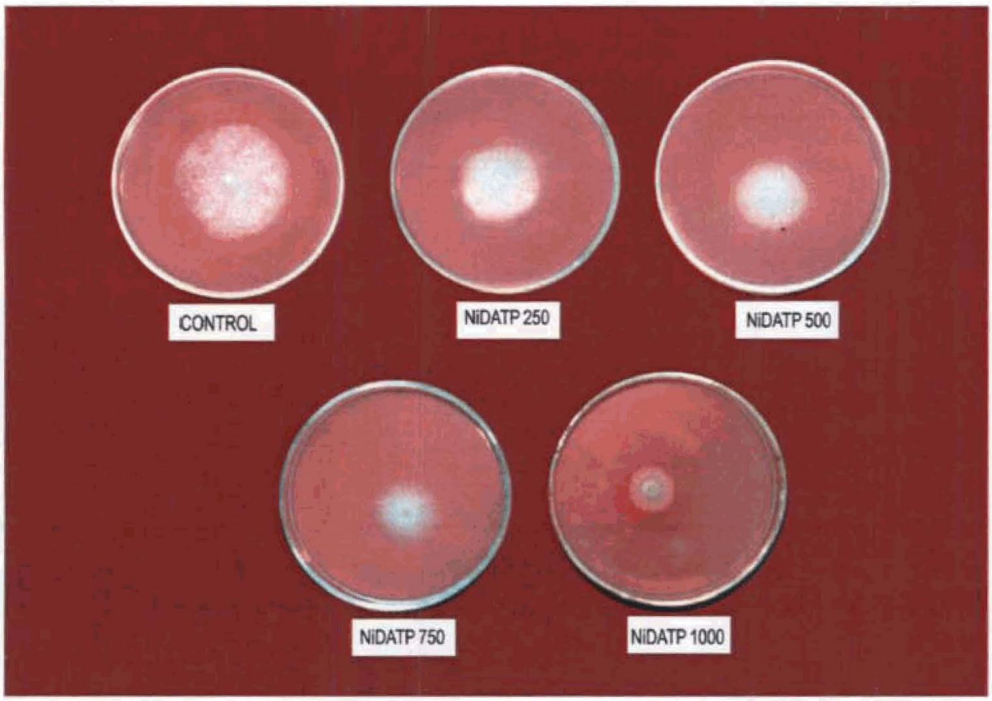
CONTROL
NiDATP 250
NiDATP 500
NiDATP 750
NiDATP 1000

Photo.9
Effect of [Ni $(PAP)_2$ $(H_2O)_2$]
On mycelial growth of *Phytophthora capsici*

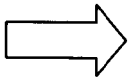

Photo.10
Effect of [Ni $(CAP)_2$ $(H_2O)_2$]
On mycelial growth of *Phytophthora capsici*

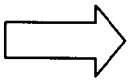

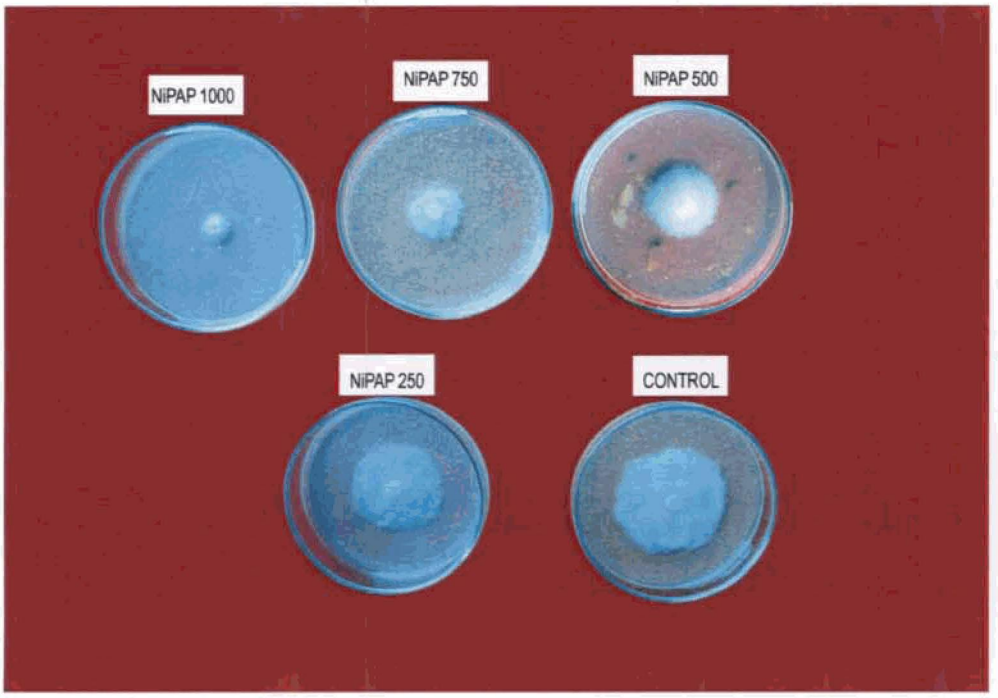
NiPAP 1000
NiPAP 750
NiPAP 500
NiPAP 250
CONTROL

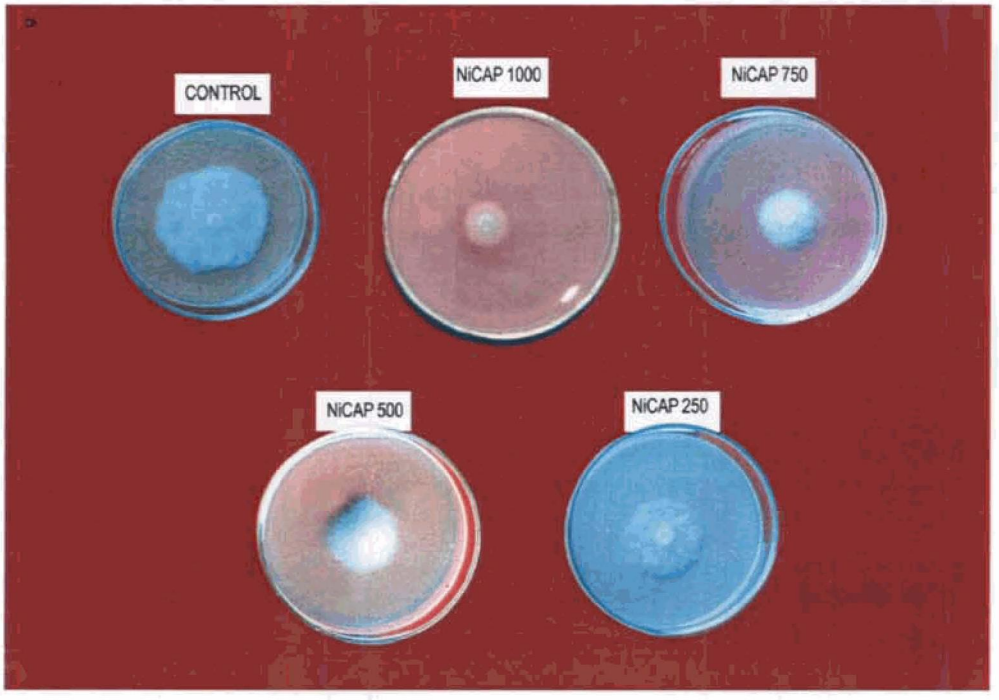
CONTROL
NiCAP 1000
NiCAP 750
NiCAP 500
NiCAP 250

Photo.11
Effect of [Cu (DAP) $(H_2O)_2$]
On mycelial growth of *Phytophthora capsici*

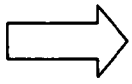

Photo.12
Effect of [Cu (DATP) $(H_2O)_2$]
On mycelial growth of *Phytophthora capsici*

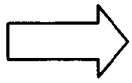

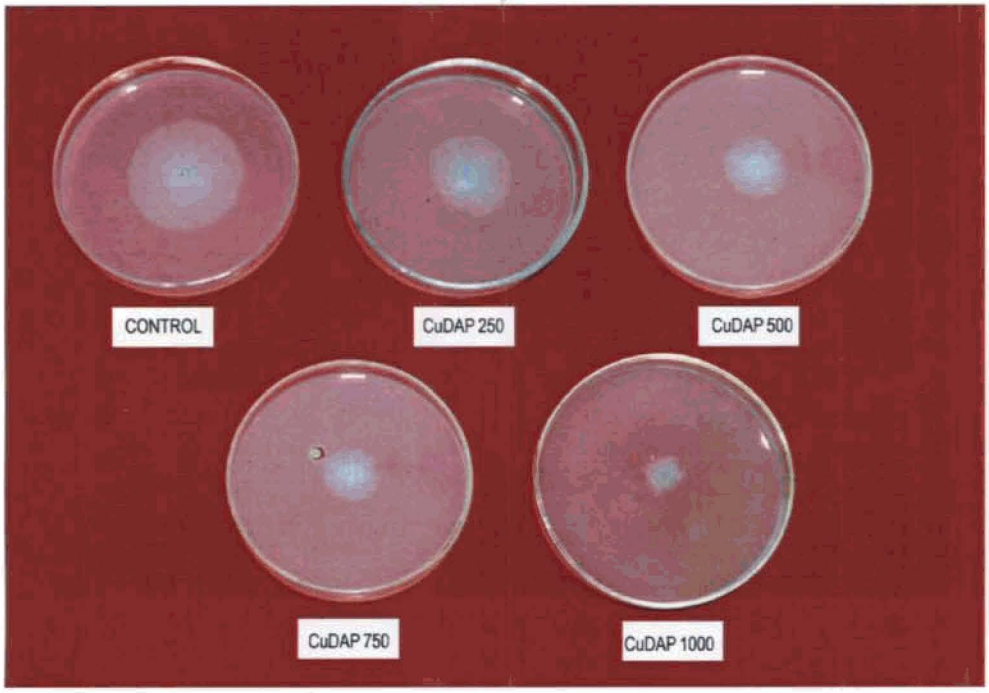
CONTROL
CuDAP 250
CuDAP 500
CuDAP 750
CuDAP 1000

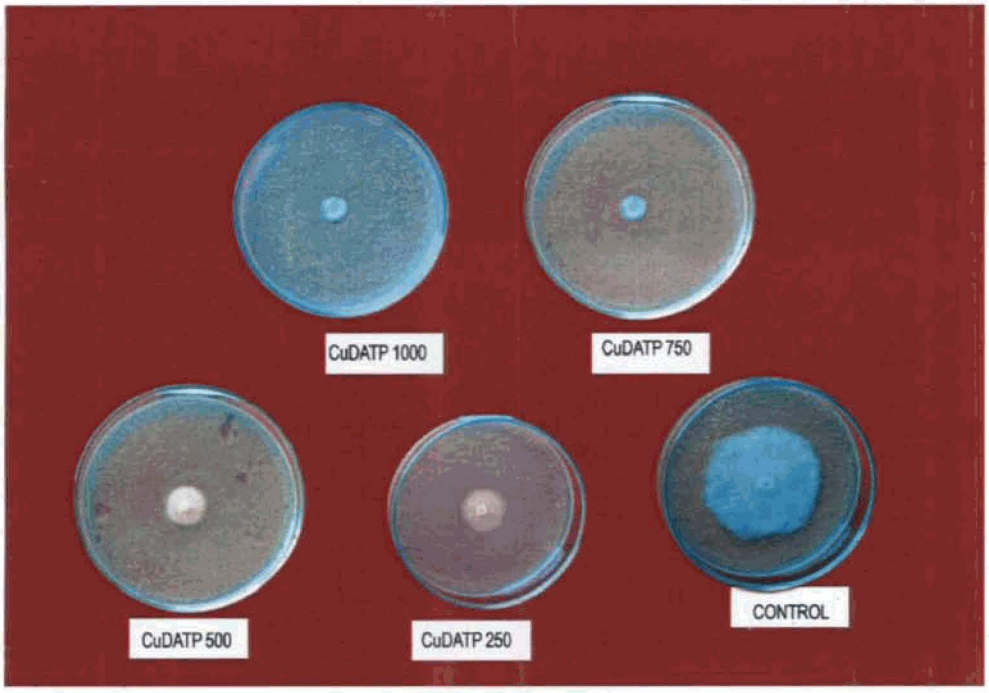
CuDATP 1000
CuDATP 750
CuDATP 500
CuDATP 250
CONTROL

Photo.13
Effect of [Cu $(PAP)_2$ $(H_2O)_2$]
On mycelial growth of *Phytophthora capsici*

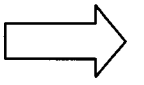

Photo.14
Effect of [Cu $(CAP)_2$ $(H_2O)_2$]
On mycelial growth of *Phytophthora capsici*

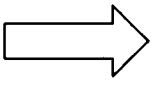

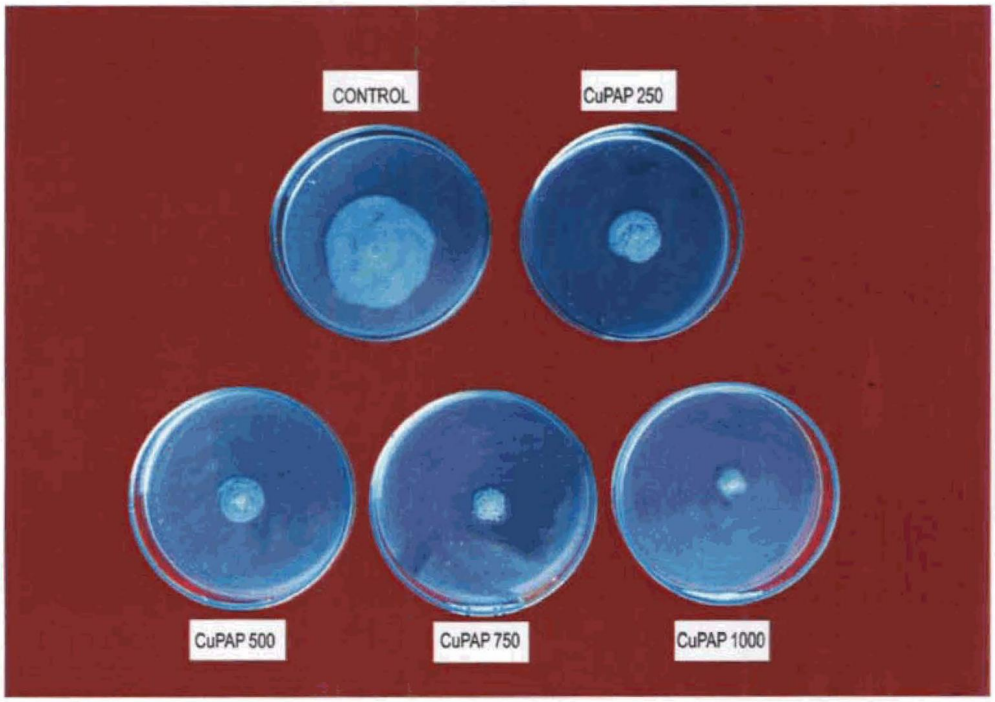
CONTROL
CuPAP 250
CuPAP 500
CuPAP 750
CuPAP 1000

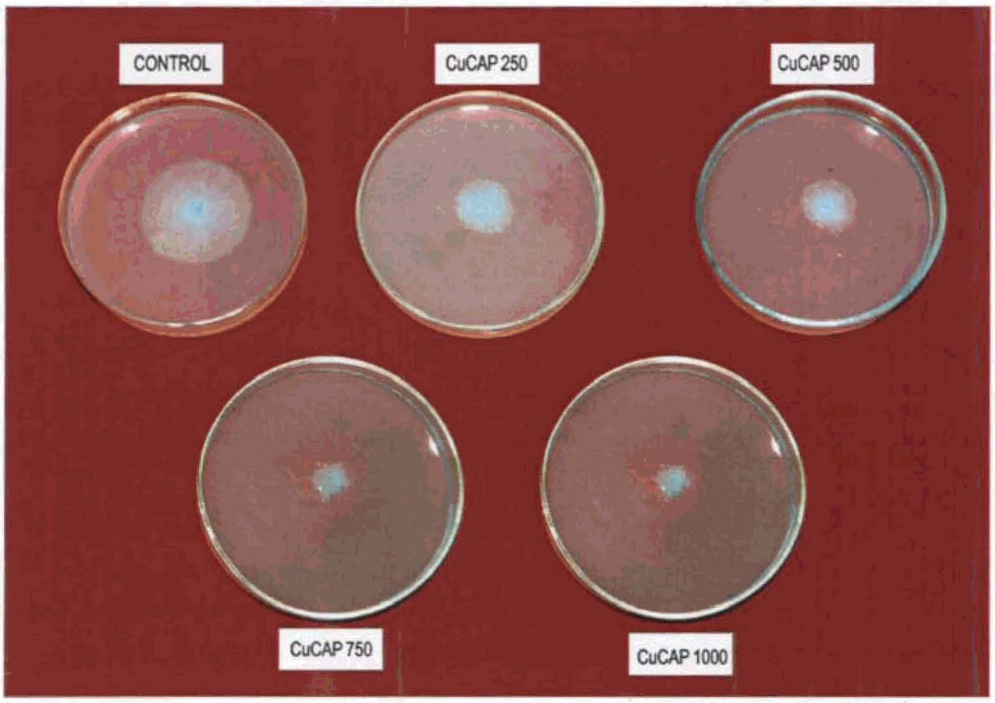
CONTROL
CuCAP 250
CuCAP 500
CuCAP 750
CuCAP 1000

Photo.15
Effect of [Zn $(PAP)_2$]
On mycelial growth of *Phytophthora capsici*

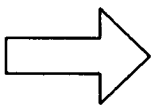

Photo.16
Effect of [Zn $(CAP)_2$]
On mycelial growth of *Phytophthora capsici*

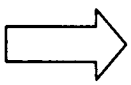

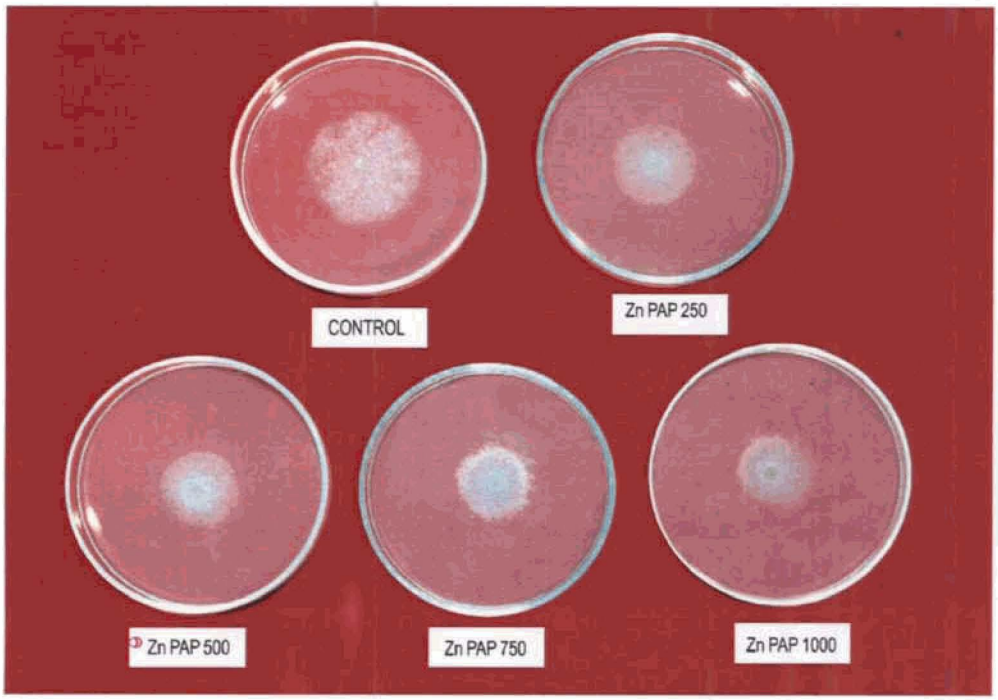
CONTROL
Zn PAP 250
Zn PAP 500
Zn PAP 750
Zn PAP 1000

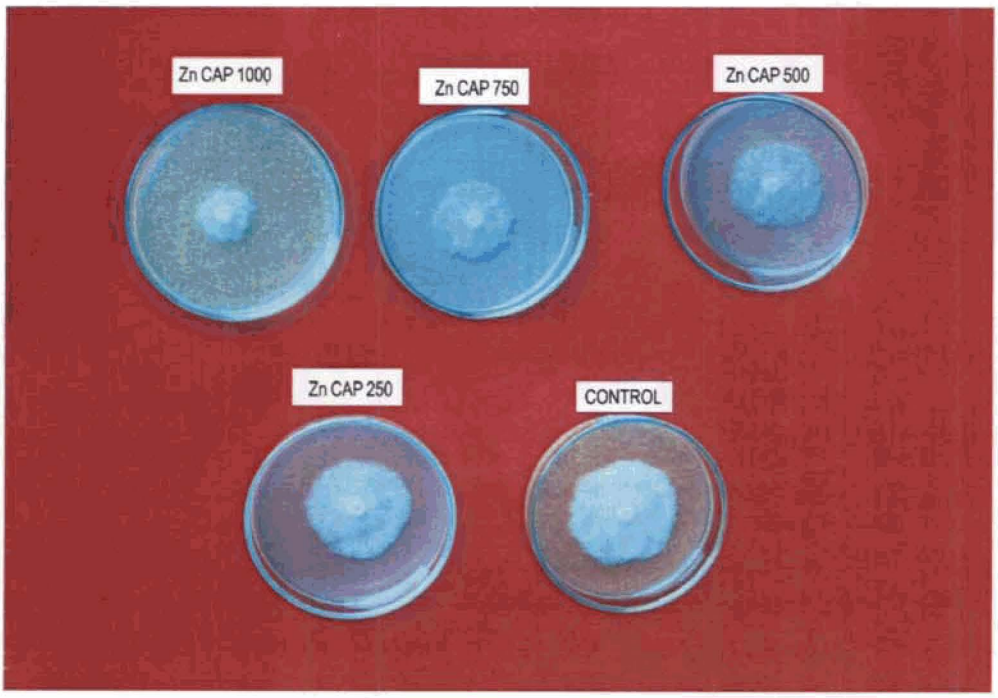
Zn CAP 1000
Zn CAP 750
Zn CAP 500
Zn CAP 250
CONTROL

Photo.17
Effect of [Zn (DAP)]
On mycelial growth of *Phytophthora capsici*

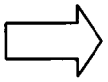

Photo.18
Effect of [Zn(DATP)]
On mycelial growth of *Phytophthora capsici*

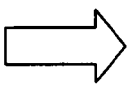

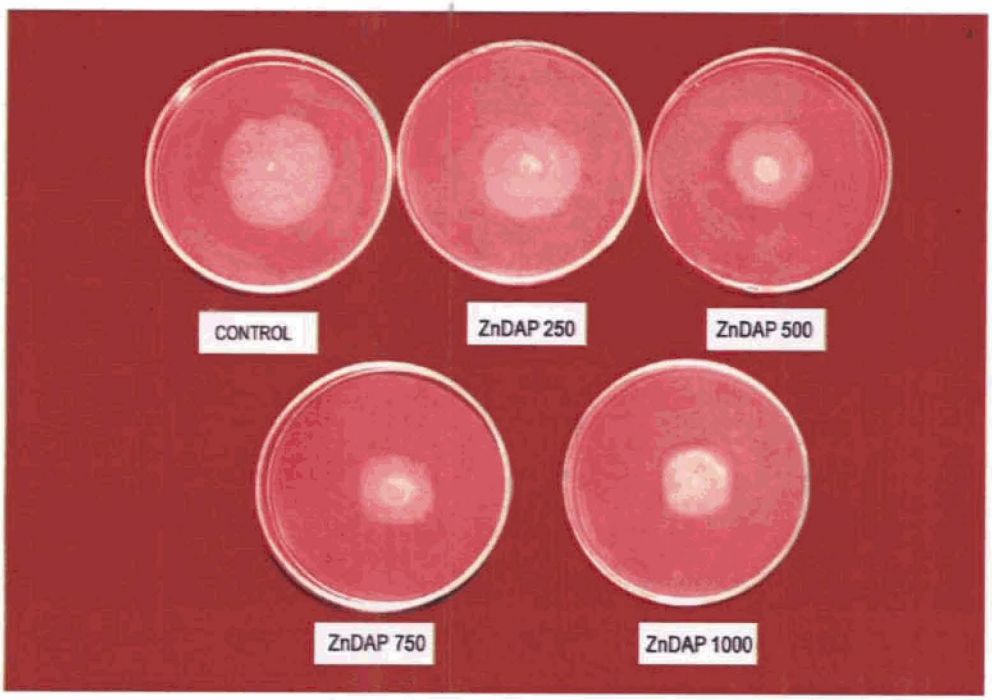
CONTROL
ZnDAP 250
ZnDAP 500
ZnDAP 750
ZnDAP 1000

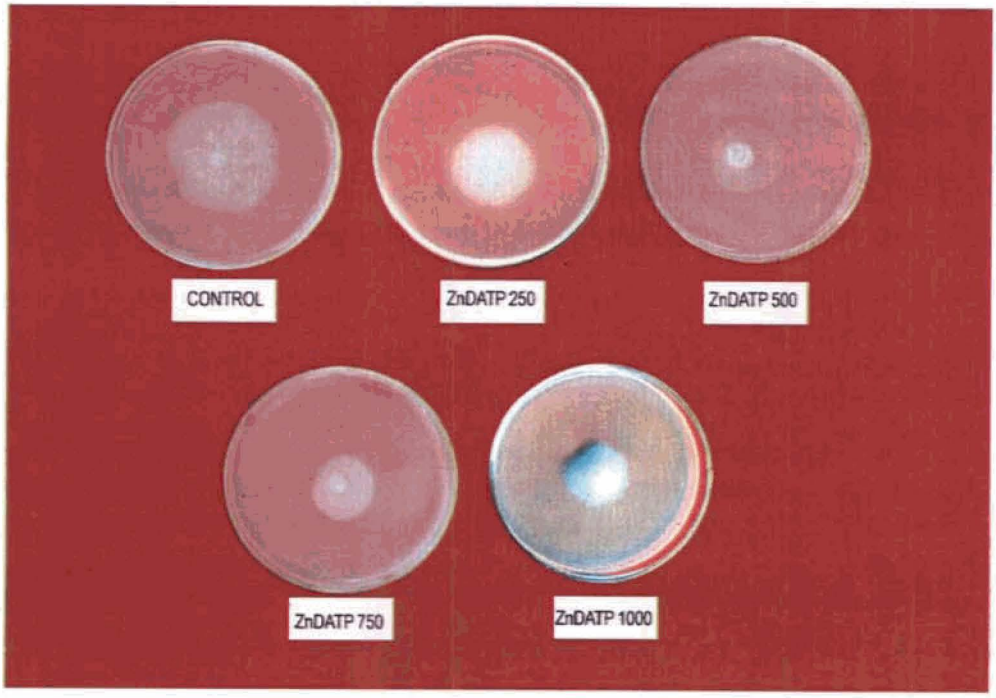
CONTROL
ZnDATP 250
ZnDATP 500
ZnDATP 750
ZnDATP 1000

References

1) Sarma, Y. R.; Anandaraj, M.; Venugopal, M. N. *Biological control of diseases of spices*; Anandaraj, M.; Peter, K. V.,eds.; Biological control in spices, Indian Institute of Spices Research, Kozhikode, Kerala, India, **1997**, 1-19.

2) Samraj, J.; Jose, P.C. *Sci. and Cult.* **1966** , 32 , 90-92.

3) Sarma, Y. R .; Ramachandran, N.; Anandaraj. M. *Black Pepper Diseases in India;* Sarma, Y. R .; Premkumar., eds.; Diseases of Black Pepper, National Research Center for Spices, Calicut, **1991**,55-94.

4) Sarma, Y. R.; Anandaraj, M.; Venugopal.M.N. *Diseases of Spice Crops*; Chadha K .L.; Rethinam, P., eds.; Advances in Horticulture, Malhothra Publishing House,New Delhi,**1994**, 1015-1057.

5) Anandaraj. M.; Sarma, Y. R. *J.Spices and Aromatic Crops.***1995,** 4,17-23.

6) Prabhakaran, P. V. *Journal of Spices and Aromatic Crops.* **1997**, 6,1, 31.

7) Alexopaulose, C. J.; Mims, C. W.; Blackwell,M. *Introductory Mycology,* Fourth Edition, John Wiley& son inc, **1996,** *869 pp* .

8) Webster, J. *Introduction to Fungi*, Cambridge University Press, **1993** , 669pp.

9) Erwin, D. C.; Ribeiro, O. K. *Phytophthora diseases worldwide*, APS Press, The American Phytopathological Society, St. Paul, Minnesota, **1996,** 562pp.

10) Ribeiro, O. K. *A Source book of the genus Phytophthora;* Gantner ; Verlag. K .– G.,9490 , Vaduz . **1978**, 417pp.

11) Desjardins, P. R.;Zentmyer G. A.; Reynolds , D. A. *Can .J. Bot* .**1969**, 47,1077-1079.

12) Slusher, R . L.; Sinclair, J. B. *Phytopathology.* **1973**,63,1168-1171.

13) Bartinicki-Garia, S. *Phytopathology.* **1969**, 59,10665-1071.

14) Bartinicki-Garica, S. *The cell wall; a crucial structure in fungal evolution*; Rayner, A. D. M..; Brasier, C. M.;.Moore. D., eds.; Evolutionary Biology of the fungi, Cambridge University Press,**1987**, 389-403.

15) Brasier, C. M.; Hansen. E . M. *Annual Review of phytopathology* .**1992**,30,173-200.

16) Hendrix, J. W. *Annu.Rev.Phytopathology.* **1970** ,811-130.

17) Ramachandran, N.;Sarma Y. R.; Anandraj ,M.; Abraham, J. *.Journal of Plantation Crops.* **1988** , 16,110-118.

18) Ananadraj, M. PhD Thesis. University of Calicut. **1997**, 154pp.

19) Ramachandran, N.; SarmaY. R.; Anandraj, M. *Management of Phytophthora infections in black pepper.* Sarma,Y. R.; Premkumar, T.;eds.; Diseases of black pepper, National research center for spices, Calicut , India .**1991**,158-174.

20) Cook, J.; Baker, K. F. *The Nature and practise of biological control of plant pathogens,* American phytopathological society, St Paul , Minnesota,**1983**, 539 pp .

21) Rajan, P. P. *Approaches towards integrated disease management of Phytophthora infection of black pepper* (*Piper nigrum* L.).Ph.D. Thesis, University of Calicut, Calicut, **1999**,190pp.

22) Singh,U. P.;Chowhan.W. B.;Wagner.K. G.; Anil Kumar. Effect of Ajoene,a compound from garlic (*Alium sativum)* on *Phytophthora drechsleri* f. sp. *cajani.Mycologia.* **1992**,*84 ,105-8.*

23) Heitefuss, R.*Crop and Plant protection;* Practical Foundation, New York, Halsted Press. **1989**, 261pp.

24) Timmer, L.W. *Phytopathology.* **1977**, 67, 1149-1154.

25) Schwinn, F. J.; Margot, P. *Control with Chemical* ; Ingram D.S. Willams P.H.eds.; *Phytopthora Infestans,* Cause of Late Blight of Potato, *Adv.Plant pathol*, Academic Press, **1991**,7,273.

26) Nene, Y. L.; Tapliyal.P. N . *Fungicides in plant disease control;* 3 rd edn ,Oxford I B H publishing company, New Delhi. **1993**,691pp.

27) Iwan, J.; Hertel.;Radzuweit, J. *Neth.J.Plant Pathol.* **1977** ,83 ,277-284.

28) Kerkenaar, A.;Kaars, A.; *Neth. J. Plant. Pathol.* **1977**, 83,145-152.

29) Schwinn F. J.; Staub T. *Phenylamides and other Fungicides against Oomycetes*, L.Horst.,ed,; Modern Selective Fungicides , Properties , Applications and Mechanism of Action , Scientific and Technical ,Longman, England, **1987**, 383.

30) Ramachandran, N. *Bioefficancy of Systemic Fungicides against Phytophthora Infections in Black pepper*. Ph.D. Thesis, Dept. Botany, Calicut University, Calicut,**1990** ,138.

31) Jejukumar, C. R.; Ketan Parikh. *Asian J.Chem.* **1997**, 9,4, 624 – 629.

32) Satpathy, K.C.;Mishra ,H. P.; Prahgha, G. C. *J.Indian Chem. Soc.* **1981**,58,844.

33) Rao, D.S.; Ganorkar, M.C. *J.Indian chem.Soc.***1981**.58,217.

34) Coyle, B.; Kavanagh. K.; McCann, M.; Devereux, M.; Geraghty, M. *Biometals.* **2003**, 16,2, 321-329.

35) Hans.R.; Hohl.; *Nutrition of Phytophthora* ,. Erwin D .C.; Bartnicki-Garcia, S.; Taso. P.H. eds. ; Phytophthora ,The American Pathological Society, **1983**.

36) Rubbo, S. D.; Albert, A.; Gibson N. I. *Brit.J.Exptl.Path.***1960**, 31,425.

37) Robbins .; Mcwigh. *Am.J.Bot.* **1946**,33.

38) Srivastava, R . S. *Inorg.Chem.Acta.* **1981**,56, 65.

39) Fahmi, N.; Singh, R . V. *Trans. Metal Chem.***1994**, 1219.

SUMMARY

SUMMARY

Metal complexes of Schiff bases have occupied a central role in the development of coordination chemistry. Biological activity, industrial applications, catalysis and mimic activities are some of the practical applications of these complexes. Recently these complexes are becoming a major alternate in the field of chemical science .

Transition metal complexes especially Schiff base complexes play a vital role in biological systems. Its remarkable antimicrobial activity that gave much inspiration for developing Schiff bases as potential ligands. This investigation is expected to provide valuable insight into the nature of the metal ligand bonds and their thermal stability. It is also proposed to find out some new applications of the Schiff bases and their transition metal chelates.

The present study is focused mainly on the metal complexes of Schiff bases derived from dimedone, cyclohexanone and pyrolidone. Seven new ligands viz dimedone bis semicarbazone (H_2DSC), dimedone bis -2-aminophenol (H_2DAP), dimedone - bis -2-aminothiophenol (H_2DATP), cyclohexanone-2-aminophenol (HCAP), cyclohexanone 2-aminothiophenol (HCATP) pyrolidone-2-aminophenol

(HPAP) and pyrolidone-2-aminothiophenol (HPATP) and their transition metal chelates have been synthesized and characterized .

The thesis is divided into three parts. Part I deals with the synthesis and characterization of the various complexes derived from the Schiff base ligands. Part I comprises six chapters. The first chapter consists of an introduction and a critical review of the published work on metal complexes of Schiff bases. In the second chapter, materials, methods and instruments used for the various studies are described.

Synthesis and characterization of Mn (II), Co (II), Ni (II), Cu (II), Zn (II) and Cd (II) complexes of H_2DSC is described in chapter III. Structural elucidation of these complexes has been made on the basis of micro analytical, spectral and magnetic data. These data suggest that H_2DSC behave as neutral tetradentate ligands for the metal ions. All these complexes possess 1:1 metal ligand stochiometry and they are non-electrolytes. Based on the above physiochemical studies, an octahedral structure is suggested for Mn (II), Co (II), Ni (II), Cu (II) complexes and a tetrahedral geometry has been assigned for Zn (II), Cd (II) complexes. Zn (II) and Cd (II) complexes are found to be diamagnetic, while the other metal chelates showed paramagnetic behavior.

Chapter IV deals with the preparation and characterization of Mn (II), Co (II), Ni (II), Cu (II), Zn (II) and Cd (II) complexes of H_2DAP and H_2DATP. Micro analytical data reveals that there exists a 1:1 stochiometry between the metal and ligand in all these complexes. Conductance date explains the non-electrolytic nature of all these complexes. The IR spectral data reveals that the ligand acts as a bivalent tetradentate in the complexes. Mn (II), Co (II), Ni (II) and Cu (II) complexes are paramagnetic while Zn (II) and Cd (II) complexes are diamagnetic. All the above

studies suggest an octahedral structure for Mn (II), Co (II), Ni(II) and Cu(II) complexes and a tetrahedral structure for Zn (II) and Cd (II) complexes.

Synthesis and characterization of ligands HCAP and HCATP and their complexes with Mn (II), Co (II), Ni (II), Cu (II), Zn (II) and Cd (II) are presented in chapter V. and synthesis and characterization of ligands HPAP and HPATP and their complexes with Mn (II), Co (II), Ni (II), Cu (II), Zn (II) and Cd (II) are presented in chapter VI. The complexes are characterized on the basis of analytical, conductance, magnetic susceptibility, IR, NMR and electronic spectral data. All these complexes possess 1:2 stochiometry. The data are consistent with octahedral geometry for Mn (II), Co (II), Ni (II), Cu (II) complexes and tetrahedral structure for Zn (II), Cd (II) complexes. In all the above complexes, the ligand acts as monovalent bidentate.

Part I ends with references.

Part II deals with the thermal studies of 9 complexes of the above Schiff bases. This part comprises four chapters. The first chapter gives an introduction about the thermal studies and the various methods used to determine the kinetic parameters.

Thermal decomposition studies of Ni (II) Cu (II) and Zn (II) complexes H_2DSC, are discussed in chapter 2. H_2DAP are discussed in chapter 3 , H_2DATP are discussed in chapter 4. All the TG curves were subjected to kinetic analysis and the kinetic parameters, namely, energy of activation, Arrhenius frequency factor and entropy of activation, enthalpy of activation, free energy of activation of different decomposition stages have been calculated from TG data using the Coats-Redfern equation.

The inflection temperature, initial decomposition temperature and free energy of activation have been used to determine the thermal stability of the metal chelates.

A multi -stage decomposition pattern was observed for all the three complexes of H_2DSC. In the case of metal complexes of H_2DSC, the TG curve of Cu (II) and Ni (II) complexes give a three-stage decomposition pattern whereas Zn (II) chelates show a two-stage decomposition pattern. The thermal decomposition data as well as kinetic parameters are presented in Tables II.2.1-II.2.6.

Chapter 3 describes the thermal decomposition kinetics of Cu (II), Ni (II), Zn (II) chelates of DATP. The kinetic parameters calculated are n, E, A, $\Delta H^{\ddagger}$, $\Delta S^{\ddagger}$ and $\Delta G^{\ddagger}$. Results of these studies are summarized in Tables II.3.1 to Tables II.3.6.

Chapter 4 describes the thermal decomposition kinetics of Cu (II), Ni (II), Zn (II) chelates of DAP. The kinetic parameters calculated are n, E, A, $\Delta H^{\ddagger}$, $\Delta S^{\ddagger}$ and $\Delta G^{\ddagger}$. Results of these studies are summarized in Tables II.4.1 to Tables II.4.6.

Part II concludes with references.

Part III consists of studies on the antifungal activity of all the six Schiff base ligands and their sixteen metal complexes derived from Co (II), Ni (II), Cu (II), Zn (II) ions on *Phytophthora capsici*, a soil born pathogen that causes 'foot rot', also known as 'quick wilt' of black pepper. This part consists of three chapters.

The first chapter begins with an introduction about the different phases of growth of *Phytophthora capsici*, its life history and the various methods used to destroy the fungus or inhibit or suppress its growth. An integrated disease management involving cultural, biological and chemical methods of control is the suggested strategy to tackle the elusive problem of the 'foot rot' of black pepper caused by *Phytophthora capsici*.

The second chapter deals with materials and methods to find out the inhibitory effect of these ligands and metal complexes on various stages of growth of *Phytophthora capsici* viz. mycelial growth, sporangial production, zoospore

liberation and zoospore germination. For this, a group of ligands and their metal complexes at different concentrations were tested against different growth stages of *Phytophthora capsici*. It was noticed that the activity of Schiff bases increased considerably, when they were chelated with transition metal ions. Among the complexes, Cu (II) complexes were found to be the most effective in inhibiting the growth of *Phytophthora capsici* at its various stages compared to Co (II) and Ni (II) complexes. The results are summarized in Tables III.3.1 - III.3.17.

References are given at the end of Part III.